2

SAINT PETERSBURG STATE UNIVERSITY STUDIES
IN EARTH SCIENCES

Maria S. Kuznetsova

Nuclear Spin Effects in Self-assembled Quantum Dots

Saint Petersburg | 2014

The series Saint Petersburg State University Studies in Physics presents final results of research carried out in postgraduate physical programs at St. Petersburg State University. Most of this research is here presented after publication in leading scientific journals.

The supervisors of these works are well-known scholars of St. Petersburg State University and invited foreign researchers. The material of each book has been considered by a permanent editorial board as well as a special international commission comprised of well-known Russian and international experts in their respective fields of study.

Printed in Russia by St. Petersburg University Press
11/21 6th Line, St. Petersburg, 199004

ISSN 2308-6599
ISBN 978-5-288-05507-2

ABSTRACT

This work present original results of investigation of nuclear spin dynamics in nanostructure with negatively charged InGaAs/GaAs quantum dots characterized by strong quadrupole splitting of nuclear spin sublevels. The main method of the investigation is the experimental measurement and theoretical analysis of the photoluminescence polarization as the function of the transverse magnetic field (effect Hanle).

The dependence of the Hanle curve on temporal protocol of excitation is examined. Experimental data are analyzed using an original approach based on separate consideration of behavior of the longitudinal and transverse components of nuclear polarization. The rise and decay times of each component of nuclear polarization and their dependence on transverse magnetic field strength is determined.

To study the role of the Knight field in the dynamic of nuclear polarization a weak additional magnetic field parallel to the optical axis is used. This allows us to control the efficiency of nuclear spin cooling and the sign of nuclear spin temperature. The standard nuclear spin cooling theory fails to describe the experimental Hanle curves in a certain range of control fields. This controversy is resolved by taking into account the nuclear spin fluctuations. The model allows us to accurately describe the measured Hanle curves and to evaluate the parameters of the electron-nuclear spin system of the studied quantum dots.

New effect of resonant optical pumping of nuclear spin polarization in an ensemble of singly charged (In, Ga)As/GaAs quantum dots subject to a transverse magnetic field is observed. Electron spin orientation by circularly polarized light with the polarization modulated at the nuclear spin transition frequency is found to create a significant nuclear spin polarization, precessing about the magnetic field. Nuclear spin resonances for all isotopes in the quantum dots are found in that way. In particular, transitions between states splitted off from the $\langle \pm 1/2|$ doublets by the nuclear quadrupole interaction are identified.

Keywords: quantum dots, nuclear spin, electron spin, polarization, Hanle effect, quadrupole splitting.

Supervisor Professor Ivan V. Ignatiev
Department of Solid State Physics
Faculty of Physics
Saint-Petersburg State University, Russia

Opponents Professor Oleg F. Vyvenko (Chairman)
Director of the Interdisciplinary Resource Center for Nanotechnology
Faculty of Physics St. Petersburg State University, Russia

Professor Vadim F. Agekyan
Department of Solid State Physics
Faculty of Physics St. Petersburg State University, Russia

Professor Ilya I. Tupitsyn
Division of Quantum Mechanics
Faculty of Physics St. Petersburg State University, Russia

D. Sc. Vladimir L. Korenev
Laboratory of Optics of Semiconductors
Ioffe Physical Technical Institute, Russian Academy of Sciences,
Saint-Petersburg, Russia

Professor Nikolai A. Gippius
Skolkovo Institute of Science and Technology, Moscow region, Russia
Department of Oscillations
Semiconductor Nanostructure Theory Laboratory
Prokhorov General Physics Institute,
Russian Academy of Sciences , Moscow, Russia

Professor GIL Bernard
Director of the Institute of Physics at Montpellier (IPM), France
Director of the "MIPS" federation at the University of Montpellier 2, France

Doctor Alexey Greilich
Experimental Physic 2
Technical University of Dortmund, Germany,

ACKNOWLEGDEMENTS

First of all I want to express my sincere gratitude to my supervisor Ivan Ignatiev for introducing me to science, for his permanent support and stimulation for achieving heights in physics.

I want to express my gratitude to the entire faculty of the Department of Solid State Physics and Optics Laboratory for my training and fruitful discussion of the results. Particular thanks are to my colleagues Gerlovin I. Ya, Petrov M. Yu, Cherbunin R. V. for helping in understanding the experimental data, and basic understanding of the physics of nanostructures.

I also want to thank the head of the Laboratory of Experimental Physics 2 of the Technical University of Dortmund Prof. Manfred Bayer and Professor Dmitrii Yakovlev who kindly invited me to work in their lab. This collaboration has allowed me to gain experience in handling modern equipment and to obtain a lot of interesting data in the field of the spin dynamics of electron-nuclear system.

Financial support of this work was provided by Saint Petersburg State University (Russia), Russian Foundation for Basic Research and DFG projects (Germany).

LIST OF FIGURES

CONTENTS

LIST OF INCLUDED ARTICLES

PI Cherbunin R. V., Kuznetsova M. S., Gerlovin I. Ya., Ignatiev I. V., Dolgich Yu.K., Efimov Yu. P., Eliseev S. A., Petrov V. V., Poltavsev S. V., Larionov A. V., Ill'in A. I. Carrier spin dynamics in GaAs/AlGaAs quantum wells with a laterally localizing electric potential, *Physics of Solid State 51 (4), pp. 837-840,* 2009 (Web of Science, Scopus).

PII Verbin S. Yu., Gerlovin I. Ya., Ignatiev I. V., Kuznetsova M. S., Cherbunin R. V., Flisinski K., Yakovlev D., Bayer M. Dynamics of Nuclear Polarization in InGaAs Quantum Dots in a Transverse Magnetic Field, *Journal of Experimental and Theoretical Physics, 114, 4, pp. 681-690,* 2012. (Web of Science, Scopus).

PIII Kuznetsova M. S., Flisinski K., Gerlovin I. Ya., Ignatiev I. V., Kavokin K. V., Verbin S. Yu., Reuter D., Wieck A. D., Yakovlev D., and Bayer M. Hanle effect in (In,Ga)As quantum dots: Role of nuclear spin fluctuations, *Physical Review B — Condensed Matter and Materials Physics, Vol* 87, *P. 235320,* 2013. (Web of Science, Scopus).

PIV Cherbunin R. V., Flisinski K., Gerlovin I. Ya., Ignatiev I. V., Kuznetsova M. S., Petrov M. Yu., Yakovlev D. R., Reuter D., Wieck A. D., and Bayer M. Resonant nuclear spin pumping in (In,Ga)As quantum dots. *Physical Review B — Condensed Matter and Materials Physics*, *Vol. 84, № 4, P. 041304(R)*, 2011. (Web of Science, Scopus).

OTHER PUBLICATIONS

AI Kuznetsova M. S., Cherbunin R. V., Gerlovin I. Ya., Flisinski K., Ignatiev I. V., Petrov M. Yu., Verbin S. Yu., Yakovlev D. R., Reuter D., Wieck A. D. and Bayer M. Identification of optically induced nuclear spin transitions in (In,Ga)As/GaAs quantum dots. *Proceedings of 19th International Symposium "NANOSTRUCTURES: Physics and Technology",* Ekaterinburg, Russia, pp. 40–41, 2011. (ISBN 978-5-93634-042-0)

AII Kuznetsova M. S., Gerlovin I. Ya., Cherbunin R. V., Flisinski K., Ignatiev I. V., Kavokin K. V., Verbin S. Yu., Reuter D., Wieck A. D., Yakovlev D., and Bayer M. Manifestation of the state of nuclear spin system in the Hanle effect observed in (In,Ga)As quantum dots. *Proceedings of 21th International Symposium "NANOSTRUCTURES: Physics and Technology"*, St Petersburg, Russia, pp. 54-55, 2013. (ISBN 978-5-4386-0145-6)

AIII Kuznetsova M. S., Cherbunin R. V., Gerlovin I. Ya., Flisinski K., Ignatiev I. V., M. Yu. Petrov, Verbin S. Yu., Yakovlev D. R., and Bayer M. Detection and identification of optically induced nuclear spin resonances in GaAs/InGaAs quantum dots. *International Conference of Spin-Optronics,* Toulouse, France, 2013. P. 50.

AIV Kuznetsova M. S., Gerlovin I. Ya., Flisinski K., Ignatiev I. V., M. Yu. Petrov, Yakovlev D. R., and Bayer M. Nuclear magnetic resonance in InGaAs quantum dots observed by optical pumping technique. *International Conference on Optics of Excitons in Confined Systems* Rome, Italy, 2013. P. 109.

AV Verbin S. Yu., Gerlovin I. Ya., Ignatiev I. V., Kuznetsova M. S., Cherbunin R. V., Flisinski K., Yakovlev D. R., Reuter D., Wieck A. D., Bayer M. Nuclear spin dynamics of InGaAs quantum dots in transverse magnetic field. 7th International Conference on Quantum Dots (QD 2012) Santa Fe, New Mexico, USA, Abstract Book, 2012. P. 310.

AVI Ignatiev I. V., Ilya Gerlovin, Roman Cherbunin, Maria Kuznetsova, Serge Verbin, Karl Flisinski, Dirk Reuter, Andreas Wieck, Dmitrii Yakovlev, Manfred Bayer. Dynamic nuclear polarization and Hanle effect in (In,Ga)As/GaAs quantum dots. Role of nuclear spin fluctuations. *31st International Conference on the Physics of Semiconductors "ICPS-2012"*, Zurich, Switzerland, 2012. P. 224.

AVII Kuznetsova M. S., Cherbunin R. V., Gerlovin I. Ya., Flisinski K., Ignatiev I. V., Petrov M. Yu., Verbin S. Yu., Yakovlev D. R., and Bayer M. Optically induced nuclear spin transitions in GaAs/InGaAs quantum dots. *The 7th International Conference on Physics and Applications of Spin-related Phenomena in Semiconductors*. Eindhoven, the Netherlands, 2012. P. 41.

AVIII Kuznetsova M. S., Gerlovin I. Ya., Cherbunin R. V., Ignatiev I. V., Verbin S. Yu., Flisinski K., Reuter D., Wieck A. D., Yakovlev D. R., and Bayer M. Effect of nuclear spin fluctuations and dynamic nuclear polarization on shape of Hanle curves in (In,Ga)As/GaAs quantum dots. *International Conferense of Spin-Optronics*, Saint-Petersburg, Russia, 2012. P. 65.

AIX Kuznetsova M. S., Cherbunin R. V., Gerlovin I. Ya., Flisinski K., Ignatiev I. V., M. Yu. Petrov, Verbin S. Yu., Yakovlev D. R., and Bayer M. Optically induced nuclear spin transitions in GaAs/InGaAs quantum dots. *NewMaRE: New Materials and Renewable Energy*. Tbilisi, Georgia, 2012. P. 35.

AX Kuznetsova M. S., Gerlovin I. Ya., Flisinski K., Ignatiev I. V., Petrov M. Yu., Yakovlev D. R., and Bayer M. The shape of the Hanle curve in (In,Ga)As/GaAs quantum dots at the presence of additional longitudinal magnetic field. *International School of Nanophotonics and Photovoltaics.* Maratea, Italy, 2013.

AXI Kuznetsova M. S., Flisinski K. Investigation of optically induced nuclear spin transitions in InGaAs / GaAs quantum dots. *8th Winter School-Conference "Magnetic resonance and its applications.* Saint-Petersburg, Russia, 2011. P. 84. (in Russian)

1 INTRODUCTION

1.1 Intellectual merit

The spin dynamics in semiconductor quantum dots (QDs) has been an object of intense theoretical and experimental research during the past few decades (Dyakonov, 2008, Merkulov, 2002, Khaetskii, 2002, Gammon, 2001, Braun, 2006, Tartakovskii, 2007). In a QD, the spin of a confined electron is strongly coupled to the spins of the lattice nuclei. The coupling strength is given by the contact hyperfine interaction, which is enhanced due to strong localization of the electron in the QD (Merkulov, 2002, Khaetskii, 2002). The hyperfine coupling destroys electron spin polarization via interaction with random fluctuations of the effective nuclear magnetic field (Merkulov, 2002). A way to overcome this effect is to create a strong polarization of the nuclear spins (Khaetskii, 2002).

The dominant mechanism of the dynamic nuclear polarization (DNP) in semiconductors is the angular momentum transfer from optically oriented electrons to nuclei via electron–nuclear hyperfine interaction (Meier, Zakharchenya, 1984). This process is particularly effective in quantum dot heterostructures, where the electron wave function covers a limited number of nuclei, and the electron and nuclear spins make up a strongly coupled system. Since the spin polarized nuclei, in turn, generate effective magnetic field (Overhauser field) which splits electron spin sublevels, the state of the nuclear spin system can be examined by polarization and spectroscopic methods. The methods based on studying the polarization of photoluminescence (PL) were extensively explored for study of nuclear spin dynamics in bulk semiconductors (Meier, Zakharchenya, 1984, Kalevich, 2008). Nuclear spin relaxation times were found to be a few seconds or longer (Kalevich, 1982). Spectroscopic methods were widely used last fifteen years when the experimental technique was developed for study of PL spectra of single quantum (Brown, 1996, Gammon, 1996, Tartakovskii, 2007, Belhadj, 2008). These experiments allowed one to detect strong effect of nuclear magnetic field and to perform the first experiments on detection of nuclear magnetic resonance of single QD (Gammon, 1997). These measurements reported in recent years, have also shown that nuclear spin relaxation in QDs is much faster. In particular, nuclear spin relaxation in a magnetic field applied parallel to the optical axis (longitudinal field) was found to

occur over times on the order of milliseconds (Maletinsky, 2007, Chekhovich, 2010, Belhadj, 2008).

An alternative approach for detection of nuclear polarization in QDs is to measure the electron polarization created by optical pumping in an external magnetic field. This method does not require high spectral resolution and can be used to QDs ensemble characterized by extremely wide lines in the PL spectrum. As the nonequilibrium electron spin polarization is, in many cases, the magnetic-field dependent, the Overhauser field can be detected using its effect on the mean electron spin, for example, by observing the associated changes in the circular polarization of PL. In a magnetic field parallel to the optical axis (longitudinal magnetic field), the nuclear polarization created by the pumping may influence the PL polarization by suppressing electron spin relaxation (Cherbunin, 2009, Maletinsky, 2007, Maletinsky, 2007a). For optical pumping in a magnetic field perpendicular to the optical axis (transverse magnetic field), the electron spin polarization is usually destroyed with increasing magnetic field (Hanle effect). In this case, the Overhauser field modifies the width and shape of the dependence of the circular polarization of the PL on the magnetic field (Hanle curve), which can give rise to a nonmonotonous dependance, and even to a hysteresis (Meier, Zakharchenya, 1984, Cherbunin, 2009, Kalevich, 2008, Paget, 1977, Pal, 2009, Auer, 2009, Flisinskii, 2010, PIV, Masumoto, 2008, Urbaszek, 2013). In the presence of DNP, there is a specific feature in the Hanle curve near zero magnetic field (W-structure, **Fig. 1**) analyzed for the first time in Ref. (Paget, 1977). Qualitative interpretation of W-structure is typically done in the

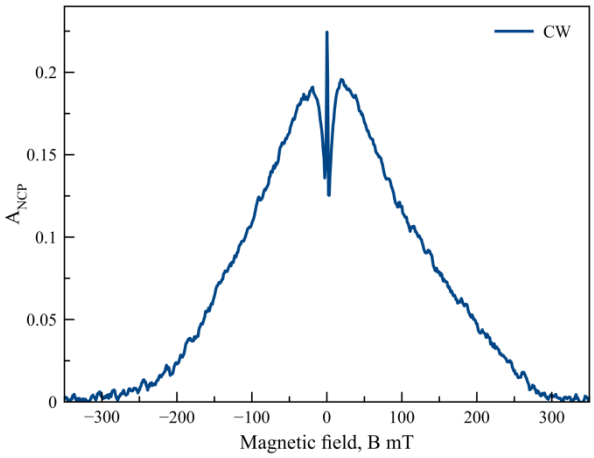

Fig. 1. Typical dependence of the degree of PL polarization in transverse magnetic field for QDs studied in present work (Hanle curve under continuous-wave pumping).

framework of the nuclear spin cooling model (A. Abraham, 1961, Meier, Zakharchenya, 1984). At the same time, this model based on thermodynamics approach does not always allow one to quantitatively analyze the dynamics of nuclear spin polarization and relaxation in QDs.

1.2 Goal of the work

The goal of present work is the investigation of main characteristics of optically created dynamical nuclear polarization in semiconductor QDs. We have performed the experimental study and theoretical modeling of the dynamics of electron-nuclear spin system in a set of nanostructures with InGaAs QDs. To quantitavely analyze the experimental data we have generalized the cooling spin model. The following tasks were solved:

- Investigation of the dynamics of the rise and decay of the spin polarization of nuclei in QDs under optical excitation (PII).
- Experimental study and theoretical modeling of the dependence of electron spin polarization in a transverse magnetic field in the QDs with strong electron-nuclear spin interaction (PIII).
- Investigation of nuclear magnetic resonance (NMR) by resonant optical pumping of nuclear polarization in the QDs under study (PIV).

1.3 Methods of investigation

In present work, the main experimental method was the investigation of the PL polarization of QDs excited by polarized optical pumping. For theoretical analysis, we used two phenomenological models: the geometric model (PII) and a generalization of the nuclear spin cooling model (PIII), allowing for adequate description the whole set of experimental data. To understand the nuclear spin dynamics, it is important to get understanding of the dynamics of electron spin. For this purpose at the first step we have studied the dynamics of polarization and relaxation of the electron spins in QDs induced by non-uniform electric field in a quantum well by the method of photo-induced magneto-optical Kerr effect (PI).

1.4 The main results

1. Behavior of the Hanle curves is studied experimentally using different temporal protocols of excitation and registration of photoluminescence of the InGaAs quantum dots.
2. The Hanle curves are analyzed by the use of an original approach based on separate consideration of behavior of the longitudinal and transverse components of nuclear polarization in QDs with strong quadruple splitting of nuclear spin states (PII).
3. This analysis made it possible to determine the rise and decay times of each component of nuclear polarization and their dependence on transverse magnetic field strength for QDs under study (PII).
4. Deformation of the Hanle curve as the function of small additional magnetic field parallel to the optical axis is studied experimentally (PIII).

5. To analyze this deformation a phenomenological model of the formation of the Hanle contour in such experimental conditions is developed. The model is based on the standard theory of nuclear spin cooling and takes into account the effect of nuclear spin fluctuations (PIII).
6. This generalized model allows us to adequately describe the experimental data and to evaluate the maximal value of the effective field of nuclear polarization created by optical pumping in QDs under study (PIII).
7. The analysis of experimental data using this model allowed us to determine the magnitude of effective field acting on the nuclei from the electron spin (Knight field) in the sample annealed at 980 ^{o}C to be of about 1 mT when the electron spin is almost totally polarized (PIII).
8. The effect of resonant optical pumping of the precessing transverse component of nuclear spin polarization in inhomogeneously broadened QD ensemble is observed for the first time under strong excitation of QDs by the circularly polarized light, which polarization is modulated with the nuclear spin precession frequency about external magnetic field (PIV).
9. Nuclear spin resonances for all isotopes in the quantum dots are identified using the calculated values of quadrupole nuclear spin splitting caused by the strain-induced gradient of crystal electric field at nucleus positions (PIV).

1.5 Practicability

The results can be applied to the study of coherent optical properties of nanostructures with quantum dots (In,Ga)As/GaAs, carrying out at the Technical University of Dortmund (Germany), Physico-Technical Institute (St. Petersburg), Novosibirsk State University and other research centers.

1.6 Appraisal of the work and publications

The results of this work were reported at the international conferences 16th International Symposium "Nanostructures: Physics and Technology" (Ekaterinburg, Russia — 2011, Saint-Petersburg, Russia — 2013), "International Conference of Spin-Optronics" (Saint-Petersburg, Russia — 2012, Toulouse, France — 2013), "International Conference on Optics of Excitons in Confined Systems" (Rome, Italy — 2013), "The 7th International Conference on Physics and Applications of Spin-related Phenomena in Semiconductors" (Eindhoven, the Netherlands — 2012), "7th International Conference on Quantum Dots" (Santa Fe, New Mexico, USA — 2012), "31st International Conference on the Physics of Semiconductors" (Zurich, Switzerland -2012), "NewMaRE: New Materials and Renewable Energy" (Tbilisi, Georgia — 2012), "School of Nanophotonics and Photovoltaics" (Maratea, Italy — 2013) and at the seminars of the Spin Optics Laboratory and the department of Solid State Physics (Saint Petersburg State University 2008 — 2013).

2 THE MAIN CONTENT

2.1 Samples and experimental setup

Heterostructures containing 20 layers of self-assembled (In,Ga)As/GaAs QDs separated by Si-δ-doped GaAs barriers were studied in this work (**Fig. 2**). Donor ionization supplies every dot with, on average, a single resident electron. The original structure was grown by molecular-beam epitaxy on a (100) GaAs substrate. Then it was separated into several pieces which were then thermally annealed at different temperatures. The annealing resulted in a reduction of the In content in the QDs due to interdiffusion of In and Ga atoms and in a high-energy shift of the lowest QD optical transition. The an-

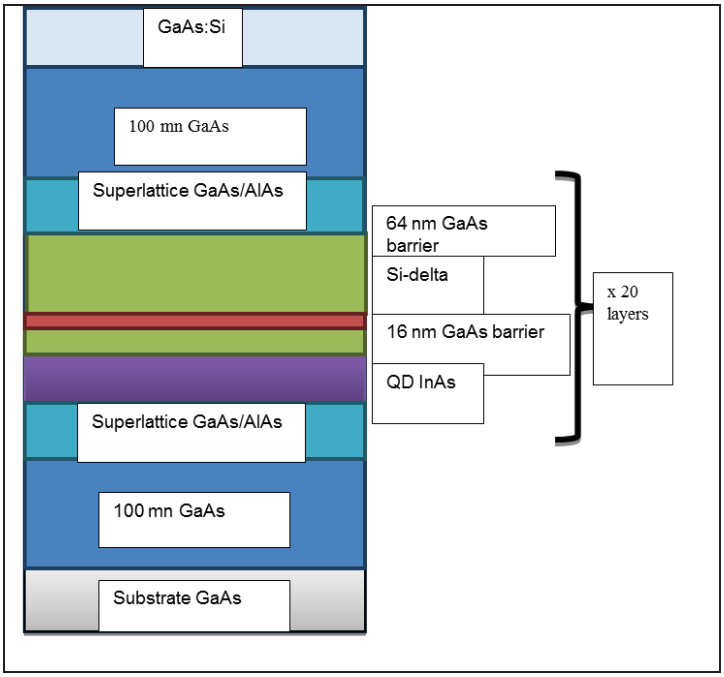

Fig. 2. Structure under study.

nealing also gave rise to the considerable decrease of mechanical stress in the QDs and, therefore, to reducing the quadrupole splitting of nuclear spin states. Besides, the enlarging of localization volume for resident electrons occurred due to the interdiffusion of In and Ga atoms.

The studied sample was immersed in liquid helium at a temperature T = 1.8 K in a cryostat with a superconducting magnet. Magnetic fields up to 100 mT were applied perpendicular to the optical axis (Voigt geometry) along to the [110] crystallographic direction of the sample. To create an additional magnetic field, perpendicular to the main magnetic field and parallel to the optical axis, a pair of small Helmholtz coils was installed outside the cryostat.

The PL of the sample is excited by circularly polarized light from a continuous-wave Ti:sapphire laser, with the photon energy tuned to the optical transitions in the wetting layer of the sample. An electro-optical modulator followed by a quarter-wave plate is used to modulate the polarization helicity of optical excitation. The degree of circular polarization of the PL is typically detected by a standard method using a photoelastic modulator and an analyzer (a Glan-Taylor prism). The modulator creates a time-dependent phase difference $\phi = (\pi / 4)\sin(2\pi f \cdot t)$, between the linear components of the PL, thus converting each of the circular components (σ+ and σ–) into linear ones (x and y) at the modulation frequency, typically $f = 50$ kHz. The analyzer selects one of the linear components, which was dispersed with a 0.5-m monochromator and detected by an avalanche photodiode. The signal from the photodiode was accumulated for each circular component separately in a two-channel photon-counting system. The PL polarization was calculated using a standard definition, $\rho = (I^{++} - I^{--})/(I^{++} + I^{--})$, where I^{++} and (I^{--}) are the PL intensity for copolarization and cross polarization of excitation and detection, respectively. The PL polarization was recorded at the wavelength corresponding to the maximum of the PL band of the sample. The complete optical setup is shown in **Fig. 3.** In some experiments, the PL polarization is determined from the PL signals detected for a fixed helicity of the PL but at different helicities of excitation.

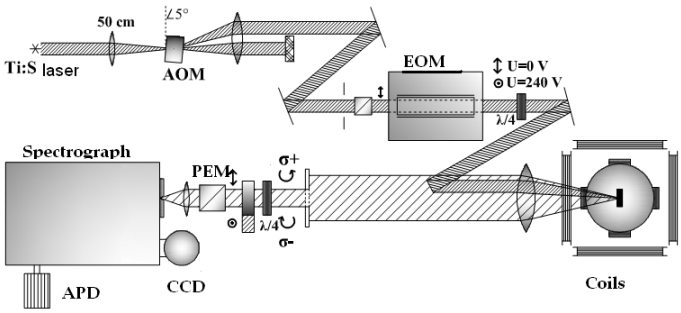

Fig. 3. Experimental setup.

To study the dynamics of nuclear polarization, we used a amplitude modulation of laser beam using an acousto-optic modulator to produce pulses with various bright and dark time durations. The spin polarization of the resident electrons is monitored through the effect of negative circular polarization (*NCP*), $\rho < 0$, of the PL observed for

singly charged QDs. The mechanism of NCP of the PL of QDs has been extensively discussed in Refs. (Cortez 2002, Ignatiev2009, Dzhioev, 1998), where it was shown that the presence of *NCP* is the result of optical orientation of the resident electrons. The amplitude of *NCP* is proportional to the projection of electron spin onto the optical axis z, averaged over the QD ensemble, (Flisinski2010)

$$A_{NCP} \sim 2S_z. \quad (1)$$

The amplitude of the PL polarization, A_{NCP}, increases with rising excitation power at relatively low excitation levels (see **Fig. 4**). A further rise of the power results in saturation

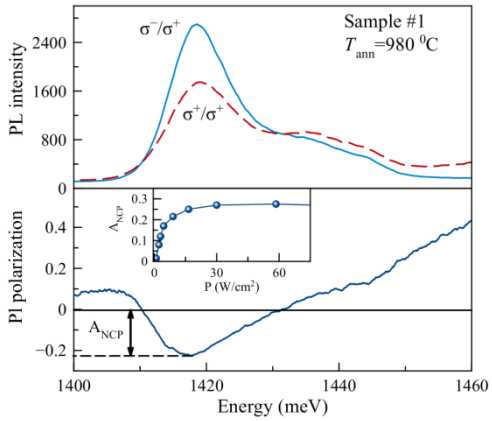

Fig. 4. Typical PL spectra (top curves) measured at σ+-excitation and co- and cross-polarized detection and the degree of circular polarization (bottom curve) for sample annealed at 980°C. The definition of amplitude of the negative circular polarization is illustrated by the arrow marked $A_{NCP.}$ Inset shows the power dependence of A_{NCP}.

of the A_{NCP}, which indicates a high level of electron spin polarization. The pump powers used in our experiments were sufficiently high to totally polarize the electron spin.

2.2. Dynamics of nuclear polarization in a transverse magnetic field

Dynamics of nuclear polarization in quantum dots in the magnetic field perpendicular to the optical axis (in Voigt geometry), until recently, did not actually investigated. An application of the transverse magnetic field reduces the degree of circular polarization of photoluminescence from semiconductors (Hanle effect). This is the effect of electron (or exciton) spins precession about the field. The shape of Hanle curve can be changed by effective magnetic field of nuclear polarization (Paget, 1977, Krebs, 2010). This makes it possible to study the dynamics of nuclear polarization experimentally by measuring the Hanle effect in the kinetic regime, i.e., with time resolution.

The first observations of the time resolved Hanle effect in an ensemble of negatively charged InGaAs/GaAs quantum dots (Cherbunin, 2010) demonstrated that experiments of this kind would provide an effective tool for examining the dynamics of a nuclear spin system. In PII we demonstrate systematic experimental data presented and analyzed to estimate the nuclear polarization buildup and decay times for the structure under study. In our experiments, we used amplitude modulated optical pumping with various dark and excitation times, t_d and t_{exc}.

The Hanle curves obtained under strong pumping for the sample under study are largely similar in shape to those observed previously for donor-bound electrons, in qualitative agreement with predictions of a classical model of DNP in a transverse magnetic field (Meier and Zakharchenya, 1984, Kalevich, 2008). However, the classical model fails to explain an increase in Hanle curve width with optical pumping intensity observed in our experiments. Following (Cherbunin, 2010, Dzhioev, 2007), we suppose that the Hanle curve broadening is due to nuclear polarization stabilized by quadrupole splitting of nuclear spin states. An analysis of time resolved measurement data provides quantitative estimates of the rise and decay times for longitudinal and transverse nuclear fields in the structures under study.

To examine nuclear polarization buildup, we measure *NCP* as a function of time after a pump pulse had arrived using the multichannel photon counting system.

Nuclear spin relaxation was examined by detecting photoluminescence during a short interval $t_{det} = 1$ ms at the start of pumping after various dark times. Pumping was supposed to have a weak effect on nuclear polarization during the detection time. The degree of polarization was measured as a function of dark time by varying t_d from 20 μs to 50 ms. **Fig. 5a** shows the Hanle curves obtained for several dark times, and **Fig. 5b** shows their central portions. It is clear that the curves corresponding to short dark times are similar to that obtained under CW pumping (see **Fig. 1**). In particular, a pronounced W profile is observed, and the curve is wider. An increase in dark time smoothies out the W profile and reduces the width of the Hanle curve.

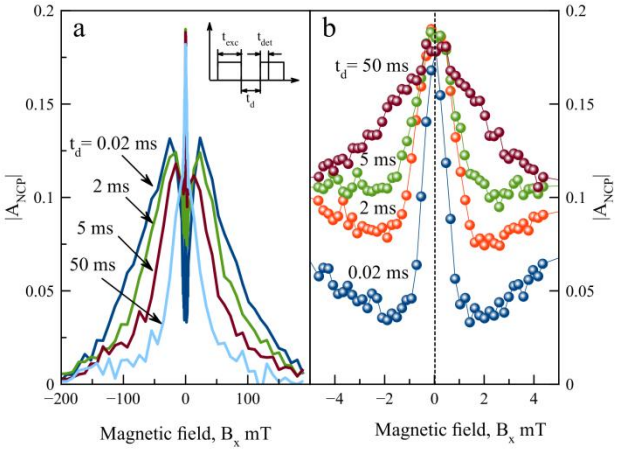

Fig. 5. Hanle curve at constant excitation time $t_{exc} = 100$ ms, parameterized by dark time t_d: (a) complete curves; (b) central portion of curves.

Our experimental findings suggest that the development of nuclear polarization generally leads to a decrease in electron spin polarization in weak transverse magnetic fields and its increase in strong fields. It is obvious that these effects are associated with two different processes.

This implies that dynamics of the longitudinal component $B_{DNP||}$ of nuclear field can be inferred from the time evolution of the dips around the central peak.

Information about behavior of the transverse component $B_{DNP\perp}$ of nuclear field can be extracted by analyzing the width of the Hanle curve. Its large width has been attributed to the formation of a transverse component $B_{DNP\perp}$ of nuclear field stabilized by quadrupole splitting of nuclear spin states along the optical axis (Dzhioev, 2007). Since the longitudinal component $B_{DNP||}$ plays no significant role in strong applied magnetic fields (Meier and Zakharchenya, 1984, Kalevich, 2008), dynamics of $B_{DNP||}$ and $B_{DNP\perp}$ can be inferred separately from behavior of electron spin polarization in weak and strong fields, respectively. Accordingly, to analyze experimental data, expressions are required that relate the degree of electron polarization to the magnitudes of the corresponding DNP components.

Measured degree of photoluminescence polarization is proportional to the electron spin projection on the viewing direction.

$$S_z = S^* \cos\vartheta^2 = S\frac{B_{tot,z}^2}{B_{tot}^2}. \tag{2}$$

Here S quantifies the degree of optically induced spin orientation and ϑ is the angle between the viewing direction and the total field $B_{tot} = B + B_N$, which is the sum of the applied field B and the nuclear field, $B_N = B_f + B_{DNP}$, including the effective nuclear spin fluctuation field, B_f, generated by randomly oriented nuclear spins (Merkulov, 2002). Since the electron spin in a quantum dot interacts with limited number of nuclear spins, the contribution due to fluctuations is significantly larger than that for donor bound electron spins in a bulk material, amounting to several tens of milliteslas (Petrov, 2009). Therefore, we can evaluate only an ensemble averaged spin.

In summary, the degree of electron spin polarization can be represented by the general expression

$$\rho = \langle S_z \rangle / S = \frac{\left(B_{DNP\perp}^2 + 0.5B_{f\perp}^2\right)}{\left(B + B_{DNP||}\right)^2 + B_{DNP\perp}^2 + B_f^2}, \tag{3}$$

where $\left\langle B_f^2 \right\rangle = \left\langle B_{f||}^2 \right\rangle + \left\langle B_{f\perp}^2 \right\rangle = 3\left\langle B_{f||}^2 \right\rangle$. The last relation holds when dynamic nuclear polarization is insignificant and nuclear spin fluctuations are statistically isotropic.

Experimental data can be analyzed by simplifying expression (3) in two special cases of particular importance. According to (Meier and Zakharchenya, 1984), the longitudinal component $B_{DNP||}$ of nuclear field appears only in the W-profile region of the Hanle

curve, where the applied field is negligible compared to the nuclear spin fluctuation field (Dzhioev, 2002, Merkulov, 2002). Then, it holds for this region that

$$\rho \approx \frac{\left(B_{DNP\perp}^2 + 0.5\left\langle B_{f\perp}^2 \right\rangle\right)}{\left(B_{DNP\|}\right)^2 + B_{DNP\perp}^2 + 3\left\langle B_{f\|}^2 \right\rangle}. \tag{4}$$

In strong applied magnetic fields (as $B_{DNP\|} \to 0$), the degree of polarization becomes

$$\rho \approx \frac{\left(B_{DNP\perp}^2 + 0.5\left\langle B_{f\perp}^2 \right\rangle\right)}{B^2 + B_{DNP\perp}^2 + 3\left\langle B_{f\|}^2 \right\rangle}. \tag{5}$$

Thus, we can examine the time dependence of ρ in strong and weak magnetic fields to determine the respective kinetics of the longitudinal and transverse components of nuclear polarization

For describing the rise and decay of the longitudinal component of nuclear polarization were found the following expression:

$$\rho \approx \frac{a^2 + 1}{c^2\left(1 - e^{-t/\tau}\right)^2 + a^2 + 3}, \tag{6}$$

$$\rho \approx \frac{a^2 + 1}{c^2 e^{-2t/\tau} + a^2 + 3}. \tag{6′}$$

Expression (5), valid for strong applied magnetic fields, can be written analogously to describe the rise and decay of the transverse component of nuclear polarization, respectively:

$$\rho \approx \frac{\left(1 - e^{-t/\tau}\right)^2 + c'^2}{a'^2 + \left(1 - e^{-t/\tau}\right)^2 + 3c'^2}, \tag{7}$$

$$\rho \approx \frac{e^{-2t/\tau} + c'^2}{a'^2 + e^{-2t/\tau} + 3c'^2}. \tag{7′}$$

Figure 6, 7 shows the results of an analysis of the time dependent Hanle curves, which are measured after the start of optical pumping. The values of ρ are refined by taking into account photoluminescence depolarization due to contributions from neutral quantum dots. Experimental data were processed to determine the time resolved degrees of polarization

corresponding to several applied magnetic field strengths. **Figure 6** demonstrates a wide difference between kinetics of degree of polarization under weak and strong field conditions (few milliteslas and higher than 20 mT, respectively).

At $B = 2$ mT (the lowest point of a dip), where the dominant role is played by $B_{DNP||}$, the degree of electron spin polarization ρ decreases with time elapsed (**Fig. 6**), signifying an increase in $B_{DNP||}$. We found that the time dependent degree of polarization determined from experimental data can be fitted by Expression (6) only if the transverse component of nuclear field is sufficiently weak, $B^2_{DNP\perp} \ll \left\langle B^2_f \right\rangle$. Using the resulting approximation, we estimated the characteristic rise time for $B_{DNP||}$, $\tau_{||} \approx 6$ ms.

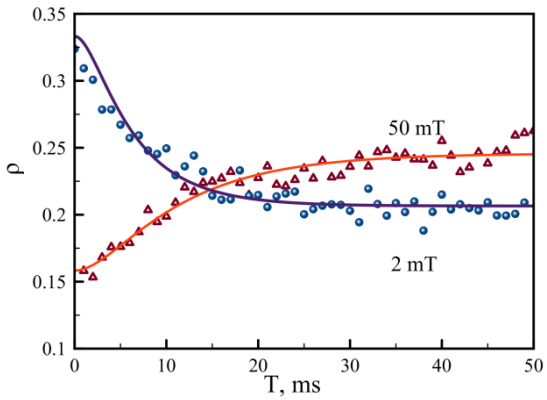

Fig. 6. Example of time-dependent degree of polarization. Symbols represent experimental results; solid curves are approximations by functions (6) and (7).

Figure 7 shows the rise time τ of the transverse component of nuclear polarization. It demonstrates that the time linearly increases from approximately 2.5 to 15 ms with an applied field between 20 and 100 mT.

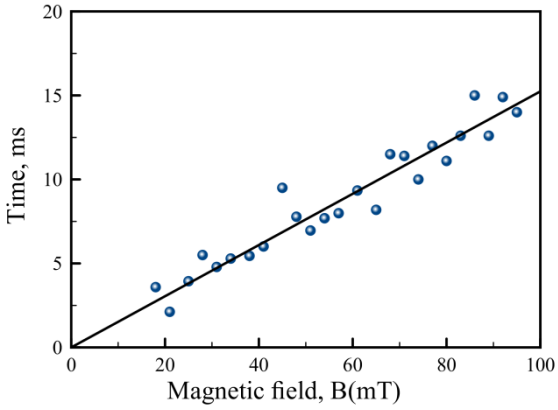

Fig. 7. Field dependence of the build-up time of the transverse DNP field component.

An analogous procedure was used to analyze the shape of the Hanle curve as a function of dark time (**Fig. 5**). Measurement results were converted into spin polarization kinetics for several values of applied magnetic field strength (as in **Fig. 6**), and the resulting curves were fitted by (6′) and (7′). The curves in **Fig. 8** are examples of such fits. The fitting parameters were used to evaluate the initial longitudinal and transverse nuclear fields, as well as the corresponding decay times. The decay time of the longitudinal component calculated by using the data for $B = 2$ mT was found to be $\tau \approx 5.5$ ms, which is close to the corresponding rise time reported above.

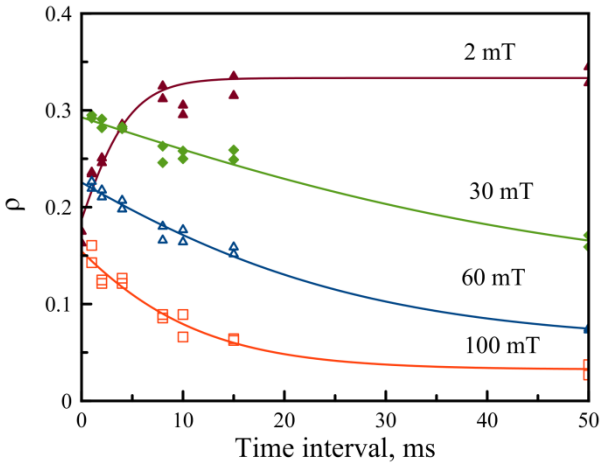

Fig. 8. Kinetics of degree of polarization at several magnetic field strengths, obtained by analyzing measurements results for various dark times. Symbols represent experimental data, solid curves are approximations by functions (6′) and (7′).

However, the decay time of the transverse component of nuclear polarization differs significantly from its rise time. Moreover, its time variation in an applied magnetic field exhibits an opposite trend: whereas the rise time increases with field strength (**Fig. 7**), the decay time rapidly decreases (**Fig. 9**). Accordingly, these times are approximately equal in strong magnetic fields but differ by a factor of several tens at B = 20 mT.

Our analysis shows that the longitudinal and transverse components of nuclear polarization in the quantum dots under study exhibit widely different dynamical patterns. The behavior of longitudinal polarization is relatively simple. After the start of optical pumping, this component increases with a characteristic time of approximately 6 ms to a limit magnitude corresponding to an effective nuclear field of 30 to 40 mT. After the end of pumping, the longitudinal component decays over a similar time scale.

The behavior of the component of dynamic nuclear polarization perpendicular to the applied magnetic field is much more complicated. Observations that defy any straightforward explanation include difference between the buildup and decay times, their opposite variation with applied magnetic field, and increase in magnitude of this component with applied field strength.

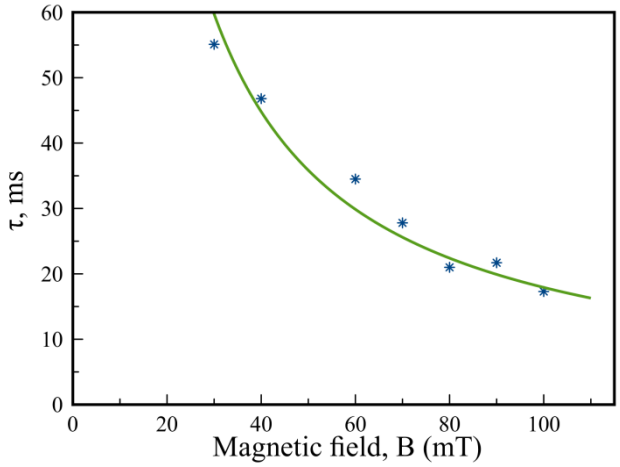

Fig. 9. Field dependence of decay time of the transverse DNP-field component.

In our view, these differences are mainly due to the fact that the dominant contributions to the buildup of longitudinal and transverse polarization components come from states with different spin projections on the viewing direction.

In PII we performed an experimental study of time dependent circular polarization of photoluminescence from quantum dots as a function of magnetic field applied perpendicular to the optical axis (time resolved measurements of the Hanle effect). Experimental data were analyzed using an original approach based on separate treatment of the longitudinal and transverse components of nuclear polarization in quantum dots characterized by strong quadrupole splitting of nuclear spin states. The phenomenological model proposed here takes into account the contribution of nuclear spin fluctuations, which were ignored in previous analyses of experimental data on the Hanle effect. The model is validated both by our finding that nuclear spin fluctuation field is independent of applied field and by good quantitative agreement with results of other studies (Cherbunin, 2009, Petrov, 2009). Using this model to analyze experimental results, we obtained detailed information about the rise and decay times of each component of nuclear polarization in quantum dots in a transverse magnetic field. The rise and decay times of the component parallel to the applied field were found to be almost equal (approximately 5 ms). However, the dynamics of the transverse component is much more complicated: the corresponding rise and decay times differ widely and have opposite dependence on magnetic field strength. Furthermore, the magnitude of the transverse component created by continuous wave pumping significantly increases with applied field strength. We attribute this unexpected behavior of nuclear polarization to nuclear spin relaxation via interaction with photo excited carriers.

2.3 Role of nuclear spin fluctuations

In PIII, we report on detailed measurements of the Hanle effect in (In,Ga)As/GaAs QDs in the weak-field range (0–20 mT field strength), where the effect of the nuclear spin fluctuations (NSF) is expected to be the strongest. We have measured a set of Hanle curves under optical excitation of moderate intensity and at different strengths of an additional magnetic field applied along the optical axis (longitudinal magnetic field). The experimental Hanle curves are compared with the results of calculations using two models, one including NSF and the other one taking into account only mean Overhauser fields. In both theories, the mean Overhauser field has been calculated within the spin temperature approach. Our analysis shows that the mean-field model fails to describe the features of the Hanle curve around zero transversal field, where the so-called W structure appears in a certain range of longitudinal fields B_z. The model including NSF, on the other hand, yields good fits of the experimental data, with a reasonable choice of parameters, for all experimental conditions except for the exact compensation of the Knight field with B_z. In the latter case, nuclear quadruple effects due to strain in the QDs probably play the dominant role.

The effect of the longitudinal magnetic fields, ranging from −20 to +20 mT, on the Hanle curve and the dependences calculated in the framework of the nuclear spin cooling model are investigated. For positive B_z, which, for the helicity of excitation used in our experiments, is codirected to the Knight field the experimental and calculated curves are in qualitative agreement with each other. The analysis shows that the effective nuclear field in this case is codirected to the external magnetic field and thus "amplifies" it. This amplification results in a gradual decrease of spin polarization and, correspondingly, of PL polarization beyond the central peak with rising B_z.

When B_z is negative, the effective field is antiparallel to the Knight field. If $B_z = -B_e$, the compensation of the longitudinal component of total field occurs. According to Refs. (Meier and Zakharchenya, 1984, Page, 1977), nuclear spin cooling is not possible in this case. This should result in the disappearance of the W structure, as it is shown in **Fig. 10** for the Hanle curve calculated for $B_z = -1$ mT. At more negative B_z, the W structure appears again, but the additional maxima run away from the central peak with increasing $|B_z|$, maintaining the same amplitude as the central peak. This behavior of the calculated Hanle curves is explained by the fact that in this case the nuclear field is directed against the total effective magnetic field affecting the nuclei. The x component of the nuclear field, B_{Nx}, is compensated by the transverse magnetic field B_x at some magnitude of B_x, giving rise to the additional maxima.

These numerical results, however, are in strong contradiction to our experimental observations (**Fig. 10**).The central peak of the measured Hanle curves is higher than the other parts of the Hanle curve at any negative B_z. We want to stress that the disagreement between the theory and the experiment cannot be eliminated for any set of values of the adjustable parameters. Therefore this contradiction is of principal importance and indicates that the model of mean nuclear field ignores some mechanism causing depolarization of the electron spin at nonzero transverse magnetic field, including points where it is totally compensated by the nuclear field. In the cooling model, such mechanisms are not provided which does not get a description of the experimental data.

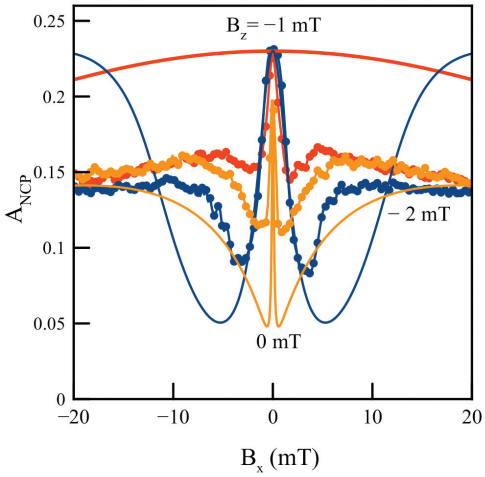

Fig. 10. Comparison of Hanle curves calculated in the framework of standard cooling model (solid lines) with the experimental data (points) for negative longitudinal external fields B_z.

To extend the standard cooling model, we suppose that the effective nuclear field consists of a regular component, B_N, created by the nuclear polarization, and a fluctuating component, B_f, appearing due to the random orientation of the limited number of nuclear spins interacting with the electron spin (Merkulov, 2010). The estimates given in (Ikezawa, 2005, Pal, 2009) for similar QDs show that the average magnitude of the fluctuating nuclear field is of the order of tens of milliteslas.

The dependence of the average electron spin polarization on the transverse external magnetic field within this approximation is a bell-like curve, which can be well fitted by a Lorentzian:

$$\rho(B) \approx \frac{\left\langle B_{fz}^2 \right\rangle}{B^2 + \left\langle B_f^2 \right\rangle}. \tag{8}$$

Some generalization of Eq. (8) is required to describe electron spin polarization under our experimental conditions. We need to take into account the regular nuclear field B_N with nonzero components B_{Nx} and B_{Nz} created by the dynamic polarization of nuclei. In addition, in our experiments, the external magnetic field has not only the transverse component but also some longitudinal one. For this case we can write down the following expressions for the z and x components of the averaged electron spin $\boldsymbol{S}_{\|}$:

$$S_z = S_0 \frac{\left(B_z + B_{Nz}\right)^2 + \left\langle B_{fz}^2 \right\rangle}{\left(B_x + B_{Nx}\right)^2 + \left(B_z + B_{Nz}\right)^2 + \left\langle B_f^2 \right\rangle}, \tag{9}$$

$$S_x = S_0 \frac{\left(B_z + B_{Nz}\right)\left(B_x + B_{Nx}\right)}{\left(B_x + B_{Nx}\right)^2 + \left(B_z + B_{Nz}\right)^2 + \left\langle B_f^2 \right\rangle}. \tag{9′}$$

Here we assume that the regular nuclear field B_N is directed along the total effective field B_{Ntot} acting on the nuclei, which consists of the external magnetic field $B_x + B_z$, and the Knight field $B_e = b_e S_{||}$, created by hyperfine interaction with the electron spin. According to standard cooling model we can write the nuclear field the following way

$$\boldsymbol{B}_N = \boldsymbol{B}_{tot}^{(N)} \frac{b_N \left(\boldsymbol{B}_{tot}^{(N)} \cdot \mathbf{S}_{||}\right)}{B_{tot}^{(N)2} + \xi B_L^2} \cdot 4I(I+1)/3\,. \tag{10}$$

The above equation allows one to obtain the following expressions for the x and z components of the nuclear field:

$$B_{Nx} = \left(B_x + b_e S_x\right) \frac{b_N \left(B_z S_z + B_x S_x + b_e S_x^2 + b_e S_z^2\right)}{\left(B_x + b_e S_x\right)^2 + \left(B_z + b_e S_z\right)^2 + \xi B_L^2}, \tag{10′}$$

$$B_{Nz} = \left(B_z + b_e S_z\right) \frac{b_N \left(B_z S_z + B_x S_x + b_e S_x^2 + b_e S_z^2\right)}{\left(B_x + b_e S_x\right)^2 + \left(B_z + b_e S_z\right)^2 + \xi B_L^2}. \tag{10″}$$

The coefficient b_e is given, in principle, by $be = -(16\pi/3)\mu_B \xi^2$, where μ_B is the Bohr magneton and ζ is the electron density on a nuclear site. The negative sign means that the direction of the Knight field is opposite to that of the electron spin. Because the electron density is dependent on the QD size, which can sufficiently vary from dot to dot, the value of ζ is unknown a priori.

We solved the whole system of Eqs. (9), (9′), (10′), and (10″) and used their real roots for modeling the Hanle curves, slightly varying the fitting parameters. Examples of the calculated Hanle curves are shown in **Fig. 11.** As seen, reasonable agreement between calculated and measured curves is observed for negative B_z. Some deviations from the experiment occur for magnetic fields B_z in the range from −0.5 to −1 mT, where the theoretically calculated amplitude of the central peak is considerably smaller than the one observed experimentally (see inset in **Fig. 11**). The strong decrease of the peak amplitude obtained in the calculations is due to the depolarization of the electron spin by the nuclear spin fluctuations, when the longitudinal component of total field disappears and the nuclear field does not build up. Experiments also show a decrease of the central peak of about 20%, which is, however, significantly smaller than the one predicted theoretically. A possible reason for this discrepancy between the theory and the experiment could be related to the spread of Knight fields in the QD ensemble, which is ignored in

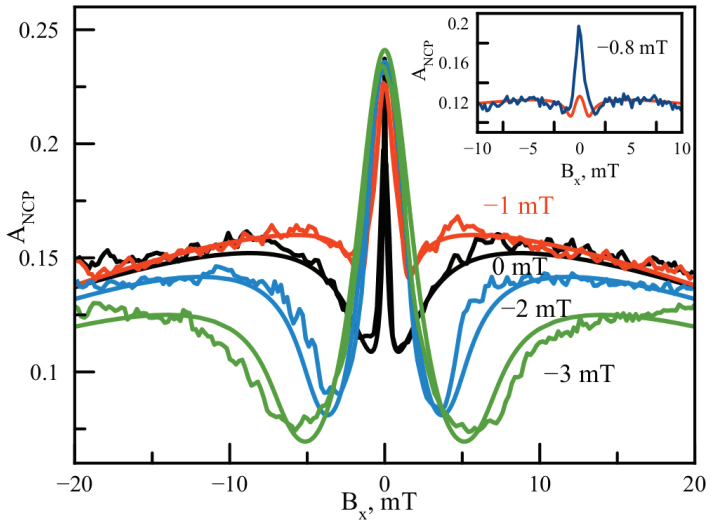

Fig. 11. Experimentally measured curves (noisy lines) and results of calculations taking into account the NSF (smooth solid lines) for negative longitudinal external fields B_z.

the theory. Another possible reason is the polarization of quadrupole-split nuclear spin states, which can stabilize the electron spin polarization (Dzhioev, 2007). Further study is needed to clarify this problem.

The results of the calculations allow us to conclude that the effect of nuclear spin fluctuations is indeed important for the QDs under study. The good agreement between theory and experiment for the whole range of B_z (with the only exception mentioned above) allows us to consider in more detail the physical meaning of the parameters obtained from the fitting and their dependence on the longitudinal magnetic field

We find that the NSF amplitude, $\sqrt{\left\langle B_{fz}^2 \right\rangle}$, can be chosen close to 25 mT for all the Hanle curves measured at various longitudinal magnetic fields. The good overall correspondence of the simulated and measured Hanle curves confirms the validity of the model developed.

The analysis of experimental data has confirmed the prediction of (Merkulov, 2002) about the significant influence of nuclear spin fluctuations on the electron spin orientation due to strong localization of the electron in QDs. The observed behavior is considerably different from that in bulk semiconductor alloys studied in many works (Meier and Zakharchenya, 1984), in which the electron density is spread out over a huge number of nuclei and the effect of the NSF, as a rule, is negligibly small. The analysis allows us to evaluate the maximal value of the effective field of nuclear polarization created in studied quantum dots by optical pumping to be about 200 mT. We have also found that the effective field acting on the nuclei from the electron spin (Knight field) in the sample under study is near 1 mT when the electron spin is almost fully oriented.

2.4. Resonant nuclear spin pumping

In PIV it is discussed the observation of resonant optical pumping of nuclear spin polarization in an ensemble of singly charged (In,Ga)As/GaAs quantum dots subject to a transverse magnetic field. Electron spin orientation by circularly polarized light with the polarization modulated at the nuclear spin transition frequency is found to create a significant nuclear spin polarization, precessing about the magnetic field.

An efficient technique to reach significant nuclear spin polarization (NSP) is optical pumping (Meier and Zakharchenya, 1984). A relatively strong nuclear polarization (tens of percent) can be created by optical pumping of QDs in a magnetic field parallel to the optical axis (longitudinal field) (Gammon, 2001, Braun, 2006, Tartakovskii, 2007). Optical pumping can create dynamic nuclear polarization also in a transverse magnetic field (Paget, 1977, Krebs, 2010). It is commonly accepted (Dyakonov, 2008) that the nuclear polarization is directed along the external magnetic field. The appearance of this longitudinal component corresponds to a difference in population of nuclear Zeeman sublevels and, therefore, is usually treated in terms of "nuclear spin cooling."

In PIV we experimentally demonstrate that not only longitudinal but also transverse NSP components of remarkable magnitude can be created in QDs. We find that polarization-modulated optical excitation of singly charged (In,Ga)As/GaAs QDs results in a strong change of the dependence of photoluminescence (PL) polarization on a transverse magnetic field (Hanle curve). We identify resonances related to spin transitions of the gallium, indium, and arsenic nuclei which are influenced by magnetic field and quadrupole interaction. We suggest that the observed effect is a clear indication of a phasing of the nuclear spin states that corresponds to the creation of transverse NSP components precessing about the magnetic field.

Figure 12 shows the magnetic field dependence of the NCP amplitude measured for different excitation protocols. All curves show a decrease of NCP (the Hanle effect) with increasing magnetic field. For continuous-wave (cw) excitation with fixed polarization helicity the Hanle curve consists of a narrow central peak and broad shoulders, together forming the so-called W structure (Paget, 1977). The W structure clearly indicates NSP that has built up for these excitation conditions. When amplitude modulation (AM) with a low on-off time ratio is used, the Hanle curve has a Lorentzian shape. Switching on polarization modulation (PM) in addition to the amplitude modulation ("AM + PM" protocol in the inset of **Fig. 12**) does not change notably the Hanle curves, meaning that nuclear polarization does not develop under such excitation conditions and the Hanle curve is determined solely by electron spin dynamics. Therefore we call the curve measured in that way the electronic peak ("*e* peak").

The Hanle curve measured for polarization modulation only [curve (3) in Fig. 12] shows two additional maxima at approximately $B = \pm 10$ mT. The appearance of such additional maxima is the main topic of PIV. The position of these additional maxima, resonances, strongly depends on the polarization modulation frequencies (**Fig. 13**). The positions are shifted to higher fields with increasing modulation frequencies. The frequency shift of the shoulders indicates their resonant character.

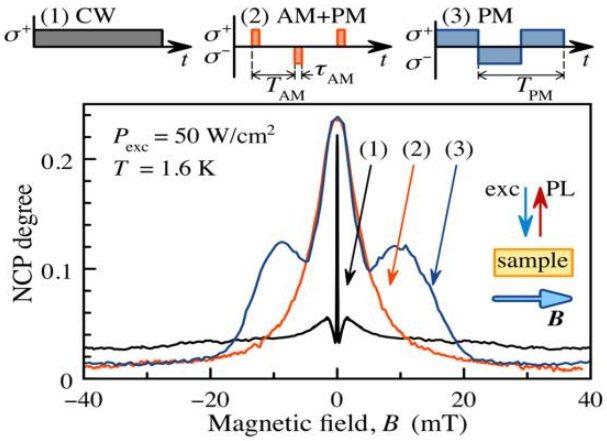

Fig. 12. Hanle curves measured for cw optical excitation [curve (1)], for modulated polarization of the excitation [$T_{PM} = 40$ μs, curve (3)], and for polarization and amplitude modulation of the excitation [$T_{AM} = 20$ μs, $\tau_{AM} = 5$ μs, curve (2)]. The top panels sketch these different timing protocols.

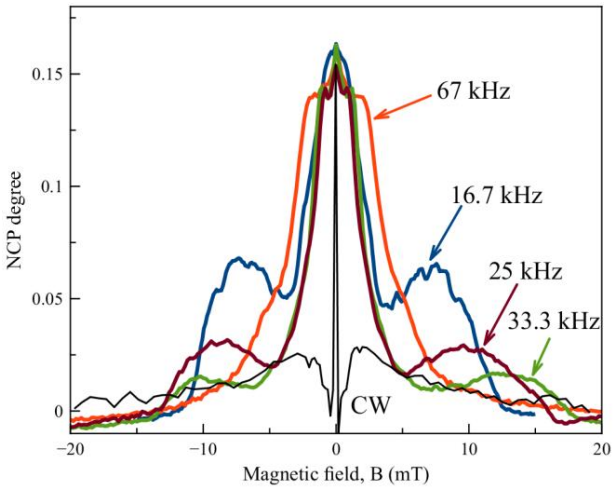

Fig. 13. Hanle curves measured for excitation polarization modulated at different frequencies.

Even stronger modification of the Hanle curves is observed when a radio-frequency (RF) field that is synchronous with the modulation of polarization is applied. The RF field generated with a magnetic component directed along the optical axis (**Fig. 14**).

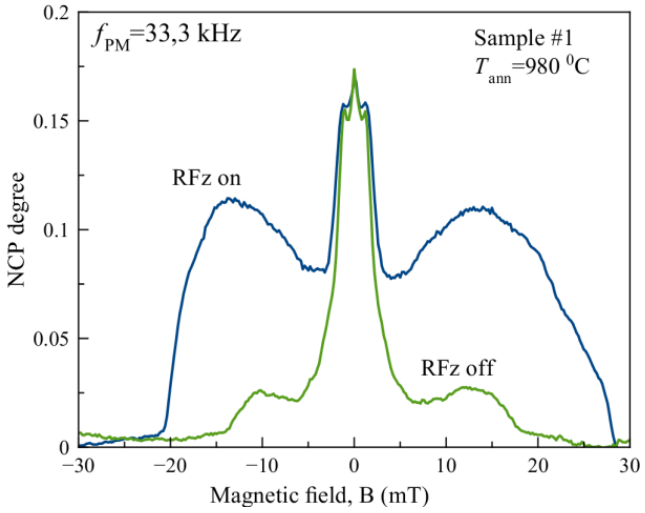

Fig. 14. The blue curve is measured with applying a Rfz-field. The green curve is measured with no RF-field.

To identify the resonances which contribute to the Hanle curves, we analyze the nuclear spin splitting in a transverse magnetic field (**Fig. 15**). The calculations are made taking into account the quadrupole splitting of nuclear spin states caused by the strain-induced gradient of the crystal field as well as by the statistical population of crystal sites by Ga and In atoms. The QDs under study contain several types of nuclei (including isotopes): ^{69}Ga, ^{71}Ga, ^{75}As, ^{113}In, and ^{115}In. The principle axis of the strain-induced gradient is directed along the growth axis (*z* axis).

We calculate the splitting of nuclear spin states by the magnetic field and the quadrupole interaction assuming a strain magnitude $\varepsilon_b = 0.01$ as estimated in Flisinskii, 2010 for sample annealed at T = 980 °C. Each resonance at a calculated energy is modeled by a Gaussian with amplitude and width as fit parameters. Our analysis shows that the Hanle curves measured at different modulation frequencies can be described well using the calculated resonance energies.

The analysis of a Hanle curve measured with RF-field application is shown in **Fig. 16**. To work out the resonances more clearly, we subtracted the *e* peak from the experimentally measured Hanle curve. The central part of the curve is given by the resonances $\langle +1/2| \leftrightarrow |-1/2\rangle$. The wide part of the Hanle curve can be well described by the resonances $\langle +3/2| \leftrightarrow |-3/2\rangle$ or the In and Ga nuclei, as well by the resonances $\langle +5/2| \leftrightarrow |-5/2\rangle$ for the In nuclei.

At higher modulation frequencies, additional maxima appear at the Hanle curves as it is shown in **Fig. 17**. According to the calculations of energy splitting of the nuclear spin states (see **Fig. 15**), these maxima can be attributed to "quadrupole" resonances

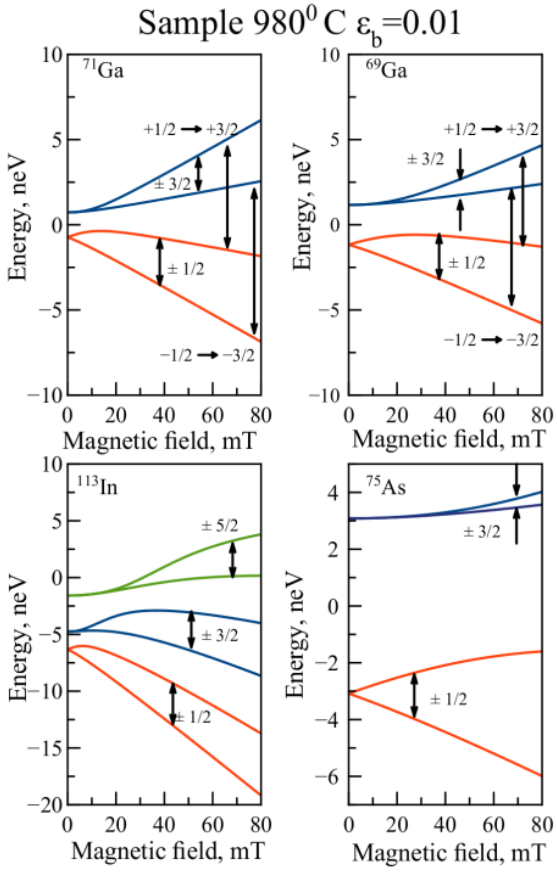

Fig. 15. Calculated energies of nuclear spin sub-levels for isotopes ^{71}Ga, ^{69}Ga, ^{113}In, and ^{75}As as functions of magnetic field.

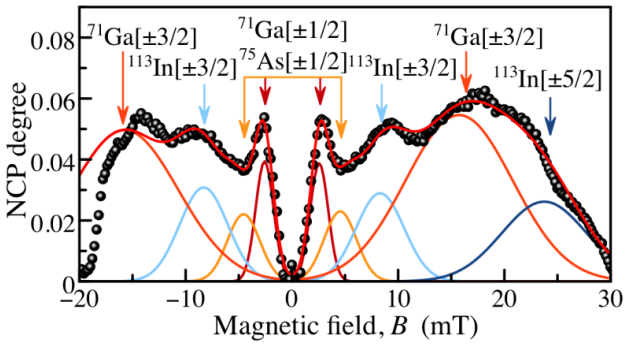

Fig. 16. Gaussian decomposition of Hanle curve measured at fPM = 67 kHz in presence of RFz field for the sample 980°C.

+1/2 ↔ +3/2 and –1/2 ↔ –3/2. As seen in **Fig. 17**, inclusion of these resonances into consideration allows one to adequately describe the experimentally measured Hanle curve.

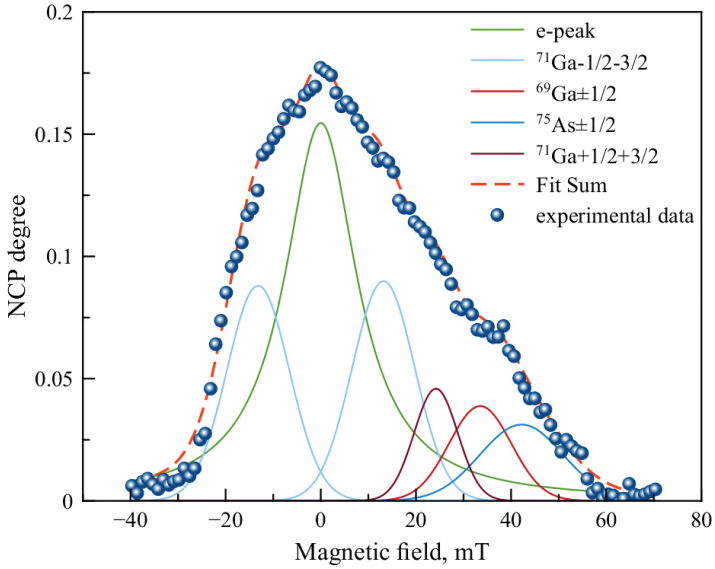

Fig. 17. Gaussian decomposition of Hanle curve measured at $f_{PM} = 600$ kHz in presence of RFz field for the sample 980°C. The colored Gaussians model resonances, whose positions are fit parameters.

The comparizon of the resonance positions obtained from the experiment with those obtained from the calculation of Zeeman splitting of nuclear spin states are shown in **Figs. 18, 19. Fig. 18** demonstrate the data for observed transitions $+1/2 \leftrightarrow -1/2, +3/2 \leftrightarrow -3/2$, and $+5/2 \leftrightarrow -5/2$.

Figure 19 demonstrates similar data for transitions +1/2 ↔ +3/2 and –1/2 ↔ –3/2. Resonant frequencies for these transitions are determined with less accuracy however

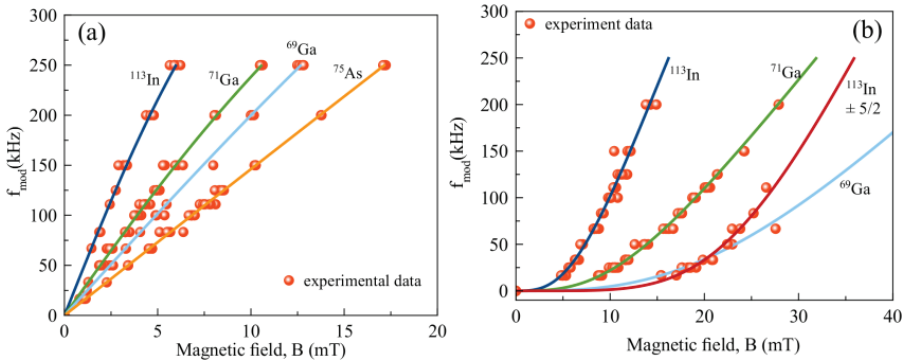

Fig. 18. Theoretically calculations of frequency dependence on magnetic field for nuclear spin states Ga, In, As and compare it with experimental data (a) for transitions and (b) for +3/2 ↔ –3/2, +5/2 ↔–5/2.

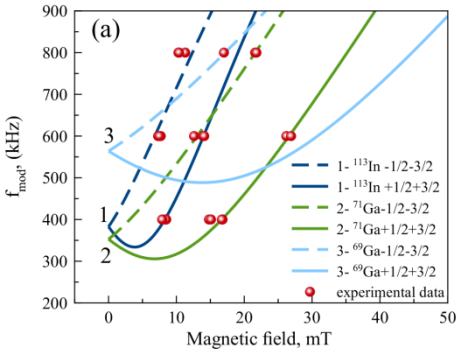

Fig. 19. Theoretically calculations of frequency dependence on magnetic field for nuclear spin states Ga, In and compare it with experimental data.

the Hanle curve cannot be adequately described with no consideration of these resonances.

We want to note here that the explanation of the Hanle curve peculiarities by peaks centered at certain resonance fields is not generally accepted, but rather the object of discussion. Further, the authors of Refs. Tartakovskii, 2007, Kalevich, 1980, Eickhoff, 2002 observed experimentally dispersion like peculiarities superimposed on a smooth Hanle curve.

We assume that the key point for understanding the origin of the resonances observed in our work is the appearance of a significant component of nuclear polarization in the plane perpendicular to the external magnetic field (transverse component).

The creation of a transverse component is a resonant process, as our experiments show. For excitation with constant polarization of light, polarized nuclear spins are created with arbitrary phases so that a transverse component is not created. Only resonant modulation of the optical polarization results in cophase pumping of a large number of nuclear spins, giving rise to resonant amplification of the transverse component of nuclear polarization.

In conclusion, we have observed a significant nuclear polarization in the plane perpendicular to the external magnetic field in semiconductor QDs. The polarization is created by circularly polarized optical pumping modulated at a frequency that is resonant to one of the nuclear spin transitions. The effect, which may be termed resonant optical pumping of nuclear spin polarization, is evidenced by several intense peaks in the Hanle curve. The number and amplitude of peaks increase for joint action of polarization modulation of optical excitation and synchronous RF-field application. In particular, the RF-field enhances resonances related to transitions between $|\pm 3/2\rangle$ nuclear states split off from the $|\pm 1/2\rangle$ states by a quadrupole interaction.

REFERENCES

Abragam, A. (1961). Principles of Nuclear Magnetism. Oxford University Press. ISBN 0 19 852014.

Artemova, E. S. and *Merkulov, I. A.* (1985). The theory of nuclear polarization in semiconductor by oriented electrons in a strong quadrupole splitting of the nuclear spin levels. Sov. Phys. Solid State 27 (4), 694. (in Russian)

Auer, T., Oulton, R., Bauschulte, A., Yakovlev, D. R., Bayer, M., Verbin, S. Yu., Cherbunin, R. V., Reuter, D., and Wieck, A. D. (2009). Measurement of the Knight field and local nuclear dipole-dipole field in an InGaAs/GaAs quantum dot ensemble. Physical Review B: Condensed matter 80, 205303. DOI: 10.1103/PhysRevB. 80.205303

Belhadj, T., Kuroda, T., Simon, C. -M., Amand, T., Mano, T., Sakoda, K., Koguchi, N., Marie, X., and Urbaszek, B. (2008). Optically monitored nuclear spin dynamics in individual GaAs quantum dots grown by droplet epitaxy. Physical Review B: Condensed matter 78, 205325. DOI: 10.1103/PhysRevB. 78.205325.

Braun, P. F., Marie, X., Lombez, L., Urbaszek, B., Amand, T., Renucci, P., Kalevich, V. K., Kavokin, K. V., Krebs, O., Voisin, P., and Masumoto, Y. (2005). Direct Observation of the Electron Spin Relaxation Induced by Nuclei in Quantum Dots. Physical Review Letters 94, 116601. DOI:~10.1103/PhysRevLett.94.116601.

Braun, P. -F. Urbaszek, B. Amand, T., Marie, X. Krebs, O., Eble, B., Lemaitre, A., and Voisin P. (2006). Bistability of the nuclear polarization created through optical pumping in $In_{1-x}Ga_xAs$ quantum dots. Physical Review B: Condensed matter 74, 245306 DOI: 10.1103/PhysRevB. 74.245306.

Brown, S. W., Kennedy, T. A., Gammon, D., and Snow, E. S. (1996). Spectrally resolved Overhauser shifts in single GaAs/$Al_xGa_{1-x}As$ As quantum dots. Physical Review B: Condensed matter 54, 17339 (R). DOI:~10.1103/PhysRevB. 54.R17339.

Chekhovich, E. A., Makhonin, M. N., Skiba-Szymanska, J., Krysa, A. B., Kulakovskii, V. D., Skolnick, M. S., and Tartakovskii, A. I. (2010). Dynamics of optically induced nuclear spin polarization in individual InP/$Ga_xIn_{1-x}P$ quantum dots. Physical Review B: Condensed matter 81, 24, 245308. DOI:10.1103/PhysRevB. 81.245308

Cherbunin, R. V., Verbin, S. Yu., Auer, T., Yakovlev, D. R., Reuter, D., Wieck, A. D., Gerlovin, I. Ya., Ignatiev, I. V., Vishnevsky, D. V. and Bayer, M. (2009). Dynamics of the nuclear spin polarization by optically oriented electrons in a (In,Ga)As/GaAs quantum dot ensemble. Physical Review B: Condensed matter 80, 035326. DOI: 10.1103/PhysRevB. 80.035326.

Cherbunin, R. V., Kuznetsova, M. S., Gerlovin, I. Ya., Ignatiev, I. V., Dolgich, Yu.K., Efimov, Yu.P., Eliseev, S. A., Petrov, V. V., Poltavsev, S. V., Larionov, A. V., Ill'in, A. I. (2009). Carrier spin dynamics in GaAs/AlGaAs quantum wells with a laterally localizing electric potential. Physics of Solid State 51 (4), pp. 837-840. DOI: 10.1134/S1063783409040349

Cherbunin, R. V., Verbin, S. Yu., Flisinski, K., Gerlovin, I. Ya., Ignatiev, I. V., Vishnevsky, D. V., Reuter, D., Wieck, A. D., Yakovlev, D. R., and Bayer, M. (2010). Time-resolved Hanle effect in (In,Ga)As/GaAs quantum dots. Journal of Physics: Conference Series 245, 012055. doi:10.1088/1742-6596/245/1/012055.

Cherbunin, R. V., Flisinski, K., Gerlovin, I. Ya., Ignatiev, I. V., Kuznetsova, M. S., Petrov, M. Yu., Yakovlev, D. R., Reuter, D. Wieck, A. D., and Bayer, M. (2011). Resonant nuclear spin pumping in (In,Ga)As quantum dots. Physical Review B: Condensed matter 84, 041304 (R). DOI: 10.1103/PhysRevB. 84.041304.

Cortez, S., Krebs, O., Laurent, S., Senes, M., Marie, X., Voisin, P., Ferreira, R., Bastard, G., Gërard, J-M., and Amand, T. (2002). Optically Driven Spin Memory in n-Doped InAs-GaAs Quantum Dots. Physical Review Letters 89, 207401. DOI: 10.1103/PhysRevLett.89.207401.

Crooker, S. A., Awschalom, D. D., Baumberg, J. J., Flack, F., and Samarth, N. (1997). Optical spin resonance and transverse spin relaxation in magnetic semiconductor quantum wells. Physical Review B: Condensed matter, 56, 7574. DOI: 10.1103/PhysRevB. 56.7574.

D'yakonov, M. I. and Perel', V. I. (1975). Cooling of a system of nuclear spins following optical orientation of electrons in semiconductors. Sov. Phys. Journal of Experimental and Theoretical Physics 41 (4), 759.

Dzhioev, R. I., Merkulov, I. A., Tkachuk, M. N., and Fleisher, V. G. (1982). Nonlinear effects in the electron-nuclear spin system of a semiconductor following absorption of light of variable circular polarization. Journal of Experimental and Theoretical Physics 56, 1304.

Dzhioev, R. I., Zakharchenya, B. P., Korenev, V. L., Pak, P. E., Vinokurov, D. A., Kovalenkov, O. V., and Tarasov, I. S. (1998). Optical orientation of donor-bound excitons in nanosized InP/InGaP islands. Physics of the Solid State 40 (9), 1587-1593.

Dzhioev, R. I., Korenev, V. L., Merkulov, I. A., Zakharchenya, B. P., Gammon, D., Efros, Al. L., and Katzer, D. S. (2002). Manipulation of the Spin Memory of Electrons in n-GaAs. Physical Review Letters, 88, 25 256801. DOI: 10.1103/PhysRevLett.88.256801

Dzhioev, R. I. and Korenev, V. L. (2007). Stabilization of the Electron-Nuclear Spin Orientation in Quantum Dots by the Nuclear Quadrupole Interaction Physical Review Letters 99,037401. DOI:~10.1103/PhysRevLett.99.037401.

Eickhoff, M., Lenzman, B., Flinn, G., and Suter, D. (2002). Coupling mechanisms for optically induced NMR in GaAs quantum wells. Physical Review B: Condensed matter 65, 125301 DOI: 10.1103/PhysRevB. 65.125301

Fleisher, V. G., Dzhioev, R. I., and Zakharchenya, B. P. (1976). Optical cooling of a nuclear spin system of a conductor in a weak oscillating magnetic field. Sov. Phys. Journal of Experimental and Theoretical Physics Lett. 23, 18.

Flisinski, K., Gerlovin, I. Ya., Ignatiev, I. V., Petrov, M. Yu., Verbin, S. Yu., Yakovlev, D. R., and Bayer, M. (2010). Dynamical nuclear polarization and nuclear magnetic resonance in a (In,Ga)As/GaAs quantum dot ensemble. Journal of Physics: Conference Series 245, 012056. doi:10.1088/1742-6596/245/1/012056

Flisinski, K., Gerlovin, I. Ya., Ignatiev, I. V., Petrov, M. Yu., Verbin, S. Yu., R. V., Yakovlev, D., Reuter, D., Wieck, A. D., and Bayer. M. (2010a). Optically detected magnetic resonance at the quadrupole-split nuclear states in (In,Ga)As/GaAs quantum dots. Physical Review B: Condensed matter 82, 081308(R). Doi: 10.1103/Phys.Rev. B82.081308.

Gammon, D. Snow, E. S., Shanabrook, B. V., Katzer, D. S., and Park, D. (1996).Fine Structure Splitting in the Optical Spectra of Single GaAs Quantum Dots. Physical Review Letters 76, 16 3005. DOI: 10.1103/PhysRevLett.76.3005

Gammon, D., Brown, S. W., Snow, E. S., Kennedy, T. A. Katzer, D. S., Park, D. (1997). Nuclear Spectroscopy in Single Quantum Dots: Nanoscopic Raman Scattering and Nuclear Magnetic Resonance. Science *277,* 85 *DOI: 10.1126/science.277.5322.85*

Gammon, D., Efros, Al. L., Kennedy, T. A., Rosen, M., Katzer, D. S., Park, D., Brown, S. W., Korenev, V. L., and Merkulov, I. A. (2001). Electron and Nuclear Spin Interactions in the Optical Spectra of Single GaAs Quantum Dots. Physical Review Letters 86, 5176. DOI:~10.1103/PhysRevLett.86.5176.

Gerlovin, I. Ya., Dolgikh, Yu.K., Eliseev, S. A., Ovsjankin, V. V., Efimov, Yu.P., Ignatiev, I. V., Petrov, V. V., Verbin, S. Yu., and Masumoto, Y. (2004). Spin dynamics of carriers in GaAs quantum wells in an external electric field. Physical Review B: Condensed matter, 69, 035329. DOI: 10.1103/PhysRevB. 69.035329.

Ignatiev, I. V., Verbin, S. Yu., Gerlovin, I. Ya., Cherbunin, R. V., and Masumoto, Y. (2009). Negative circular polarization of InP QD luminescence: Mechanism of formation and main regularities. Optics and Spectroscopy 106 (3), 375. DOI: 10.1134/ S0030400X09030114.

Ikezawa, M., Pal, B., Masumoto, Y., Ignatiev, I. V., Verbin, S. Yu., and Gerlovin, I. Ya. (2005). Submillisecond electron spin relaxation in InP quantum dots. Physical Review B: Condensed matter 72, 153302. DOI:~10.1103/PhysRevB. 72.153302.

Jeffries, C. (1963). Dynamic Nuclear Orientation Interscience,New York

Kalevich, V. K., Kulkov, V. D., and Fleisher, V. G. (1980) Optical cooling of the spin-lattice nuclei swstem of the semiconductor in a rotating coordinate system. Sov. Phys. Solid State 22, 1208. (In Russian)

Kalevich, V. K., Kul'kov, V. D. and Fleisher, V. G. (1982). Onset of a nuclear polarization front due to optical spin orientation in a semiconductor. Journal of Experimental and Theoretical Physics Letters. 35 (1), 20. ISSN: 0370-274X.

Kalevich, V. K., Kavokin, K. V., and Merkulov, I. A. (2008). Dynamic Nuclear Polarization and Nuclear Fields. In Spin Physics in Semiconductors, Ed. by M. I. Dyakonov, Chap. 11, p. 309. ISBN 978-3-540-78819-5/ISSN 0171-1873.

Kavokin, K. V. (2008). Spin relaxation of localized electrons in n-type semiconductors. Semiconductor Science and Technology. 23, 114009. doi:10.1088/0268-1242/23/11/114009.

Khaetskii, A. V. and Nasarov, Yu. V. (2000). Spin relaxation in semiconductor quantum dots. Physical Review B: Condensed matter, 61, 12639. DOI: 10.1103/PhysRevB. 61.12639.

Khaetskii, A. V., Loss, D., and Glazman, L. (2002). Electron Spin Decoherence in Quantum Dots due to Interaction with Nuclei. Physical Review Letters 88, 186802. DOI: 10.1103/PhysRevLett.88.186802.

Kikkawa, J. M. and Awschalom, D. D. (1998). Resonant Spin Amplification in n-Type GaAs Physical Review Letters 80, 4113. DOI: 10.1103/PhysRevLett.80.4313.

Kozlov, G. G. (2007). Exactly Solvable Spin Dynamics of an Electron Coupled to a Large Number of Nuclei; the Electron–Nuclear Spin Echoin a Quantum Dot. Journal of Experimental and Theoretical Physics 105, 803. DOI: 10.1134/S1063776107100159.

Krebs, O., Maletinsky, P., Amand, T., Urbaszek, B., Lemaitre, A., Voisin, P., Marie, X., and Imamoglu, A. (2010). Anomalous Hanle Effect due to Optically Created Transverse Overhauser Field in Single InAs/GaAs Quantum Dots. Physical Review Letters 104, 056603. DOI:10.1103/PhysRevLett.104.056603.

Kusraev, Yu. G., Artemova, E. S., Dzhioev, R. I., Zakharchenya, B. P., Merkulov, I. A., and Fleisher, V. G. (1982). Resonant optical cooling of the nuclear spin system is a semiconductor with anisotropic g factor. Sov. Phys. Solid State 24, 2705. (in Russian)

Kuznetsova, M. S., Flisinski, K., Gerlovin, I. Ya., Ignatiev, I. V., Kavokin, K. V., Verbin, S. Yu., Reuter, D., Wieck, A. D., Yakovlev, D. and Bayer, M. (2013) Hanle effect in (In,Ga)As quantum dots: Role of nuclear spin fluctuations. Physical Review B — Condensed Matter and Materials Physics, 87, 235320.DOI:10.1103/Phys.Rev.87.235320

Maletinsky, P., Badolato, A., and Imamoglu, A. (2007). Dynamics of Quantum Dot Nuclear Spin Polarization Controlled by a Single Electron. Physical Review Letters 99, 056804. DOI:~10.1103/PhysRevLett.99.056804.

Maletinsky, P., Lai, C. W., Badolato, A., and Imamoglu, A. (2007a). Nonlinear dynamics of quantum dot nuclear spins. Physical Review B: Condensed matter 75, 035409. DOI: 10.1103/PhysRevB. 75.035409.

Maletinsky, P., Kroner, M., and Imamoglu, A. (2009). Breakdown of the nuclear-spin-temperature approach in quantum-dot demagnetization experiments. Nature Physics 5, 407. doi:10.1038/nphys1273

Masumoto, Y., Toshiyuki, K., Suzuki, Ts., and Ikezawa, M. (2008). Resonant spin orientation at the exciton level anticrossing in InP quantum dots. Physical Review B: Condensed matter 77, 115331. DOI:~10.1103/PhysRevB. 77.115331.Ed. by Meier, F. and Zakharchenya, B. P. (1984) Optical Orientation, North_Holland, Amsterdam.

Merkulov, I. A. and Tkachuk, M. N. (1982). Resonant cooling of the spin system of a superconductor lattice nuclei following optical orientation of the electrons. Journal of Experimental and Theoretical Physics 56, 342.

Merkulov, I. A., Efros, Al. L., and Rosen, M. (2002). Electron spin relaxation by nuclei in semiconductor quantum dots. Physical Review B: Condensed matter 65, 205309. DOI:10.1103/PhysRevB. 65.205309.

Merkulov, I. A., Alvarez, G., Yakovlev, D. R., and Schulthess, T. C. (2010). Long-term dynamics of the electron-nuclear spin system of a semiconductor quantum dot. Physical Review B: Condensed matter 81, 115107. DOI:~10.1103/PhysRevB. 81.115107.

Nikolyuk, V. A. and Ignatiev, I. V. (2007). The Energy Structure of Quantum Dots Induced in Quantum Wells by a Nonuniform Electric Field. Semiconductors, 41 (12), 1422. DOI: ~10.1134/S1063782607120081.

Oulton, R., Greilich, A., Verbin, S. Yu., Cherbunin, R. V., Auer, T., Yakovlev, D. R., Bayer, M., Merkulov, I. A., Stavarache, V., Reuter, D., and Wieck, A. D. (2007). Subsecond Spin Relaxation Times in Quantum Dots at Zero Applied Magnetic Field Due to a Strong Electron-Nuclear Interaction.Physical Review Letters 98, 107401. DOI:~10.1103/PhysRevLett.98.107401.

Paget, D., Lampel, G., Sapoval, B., and Safarov, V. I. (1977). Low field electron-nuclear spin coupling in gallium arsenide under optical pumping conditions. Physical Review B: Condensed matter 15, 5780. DOI: 10.1103/PhysRevB. 15.5780.

Paget, D. (1981). Optical detection of NMR in high-purity GaAs under optical pumping: Efficient spin-exchange averaging between electronic states. Physical Review B: Condensed matter 24, 3776. DOI: 10.1103/PhysRevB. 24.3776.

Pal, B. and Masumoto, Y. (2009). Spin relaxation in charge-tunable InP quantum dots. Physical Review B: Condensed matter 80, 125334. DOI: 10.1103/PhysRevB. 80.125334.

Petrov, M. Yu., Ignatiev, I. V., Poltavtsev, S. V., Greilich, A., Bauschulte, A., Yakovlev, D. R., and Bayer, M. (2008). Effect of thermal annealing on the hyperfine interaction in InAs/GaAs quantum dots. Physical Review B: Condensed matter 78, 045315. DOI: 10.1103/PhysRevB. 78.045315.

Petrov, M. Yu., Kozlov, G. G., Ignatiev, I. V., Cherbunin, R. V., Yakovlev, D. R., and Bayer, M. (2009). Coupled electron-nuclear spin dynamics in quantum dots: A graded box model approach. Physical Review B: Condensed matter 80, 125318. DOI: 10.1103/PhysRevB. 80.125318.

Rudner, M. S. and Levitov, L. S. (2007). Self-Polarization and Dynamical Cooling of Nuclear Spins in Double Quantum Dots. Physical Review Letters 99, 036602 DOI: 10.1103/PhysRevLett.99.036602.

Rudner, M. S., Koppens, F. H. L., Folk, J. A., Vandersypen, L. M. K., and Levitov, L. S. (2011). Nuclear spin dynamics in double quantum dots: Fixed points, transients, and intermittency. Physical Review B: Condensed matter 84, 075339. DOI: 10.1103/PhysRevB. 84.075339.

Shabaev, A., Stina, E. A., Bracker, A. S., Gammon, D., Efros, A. L., Korenev, V. L., and Merkulov, I. (2009). Optical pumping and negative luminescence polarization in

charged GaAs quantum dots. Physical Review B: Condensed matter 79, 035322. DOI: 10.1103/PhysRevB. 79.035322.

Tartakovskii, A. I., Wright, T., Russell, A., Fal'ko, V. I., Van'kov, A. ~B., Skiba_Szymanska, J., Drouzas, I., Kolodka, R. S., Skolnick, M. S., Fry, P. W., Tahraoui, A., Liu, H. Y., and Hopkinson, M. (2007). Nuclear Spin Switch in Semiconductor Quantum Dots. Physical Review Letters 98,026806. DOI: 10.1103/PhysRevLett.98.026806.

Urbaszek, B., Marie, X., Amand, T., Krebs, O., Voisin, P., Malentinsky, P., H¨ogele, A., and Imamoglu, A. (2013). Nuclear spin physics in quantum dots: An optical investigation. Review of Modern Physics85, 79. DOI:10.1103/RevModPhys.85.79

Verbin, S. Yu., Gerlovin, I. Ya., Ignatiev, I. V., Kuznetsova, M. S., Cherbunin, R. V., Flisinski, K., Yakovlev, D., Bayer. M. (2012). Dynamics of Nuclear Polarization in InGaAs Quantum Dots in a Transverse Magnetic Field. Journal of Experimental and Theoretical Physics, 114, 4, 681-690. DOI: 10.1134/S1063776112040176.

Yugova, I. A., Greilich, A., Yakovlev, D. R., Kiselev,A. A., Bayer, M., Petrov, V. V., Dolgich, Yu. K., Peuter, D., and Wieck, A. D. (2007) Universal behavior of the electron g factor in GaAs/$Al_xGa_{1-x}As$ quantum wells. Physical Review B: Condensed matter, 75, 245302. DOI: 10.1103/PhysRevB. 75.245302.

INCLUDED ARTICLES

PI

CARRIER SPIN DYNAMICS IN GAAS/ALGAAS QUANTUM WELLS WITH A LATERALLY LOCALIZING ELECTRIC POTENTIAL

R. V. Cherbunin, M. S. Kuznetsova, I. Ya. Gerlovin, I. V. Ignatiev, Yu. K. Dolgich, Yu. P. Efimov, S. A. Eliseev, V. V. Petrov, S. V. Poltavsev, A. V. Larionov, A. I. Ill'in

Published in: *Physics of Solid State*, 2009, 51 (4), 837–840

ISSN 1063-7834, Physics of the Solid State, 2009, Vol. 51, No. 4, pp. 837–840. © Pleiades Publishing, Ltd., 2009.
Original Russian Text © R.V. Cherbunin, M.S. Kuznetsova, I.Ya. Gerlovin, I.V. Ignatiev, Yu.K. Dolgikh, Yu.P. Efimov, S.A. Eliseev, V.V. Petrov, S.V. Poltavtsev, A.V. Larionov, A.I. Il'in, 2009, published in Fizika Tverdogo Tela, 2009, Vol. 51, No. 4, pp. 791–794.

LOW-DIMENSIONAL SYSTEMS AND SURFACE PHYSICS

Carrier Spin Dynamics in GaAs/AlGaAs Quantum Wells with a Laterally Localizing Electric Potential

R. V. Cherbunin[a], M. S. Kuznetsova[a], I. Ya. Gerlovin[a], I. V. Ignatiev[a,*], Yu. K. Dolgikh[a], Yu. P. Efimov[a], S. A. Eliseev[a], V. V. Petrov[a], S. V. Poltavtsev[a], A. V. Larionov[b], and A. I. Il'in[c]

[a] *St. Petersburg State University, Ul'yanovskaya ul. 3, Staryĭ Peterhof, St. Petersburg, 198504 Russia*
** e-mail: ivan_ignatiev@mail.ru*

[b] *Institute of Solid State Physics, Russian Academy of Sciences, Institutskaya ul. 2, Chernogolovka, Moscow Region, 142432 Russia*

[c] *Institute of Microelectronics Technology Problems and High Purity Materials, Russian Academy of Sciences, Institutskaya ul. 6, Chernogolovka, Moscow Region, 142432 Russia*

Received September 4, 2008

Abstract—The spin orientation dynamics in a GaAs quantum well with a laterally nonuniform electric potential generated by a mosaic electrode deposited on the surface of the sample has been investigated using the photoinduced magneto-optical Kerr effect. It has been found that the application of a negative potential higher than 1 V to the electrode leads to more than a hundredfold increase in the spin polarization lifetime in the sample under study. It is concluded that so strong slowing down of the relaxation is caused by a combined action of two effects, namely, the spatial separation of electron and hole, which reduces the radiative recombination rate of electron–hole pair, and the localization of electron, which is accompanied by the suppression of spin relaxation processes caused by electron motion.

PACS numbers: 73.21.Fg, 78.67.De

DOI: 10.1134/S1063783409040349

1. INTRODUCTION

The growing interest in the spin dynamics of carriers in semiconductor quantum dots witnessed presently is largely prompted by prospects of using these structures in development of long-lived spin memory. Spatial localization of carriers capable of suppressing the main mechanisms of spin relaxation would increase the electron spin lifetime in a quantum dot to hundreds of microseconds, and, possibly, even to milliseconds [1]. The main drawbacks of the quantum dots prepared by self-organization lie in the scatter of dot parameters in the ensemble and the high density of defects at interfaces which originates from the fairly large lattice mismatch between the quantum dot material and the barrier layer. It is the scatter in the quantum dot properties which makes it impossible to maintain all dots in the same charge state, which is necessary for realization of spin memory. The presence of defects, including those of paramagnetic nature, results in shortening of the electron spin lifetime, thus restricting the possibility of long-time information storage.

We report here on a study of the spin dynamics of carriers introduced into an array of specific potential quantum dots produced by application of an electric bias to an electrode deposited on the surface of the structure, which contains a system of nanoholes. The regular pattern of the nanohole size and positions precludes scatter in the parameters of the quantum dot ensemble created in this way. An essential merit of such field-induced quantum dots is also a practically complete absence of interface defects, which suppresses one of the most serious spin relaxation channels. Viewed from the standpoint of their potential application, such quantum dots have an additional merit in that they would permit, in principle, addressing any dot separately with the use of special electrodes, a feature that cannot be realized in self-organized quantum dots because of their random arrangement.

2. OBJECT OF INVESTIGATION AND EXPERIMENTAL TECHNIQUE

The object of this study was a sample containing a doped GaAs : Si layer and a GaAs quantum well about 9 nm thick confined between $Al_{0.25}Ga_{0.75}As$ barriers. A gold electrode with submicron nanoholes (the mosaic electrode) was deposited on the top surface of the heterostructure. The mosaic electrode was fabricated with the use of a JSEM-850 electron microscope equipped with a Nanomaker device for electronic lithography. The electrode combined several chips measuring 150×150 μm each, with the nanoholes 500 or 100 nm in diameter. The sample thus prepared was placed in a closed-cycle optical helium cryostat which provided cooling to a temperature of 8 K. An electric bias variable from +1 to –5 V was applied between the electrode

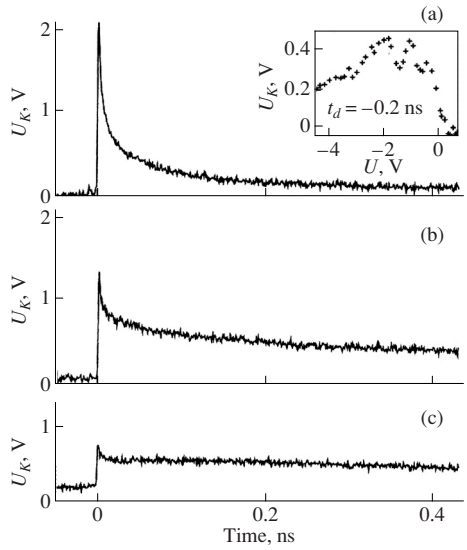

Fig. 1. Dependences of the shape of the Kerr rotation signal U_K on the bias voltage applied to the mosaic electrode. U = (a) 0.7, (b) 0.1, and (c) –2.0 V. The inset shows the dependence of the signal on the bias applied to the electrode under the same conditions at negative delays. The falloff of the signal at negative biases in excess of 2 V is most probably associated with the current flow through the sample.

and the doping layer. The cryostat with the sample was fixed between the electromagnet coils capable of generating a comparatively weak (–0.01 to +0.01 T) magnetic field.

The spin orientation dynamics in a sample was measured in the pump–probe regime detecting the signal of photoinduced (Kerr) rotation of the light polarization plane [2]. The radiation source was a titanium–sapphire laser, which produced 150-fs-long light pulses with a repetition frequency of 80 MHz. A circularly polarized pump pulse created spin orientation, which could be determined from the angle of polarization plane rotation of the linearly polarized probe beam reflected from the sample. The measurements were performed in a spectrally nondegenerated regime in which the wavelengths of the pump and probe light beams could be varied independently. A monochromator was used to vary the wavelength and spectral width of the pump beam, and the spectrum of the probe light beam was controlled by an interference filter with a transmission bandwidth of 2 nm. The signal was detected by the double locked-in technique permitting efficient suppression of the background signal generated by the pump light reflected from the mosaic electrode.

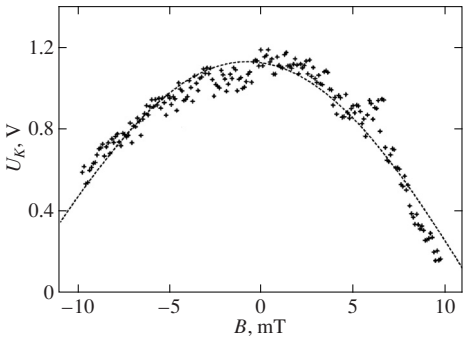

Fig. 2. Persistent Kerr effect plotted vs. transverse magnetic field. Symbols are experimental data, and the curve is the fit with function (1) for parameter $g_e = 0.12$.

3. EXPERIMENTAL RESULTS AND DISCUSSION

Figure 1 illustrates the dynamics of spin polarization at different bias voltages applied to the mosaic electrode. The measurements were performed on the part of the electrode with nanoholes 1000 nm in diameter. The dependence of Kerr rotation signal amplitude on the time delay between the probe and pump pulses has been measured. The experiments showed that, at positive bias voltages above +0.7 V, the signal on the mosaic electrode reproduces the shape of that from the free sample surface while being only one half of it in amplitude. Shifting toward negative biases is accompanied by increasing signal decay time causing a noticeable signal in the negative time delay region. The increase in the signal amplitude at negative delays is clearly seen in the inset in Fig. 1. The presence of signals at negative biases implies that the spin polarization lifetime in these conditions is comparable with the laser pulse repetition period ($T_p \approx 12.5$ ns). By assuming an exponential decay law, τ_s can be estimated from experimental data using the simple relation $\tau_s = T_p/\ln(A_0/A_-)$, where A_- and A_0 are signal amplitudes at negative and zero delays, respectively. The ratio $A_0/A_- \approx 2.4$ derived from experimental data corresponds to a relaxation time on the order of 15 ns.

That the signal at negative delays is indeed related with a long lifetime of the electronic spin is confirmed by a study of the behavior of this signal in a transverse magnetic field (Fig. 2). Electron spin precession in a transverse magnetic field gives rise to a decrease in the degree of polarization at negative time delays. In the simplest case, the field dependence of the signal should follow the relation [3]

$$\rho = \rho_0 \exp[-(\Delta t + T)/\tau_s]\cos[g_e \mu_B B(\Delta t + T)/\hbar], \quad (1)$$

where Δt is the time delay, T is the laser pulse repetition period, τ_s is the electron spin relaxation time, g_e is the

electron g-factor, μ_B is the Bohr magneton, and B is the magnetic field strength.

As is evident from Fig. 2, the field dependence of the amplitude of the long-lived signal component is fitted well with the above function, with the value of g_e close to that determined in [4] for quantum wells of similar thickness. The data obtained imply that the nonuniform electric field generated by the mosaic electrode distinctly modifies carrier spin dynamics in a planar quantum well.

Theoretical calculations [5] suggest that application of a negative electric bias to a mosaic electrode should result in generation of a nonuniform lateral potential distribution in the quantum well which will localize electrons under the nanoholes, i.e., actually in the formation of quantum dots for electrons. As follows from these calculations, the depth of a potential well for electrons may be as large as 100 mV for a realistic field between electrodes of 100 kV/cm. At a temperature of 8 K, this potential is high enough for reliable localization of electrons.

The electric potential for a positively charged hole is of the opposite sign, so that negative bias should repel the hole out of the region located above the nanohole in the electrode. This will result in a substantial decrease in the wave function overlap between the electron and the hole, which means that the exciton excited by laser light will turn out spatially indirect.

The Kerr rotation signal can originate, in principle, both from a photoexcited electron–hole pair (the exciton) and from light-oriented free electrons moved to the quantum well from the doped layer. At large negative biases, however, all free electrons are swept out of the quantum well and, thus, cannot contribute to the signal detected. Under these conditions, polarization anisotropy is determined only by the spin orientation of photoexcited carriers. The spatial separation of the electron and the hole induced by nonuniform electric field should modify substantially the exciton spin dynamics.

Indeed, the sharp decrease in the wave function overlap should be accompanied by a practically complete suppression of exchange interaction between the electron and the hole, with the result that the hole spin will rapidly relax, while the electron spin can retain its orientation for a long enough time. Significantly, not only spin relaxation but also electron–hole recombination will contribute to the polarization decay. In these conditions, the signal decay rate is governed by the sum of the rates of all relaxation processes, and the measured time should be shorter than the time of the fastest process of all.

As follows from the relevant literature [6], the exciton radiative recombination time in GaAs quantum wells of a similar thickness amounts to a few tenths of a nanosecond. The signal decay time measured by us with a negatively biased mosaic electrode exceeds by more than two orders of magnitude these values. One should, however, bear in mind that the aforementioned

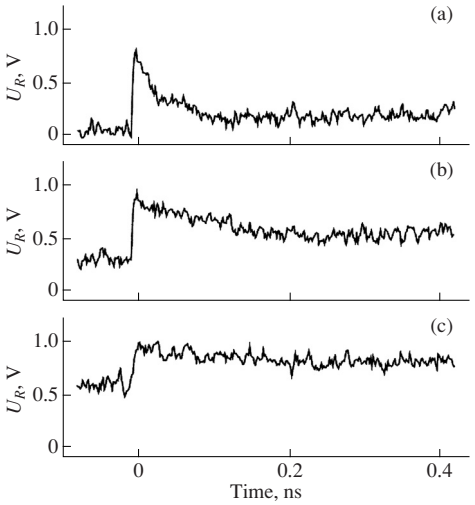

Fig. 3. Evolution of the pump-probe signal amplitude U_R for bias voltages U = (a) 0.7, (b) 0.1, and (c) –2.0 V.

decrease in wave function overlap between the electron and the hole should be accompanied by a corresponding decrease in the exciton radiative recombination rate. We come to a logical conclusion that the long-lived rotation signal originates primarily from the light-oriented spin of the electron in the photoexcited exciton whose recombination time increased strongly under application of a negative bias.

To check this assumption, we studied experimentally the dynamics of exciton state occupation in the quantum well under consideration as a function of bias voltage. The measurements were performed in the standard pump–probe regime, in which one measures the variation of the amplitude of the reflected probe beam as a function of the time delay between the pump and the probe pulses. The results of these measurements are depicted in Fig. 3. As is seen from the figure, the signal decay time, i.e., the exciton recombination time, does indeed depend strongly on bias voltage. At a positive bias of 0.7 V, which practically compensates the Schottky barrier formed at the contact with the gold electrode, the quantum well is at a zero potential. Under these conditions, absorption of a photon is accompanied by generation of a free exciton whose radiative recombination time is in this case of about 50 ps (Fig. 3c). The exciton spin affected by the anisotropic component of the electron–hole exchange interaction undergoes additional relaxation [6], so that the rotation signal decays even faster (Fig. 1).

Under negative bias, the pump–probe signal decay time grows strongly. As is seen from Fig. 3a, in the negative delay domain, the signal ranks in amplitude only

slightly below that at positive delays. The amplitude ratio for negative to zero delays is about 0.7, which corresponds to the signal decay time $\tau_r \approx 35$ ns. Thus, application of a negative bias to the mosaic electrode does indeed increase the electron–hole separation, decreasing in this way radically the probability of radiative recombination.

By comparing the data shown in Figs. 1 and 3, one can estimate the relaxation time of the electron spin τ_e, , because, as already pointed out, $1/\tau_s = 1/\tau_r + 1/\tau_e$. The estimate obtained for a bias of –2 V is $\tau_e \approx 25$ ns. It should be stressed that this is a rough estimate, because it was derived assuming an exponential character of signal decay, which, strictly speaking, is not observed in experiment. Nevertheless, this value of τ_e exceeds substantially the spin relaxation times of the electron in GaAs quantum wells of a similar thickness quoted in literature (see, e.g., [6]), which suggests that lateral electron localization of this type could be a promising approach to increasing the spin memory of electrons.

4. CONCLUSIONS

Our studies have demonstrated a possibility of using mosaic electrodes to noticeably increase the electron spin lifetime in GaAs quantum wells. We assume that this increase results from a combined action of two effects associated with electron localization under a nanohole in the electrode, more specifically of breakdown of the exchange bonding with the hole, whose spin accelerates relaxation of the electron spin, and suppression of the relaxation processes caused by electron motion.

ACKNOWLEDGMENTS

This study was supported by the Russian Foundation for Basic Research (project no. 07-02-00979a).

REFERENCES

1. A. V. Khaetskii and Yu. V. Nazarov, Phys. Rev. B: Condens. Matter **61**, 12639 (2000).
2. S. A. Crooker, D. D. Awschalom, J. J. Baumberg, F. Flack, and N. Samarth, Phys. Rev. B: Condens. Matter **56**, 7574 (1997).
3. J. M. Kikkawa and D. D. Awschalom, Phys. Rev. Lett. **80**, 4313 (1998).
4. A. Yugova, A. Greilich, D. R. Yakovlev, A. A. Kiselev, M. Bayer, V. V. Petrov, Yu. K. Dolgikh, D. Reuter, and A. D. Wieck, Phys. Rev. B: Condens. Matter **75**, 245302 (2007).
5. V. A. Nikolyuk and I. V. Ignatiev, Fiz. Tekh. Poluprovodn. (St. Petersburg) **41** (12), 1443 (2007) [Semiconductors **41** (12), 1422 (2007)].
6. I. Ya. Gerlovin, Yu. K. Dolhikh, S. A. Eliseev, V. V. Ovsyankin, Yu. P. Efimov, I. V. Ignatiev, V. V. Petrov, S. Yu. Verbin, and Y. Masumoto, Phys. Rev. B: Condens. Matter **69**, 035329 (2004).

Translated by G. Skrebtsov

PII

DYNAMICS OF NUCLEAR POLARIZATION IN INGAAS QUANTUM DOTS IN A TRANSVERSE MAGNETIC FIELD

S. Yu. Verbin, I. Ya. Gerlovin, I. V. Ignatiev, M. S. Kuznetsova, R. V. Cherbunin, K. Flisinski, D. Yakovlev, M. Bayer

Published in: *Journal of Experimental and Theoretical Physics*, 2012, 114 (4), 681–690

ISSN 1063-7761, Journal of Experimental and Theoretical Physics, 2012, Vol. 114, No. 4, pp. 681–690. © Pleiades Publishing, Inc., 2012.
Original Russian Text © S.Yu. Verbin, I.Ya. Gerlovin, I.V. Ignatiev, M.S. Kuznetsova, R.V. Cherbunin, K. Flisinski, D.R. Yakovlev, M. Bayer, 2012, published in Zhurnal Eksperimental'noi i Teoreticheskoi Fiziki, 2012, Vol. 141, No. 4, pp. 778–789.

ELECTRONIC PROPERTIES OF SOLID

Dynamics of Nuclear Polarization in InGaAs Quantum Dots in a Transverse Magnetic Field

S. Yu. Verbin[a,b,*], I. Ya. Gerlovin[a], I. V. Ignatiev[a,b,], M. S. Kuznetsova[a,b], R. V. Cherbunin[a,b], K. Flisinski[b], D. R. Yakovlev[b,c], and M. Bayer[b,***]**

[a] *Spin Optics Laboratory, St. Petersburg State University, St. Petersburg, 198504 Russia*
[b] *Technische Universität Dortmund, 44227 Dortmund, Germany*
[c] *Ioffe Physicotechnical Institute, Russian Academy of Sciences, St. Petersburg, 194021 Russia*
**e-mail: syuv54@mail.ru*
***e-mail: ivan_ignatiev@mail.ru*

Received July 24, 2011

Abstract—The time-resolved Hanle effect is examined for negatively charged InGaAs/GaAs quantum dots. Experimental data are analyzed by using an original approach to separate behavior of the longitudinal and transverse components of nuclear polarization. This made it possible to determine the rise and decay times of each component of nuclear polarization and their dependence on transverse magnetic field strength. The rise and decay times of the longitudinal component of nuclear polarization (parallel to the applied field) were found to be almost equal (approximately 5 ms). An analysis of the transverse component of nuclear polarization shows that the corresponding rise and decay times differ widely and strongly depend on magnetic field strength, increasing from a few to tens of milliseconds with an applied field between 20 and 100 mT. Current phenomenological models fail to explain the observed behavior of nuclear polarization. To find an explanation, an adequate theory of spin dynamics should be developed for the nuclear spin system of a quantum dot under conditions of strong quadrupole splitting.

DOI: 10.1134/S1063776112040176

1. INTRODUCTION

Nuclear spin orientation, or dynamic nuclear polarization (DNP), in solids has been extensively investigated since the middle of the past century [1]. The dominant DNP mechanism in semiconductors is the angular momentum transfer from optically oriented electrons to nuclei via electron–nucleus hyperfine interaction [2]. This process is particularly effective in quantum-dot heterostructures, where the electron wavefunction covers a limited number of nuclei, and electron and nuclear spins make up a strongly coupled system. Since spin-polarized nuclei, in turn, generate an effective magnetic field acting on electrons (Overhauser field), the state of the nuclear system can be examined by optical spectroscopic methods. Nuclear spin dynamics in semiconductors was extensively investigated during the last three decades [2, 3]. In bulk semiconductors and quantum wells, nuclear spin relaxation times were found to be a few seconds or longer [4]. First measurements, reported in recent years, have shown that nuclear spin relaxation in quantum dots is much faster. In particular, nuclear spin relaxation in a magnetic field applied parallel to the optical axis (longitudinal field) was found to occur over times on the order of milliseconds [5–8].

Dynamic nuclear polarization in quantum dots in a magnetic field perpendicular to the optical axis (in Voigt geometry) has not been studied until recently. An applied transverse magnetic field reduces the degree of circular polarization of luminescence from semiconductors (Hanle effect) because of the photoinduced precession of electron (or exciton) spins in the field. The effective field generated by spin-polarized nuclei can drastically change the shape of the Hanle curve [2, 9, 10]. This provides an opportunity to examine the dynamics of nuclear polarization experimentally by performing time-resolved measurements of the Hanle effect.

The first observations of the time-resolved Hanle effect in an ensemble of negatively charged InGaAs/GaAs quantum dots [11] demonstrated that experiments of this kind would provide an effective tool for examining dynamics of a nuclear spin system. In this paper, systematic experimental data presented and analyzed to estimate the nuclear polarization buildup and decay times for the structure under study. In our experiments, we used intensity-modulated optical pumping with various dark and excitation times, t_d and t_{exc}.

The Hanle curves obtained under strong pumping for the sample under study are largely similar in shape to those observed previously for donor-bound elec-

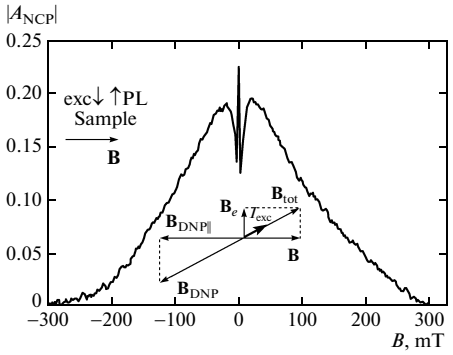

Fig. 1. Degree of luminescence polarization vs. transverse magnetic field (Hanle curve) under CW pumping with excitation intensity $I_{exc} = 40$ W/cm^2. The inserts on the left and at the bottom schematize, respectively, the experimental geometry and the formation of the effective nuclear field $\mathbf{B}_{DNP}$ acting on the electron spin (see text for details); PL = photoluminescence.

trons, in qualitative agreement with predictions of a classical model of DNP in a transverse magnetic field [2, 3]. However, the classical model fails to explain an increase in Hanle curve width with optical pumping intensity observed in our experiments. Following [11, 12], we suppose that the Hanle curve broadening is due to nuclear polarization stabilized by quadrupole splitting of nuclear spin states. An analysis of time-resolved measurement data provides quantitative estimates of the rise and decay times for longitudinal and transverse nuclear fields in the structures under study.

2. EXPERIMENTAL DETAILS

We examined a heterostructure containing 20 layers of self-assembled InGaAs/GaAs quantum dots separated by *n*-doped GaAs barriers. The doping level was adjusted to have an average of one electron per dot. The interaction time between such electrons and nuclei is not limited by their recombination time with photogenerated holes, which should facilitate creating a significant nuclear polarization. The structure was annealed at 900°C to partially reduce stresses in the quantum dots via mutual diffusion of Ga and In atoms. We measured the degree of circular polarization of photoluminescence as a function of magnetic field (Hanle curve).

Luminescence was excited with a continuous-wave Ti:Sapphire laser at frequencies corresponding to optical transitions in the wetting layer. To study dynamics of nuclear polarization, we used a square-wave intensity-modulated beam of constant circular polarization. Laser intensity was modulated with an acousto-optic modulator to produce pulses with various excitation and dark times. The radiation emitted by the sample was passed through a monochromator and detected at the quantum-dot photoluminescence band maximum by means of a single-photon counting avalanche photodiode.

Degree of polarization was measured by using a standard technique where light is passed through a photoelastic modulator and a polarization analyzer. The modulator creates a sinusoidally varying phase shift between linearly polarized beam components, $\Delta\varphi = (\pi/4)\sin(2\pi ft)$ with $f = 50$ kHz, thus converting each circularly polarized (σ^+ and σ^-) component of luminescence into linearly polarized (x and y) components. The pulses generated by the photodiode were accumulated by one of two methods. In one of these, a two-channel photon counter was used to measure the luminescence intensity detected by each channel within narrow time gates of 2.5 μs around the extrema of $\Delta\varphi$. In the other, a FAST ComTec multiscaler card (time-of-flight analyzer) was used to record the time-dependent luminescence detected after a pump pulse had arrived. Since the gate width was usually set to 1 μs, the signal produced by the photoelastic modulator and analyzer was a sine wave superimposed on a constant background. The signal was processed to compute time-dependent circular polarization of luminescence.

The quantum dots were negatively polarized; i.e., luminescence was predominantly σ^- polarized when excited by a σ^+-polarized beam [6]. The mechanism responsible for negative circular polarization (NCP) has been widely discussed in the literature [13–15]. NCP was shown to result from optically induced spin orientation of the resident electron. The amplitude of circular polarization is proportional to the projection of electron spin on the optical axis (z axis) averaged over an ensemble of quantum dots [15]:

$$A_{NCP} \propto 2\langle S_z \rangle. \quad (1)$$

This implies that the absolute value of the amplitude can be used to quantify the degree of electron spin orientation. The key factor that determines the orientation of an electron spin in a quantum dot is its hyperfine interaction with nuclear spins [2]. Therefore, analysis of electron spin dynamics can provide information about nuclear spin orientation.

The Hanle curve measured under continuous-wave (CW) pumping is W shaped with a narrow central peak (Fig. 1), indicating the occurrence of DNP [2, 9]. When the excitation pulse is sufficiently long ($t_{exc} >$ 50 ms), the shape of the Hanle curve is almost identical to that observed under CW pumping. In other words, the state of the electron–nuclear system at the end of pumping is independent of its previous dynam-

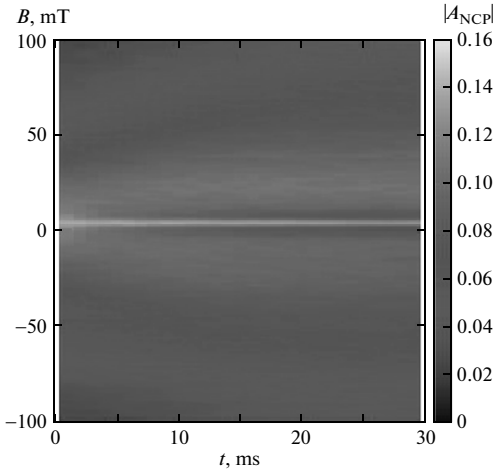

Fig. 2. Degree of polarization measured as a function of magnetic field B and time after the start of pumping (the grayscale bar on the right indicates $|A_{NCP}|$ intensity).

ics (in particular, the dark time between pulses). The shape of the Hanle curve changes with modulation parameters.

3. EXPERIMENTAL RESULTS

To examine nuclear polarization buildup, we used the multichannel photon counting system described above to measure NCP as a function of time after a pump pulse had arrived. Figure 2 demonstrates the change in shape of the Hanle curve with time elapsed after the start of pumping. Immediately after the start of pumping, the Hanle curve is smooth and narrow. The curve widens with time elapsed, and dips appear around the central peak; i.e., a W profile develops. Both W-profile width and dip depth reach maximum values under CW pumping.

Nuclear spin relaxation was examined by detecting luminescence during a short interval $t_{det} = 1$ ms at the start of pumping after various dark times. Pumping was supposed to have a weak effect on nuclear polarization during the detection time. The degree of polarization was measured as a function of dark time by varying t_d from 20 μs to 50 ms. Figure 3a shows the Hanle curves obtained for several dark times, and Fig. 3b shows their central portions. It is clear that the curves corresponding to short dark times are similar to that obtained under CW pumping (see Fig. 1). In particular, a pronounced W profile is observed, and the curve is wider. An increase in dark time smoothes out the W profile and reduces the width of the Hanle curve.

Our experimental findings suggest that the development of nuclear polarization generally leads to a decrease in electron spin polarization in weak transverse magnetic fields and its increase in strong fields. It is obvious that these effects are associated with two different processes.

According to the model proposed in [9], based on the concept of spin temperature [16], a W profile develops in the Hanle curve under strong pumping because of a significant DNP parallel to the total field B_{tot} affected the nuclear spins. This field is the sum of the applied field **B** and the effective field B_e generated by optically oriented electrons (Knight field). As the

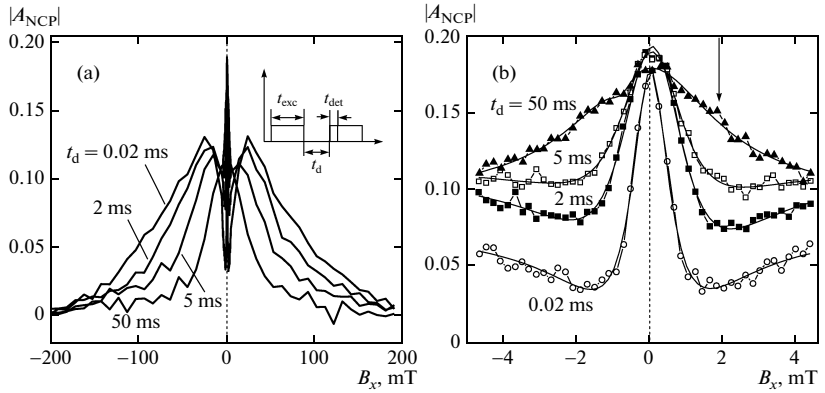

Fig. 3. Hanle curves at constant excitation time $t_{exc} = 100$ ms and intensity $I_{exc} = 40$ W/cm^2, parameterized by dark time t_d (indicated at each curve): (a) complete curves; (b) central portions of curves. The arrow points to the lowest point of a dip in a Hanle curve. The solid curves are drawn for clarity.

applied field exceeds the Knight field, the total field and, accordingly, the nuclear field begin to rotate away from the optical axis towards the applied field direction. The rotation reduces the degree of electron spin polarization, resulting in a weaker Knight field. This, in turn, additionally increases the angle of rotation. In effect, positive feedback of this kind leads to the formation of a narrow central peak in the Hanle curve.

The effective nuclear magnetic field acting on an electron spin in the system under study is parallel to the nuclear spin direction [2, 3]. When the applied magnetic field is weak (in the dip region around the central peak), the nuclear field is stronger than the applied one, and the electron spin is effectively depolarized by a high $\mathbf{B}_{\text{tot}}$. Nuclear field decreases with increasing applied field, and the ensuing increase in electron spin polarization leads to the development of a W profile in the Hanle curve. This implies that dynamics of the longitudinal component $\mathbf{B}_{\text{DNP}\|}$ of nuclear field can be inferred from the time evolution of the dips around the central peak. Note that the terms *longitudinal* and *transverse* used in the present study refer, respectively, to the nuclear field components parallel and perpendicular to the applied magnetic field (as in [16]) rather than the optical axis (e.g., see [2]).

Information about behavior of the transverse component $\mathbf{B}_{\text{DNP}\perp}$ of nuclear field can be extracted by analyzing the width of the Hanle curve. It is clear from Figs. 2 and 3 that the curve width reaches a maximum under CW pumping by a beam of constant circular polarization and decreases with increasing dark time when the pump beam is modulated. Its large width has been attributed to the formation of a transverse component $\mathbf{B}_{\text{DNP}\perp}$ of nuclear field stabilized by quadrupole splitting of nuclear spin states along the optical axis [11, 12]. Since the longitudinal component $\mathbf{B}_{\text{DNP}\|}$ plays no significant role in strong applied magnetic fields [2, 3], dynamics of $\mathbf{B}_{\text{DNP}\|}$ and $\mathbf{B}_{\text{DNP}\perp}$ can be inferred separately from behavior of electron spin polarization in weak and strong fields, respectively. Accordingly, to analyze experimental data, expressions are required that relate the degree of electron polarization to the magnitudes of the corresponding DNP components.

4. ANALYSIS OF EXPERIMENTAL DATA

4.1. Formulas for Analysis

To derive expressions for nuclear spin components, we can reasonably assume that the only time-invariant component of electron spin is its projection on $\mathbf{B}_{\text{tot}}$ because of its high precession frequency. Measured degree of luminescence polarization scales linearly with the invariant spin projection on the viewing direction,

$$S_z = S\cos^2\vartheta = S\frac{B^2_{\text{tot},z}}{B^2_{\text{tot}}}, \qquad (2)$$

where S quantifies the degree of optically induced spin orientation and ϑ is the angle between the viewing direction and the total field $\mathbf{B}_{\text{tot}} = \mathbf{B} + \mathbf{B}_{\text{N}}$ (the sum of the applied field $\mathbf{B}$ and the nuclear field $\mathbf{B}_{\text{N}} = \mathbf{B}_{\text{f}} + \mathbf{B}_{\text{DNP}}$ including the effective nuclear spin fluctuation field generated by randomly oriented nuclear spins [17]). Since the electron spin in a quantum dot interacts with just a few nuclear spins, the contribution due to fluctuations is significantly larger than that for donor-bound electron spins in a bulk material, amounting to several tens of milliteslas [18]. Therefore, we can evaluate only an ensemble-averaged spin $\langle S_z\rangle$.

In the absence of regular fields $\mathbf{B}$ and $\mathbf{B}_{\text{DNP}}$, electron spin dynamics is completely determined by nuclear spin fluctuations. A magnetic field applied perpendicular to the optical axis (hereinafter assumed parallel to the x axis) substantially changes the time-averaged electron spin polarization. It was shown in [17] that rigorous evaluation of S_z is a cumbersome task. The calculated field dependence of S_z can be described by a bell-shaped curve accurately fitted by (2) with

$$B^2_{\text{tot},z} = \langle B^2_{f,z}\rangle,$$

where $\langle B^2_{f,z}\rangle$ is the ensemble average of the nuclear spin fluctuation field z component squared and

$$B^2_{\text{tot}} = B^2 + \langle B^2_f\rangle,$$

with $\langle B^2_f\rangle = \langle B^2_{f,x}\rangle + \langle B^2_{f,y}\rangle + \langle B^2_{f,z}\rangle$. Thus, the mean ratio approximated by the ratio of means in (2),

$$\langle S_z\rangle \approx S\frac{\langle B^2_{\text{tot},z}\rangle}{\langle B^2_{\text{tot}}\rangle}, \qquad (3)$$

yields a satisfactory result under conditions specified above.

We suppose that approximation (3) holds in the presence of a regular field $\mathbf{B}_{\text{DNP}}$, with a periodically time-varying numerator:

$$B_{\text{tot},z} = B_{N\perp}\cos\omega t,$$

where $B_{N\perp}$ is the component of the total nuclear field perpendicular to the applied field and ω is the frequency of nuclear spin precession induced by the applied field. The electron pumping rate was higher than the nuclear precession frequency in the entire range of applied magnetic field magnitudes used in the experiments described here. Therefore, we can represent the numerator in (3) as

$$\begin{aligned}\langle B^2_{\text{tot},z}\rangle &= (B^2_{\text{DNP}\perp} + \langle B^2_{f\perp}\rangle)\langle\cos^2\omega t\rangle \\ &= 0.5(B^2_{\text{DNP}\perp} + \langle B^2_{f\perp}\rangle),\end{aligned} \qquad (4)$$

where

$$\langle B^2_{f\perp}\rangle = \langle B^2_{f,z}\rangle + \langle B^2_{f,y}\rangle = 2\langle B^2_{f,x}\rangle \equiv 2\langle B^2_{f\|}\rangle.$$

Analogously, the ensemble average of the total field squared (denominator in (3)) can be expressed as

$$\langle B_{\text{tot}}^2 \rangle = (B + B_{\text{DNP}\parallel})^2 + \langle B_{f\parallel}^2 \rangle + B_{\text{DNP}\perp}^2 + \langle B_{f\perp}^2 \rangle. \quad (5)$$

In summary, the degree of electron spin polarization can be represented by the general expression

$$\rho = \frac{\langle S_z \rangle}{S} = \frac{0.5(B_{\text{DNP}\perp}^2 + \langle B_{f\perp}^2 \rangle)}{(B + B_{\text{DNP}\parallel})^2 + B_{\text{DNP}\perp}^2 + \langle B_f^2 \rangle}, \quad (6)$$

where

$$\langle B_f^2 \rangle = \langle B_{f\parallel}^2 \rangle + \langle B_{f\perp}^2 \rangle = 3\langle B_{f\parallel}^2 \rangle.$$

The last relation holds when dynamic nuclear polarization is insignificant and nuclear spin fluctuations are statistically isotropic.

According to (6), the degree of electron spin polarization approaches 1/3 as $B \longrightarrow 0$ and in the absence of DNP, in full agreement with [17]. Actual measurements show that it is approximately 1.5 times lower when DNP does not develop because of a fast pump polarization modulation. In our view, the lower degree of electron spin polarization is due to the unpolarized luminescence from neutral quantum dots contributing to the recorded signal.

Experimental data can be analyzed by simplifying expression (6) in two special cases of particular importance. According to [2], the longitudinal component $B_{\text{DNP}\parallel}$ of nuclear field appears only in the W-profile region of the Hanle curve, where the applied field is negligible compared to the nuclear spin fluctuation field [17]. Then, it holds for this region that

$$\rho \approx \frac{0.5(B_{\text{DNP}\perp}^2 + \langle B_{f\perp}^2 \rangle)}{(B_{\text{DNP}\parallel})^2 + B_{\text{DNP}\perp}^2 + 3\langle B_{f\parallel}^2 \rangle}. \quad (7)$$

In strong applied magnetic fields (as $B_{\text{DNP}\parallel} \longrightarrow 0$), the degree of polarization becomes

$$\rho \approx \frac{0.5(B_{\text{DNP}\perp}^2 + \langle B_{f\perp}^2 \rangle)}{B^2 + B_{\text{DNP}\perp}^2 + 3\langle B_{f\parallel}^2 \rangle}. \quad (8)$$

Thus, we can examine the time dependence of ρ in strong and weak magnetic fields to determine the respective kinetics of the longitudinal and transverse components of nuclear polarization.

Our analysis of time-dependent nuclear polarization is based on the assumption that the increase in each component of nuclear polarization after the start of pumping and its decay during the dark time can be described by the expressions

$$y = B_{\text{DNP}}^0[1 - \exp(-t/\tau)]$$

and

$$y = B_{\text{DNP}}^0 \exp(-t/\tau),$$

where τ is the corresponding characteristic time, respectively. In the case of a weak magnetic field, we divide the numerator and denominator in (7) by $\langle B_{f\parallel}^2 \rangle$ and introduce

$$a^2 = \frac{(B_{\text{DNP}\perp}^0)^2}{\langle B_{f\parallel}^2 \rangle}$$

and

$$c^2 = \frac{(B_{\text{DNP}\parallel}^0)^2}{\langle B_{f\parallel}^2 \rangle}$$

to find respective expressions describing the rise and decay of the longitudinal component of nuclear polarization:

$$\rho \approx \frac{0.5a^2 + 1}{c^2(1 - e^{-t/\tau})^2 + a^2 + 3} \quad (9)$$

and

$$\rho \approx \frac{0.5a^2 + 1}{c^2 e^{-2t/\tau} + a^2 + 3}. \quad (10)$$

In what follows, we show that the transverse component of nuclear polarization almost vanishes in weak magnetic fields, and the parameter a can be neglected in analysis of experimental data. For this reason time dependence of this parameter is omitted in the formulas above.

Expression (8), valid for strong applied magnetic fields, can be rewritten analogously by introducing

$$a'^2 = \frac{B^2}{(B_{\text{DNP}\perp}^0)^2}, \quad c'^2 = \frac{\langle B_{f\parallel}^2 \rangle}{(B_{\text{DNP}\perp}^0)^2},$$

as

$$\rho \approx \frac{0.5(1 - e^{-t/\tau})^2 + c'^2}{a'^2 + (1 - e^{-t/\tau})^2 + 3c'^2} \quad (11)$$

and

$$\rho \approx \frac{0.5e^{-2t/\tau} + c'^2}{a'^2 + e^{-2t/\tau} + 3c'^2} \quad (12)$$

to describe the rise and decay of the transverse component of nuclear polarization, respectively.

In summary, using the expressions derived above, we can fit measured time-dependent degrees of polarization to evaluate nuclear spin relaxation times τ, as well as effective nuclear spin fluctuation fields and dynamic nuclear polarization. We note here that dynamics of the longitudinal and transverse components of nuclear polarization may be characterized by different relaxation times.

4.2. Dynamics of Nuclear Polarization Rise

Figures 4 and 5 show the results of an analysis of the time-dependent Hanle curves in Fig. 2, measured after the start of optical pumping. The values of ρ are refined by taking into account luminescence depolarization due to contributions from neutral quantum

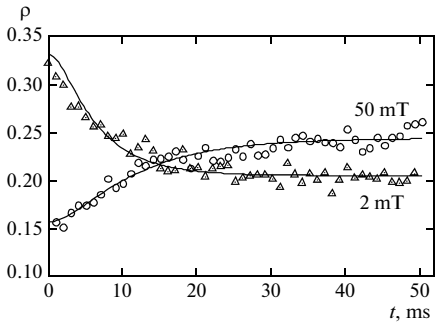

Fig. 4. Examples of time-dependent degree of polarization obtained by analyzing data presented in Fig. 2. Symbols represent experimental results for $B = 2$ and 50 mT; solid curves are approximations by functions (9) and (11).

dots. Experimental data were processed to determine the time-resolved degrees of polarization corresponding to several applied magnetic field strengths. Figure 4 demonstrates a wide difference between kinetics of degree of polarization under weak and strong field conditions (few milliteslas and higher than 20 mT, respectively).

At $B = 2$ mT (the lowest point of a dip in Fig. 3b, indicated by an arrow), where the dominant role is played by $B_{\mathrm{DNP}\|}$, the degree of electron spin polarization ρ decreases with time elapsed (Fig. 4), signifying an increase in $B_{\mathrm{DNP}\|}$ (see discussion in Section 3). We found that the time-dependent degree of polarization determined from experimental data can be fitted by (9) only if the transverse component of nuclear field is sufficiently weak, $B^2_{\mathrm{DNP}\perp} \ll \langle B_f^2 \rangle$. Using the resulting approximation, we estimated the characteristic rise time for $B_{\mathrm{DNP}\|}$, $\tau_\| \approx 6$ ms, and the parameter $c = B^2_{\mathrm{DNP}\|} / \sqrt{\langle B^2_{f\|} \rangle} \approx 1.5$.

Figure 4 shows an example of time-varying spin polarization found by processing experimental data obtained under high field conditions ($B = 50$ mT), where the dominant role is played by the transverse component of nuclear polarization. The solid curve is a fit by function (11). An analysis of the entire body of experimental data showed that all time-dependent spin polarizations measured at $B > 20$ mT are accurately approximated by this function. The parameters a' and c' calculated by fitting the polarization history for each applied magnetic field strength were then

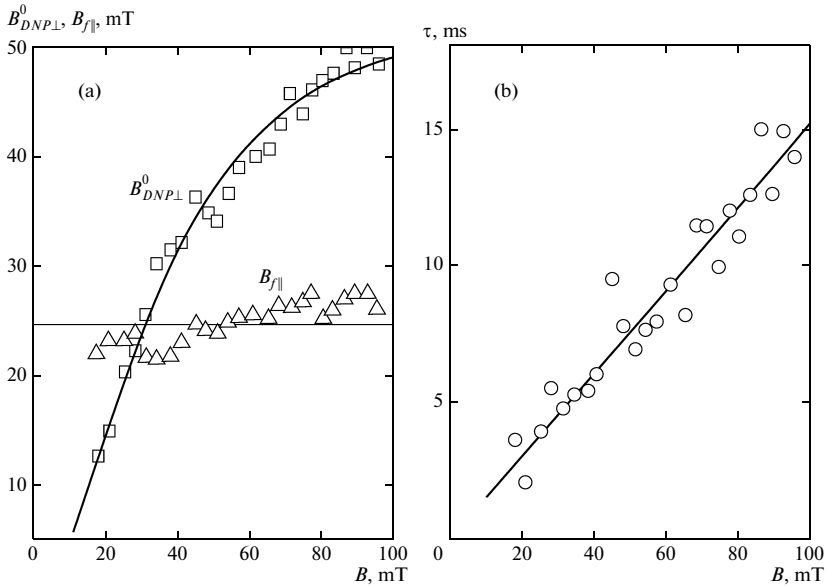

Fig. 5. (a) Limit magnitudes of the transverse nuclear field component $B^0_{\mathrm{DNP}\perp}$ and the nuclear spin fluctuation field $B_{f\|}$ vs. applied field, obtained by analyzing kinetics of spin polarization after the start of pumping (see Fig. 2). (b) Field dependence of the buildup time τ of the transverse DNP field component. The solid curves are drawn for clarity.

used to determine the limit magnitude of the transverse component of nuclear polarization,

$$B^0_{\mathrm{DNP}\perp} = B/a',$$

the rms effective nuclear spin fluctuation field,

$$B_{f\parallel} \equiv \sqrt{\langle B^2_{f\parallel}\rangle} = \frac{c'}{a'}B,$$

and their dependence on magnetic field.

Figure 5a shows $B^0_{\mathrm{DNP}\perp}$ and $B_{f\parallel}$ as functions of applied magnetic field. It is clear that the limit magnitude $B^0_{\mathrm{DNP}\perp}$ of the transverse component of nuclear polarization increases approximately from 10 to 50 mT with an applied field between 20 and 100 mT, whereas the effective nuclear spin fluctuation field $B_{f\parallel}$ remains almost constant at around 25 mT irrespective of applied field strength. This value is in good agreement with data reported in [6], where the rms nuclear spin fluctuation field was estimated at approximately 20 mT for quantum dots of similar type. Using this value and $c \approx 1.5$ obtained above, we can also calculate the maximum transverse nuclear field: $B^0_{\mathrm{DNP}\parallel} \approx 40$ mT.

Figure 5b shows the rise time τ of the transverse component of nuclear polarization. It demonstrates that the time linearly increases from approximately 2.5 to 15 ms with an applied field between 20 and 100 mT.

4.3. Dynamics of Nuclear Polarization Decay

An analogous procedure was used to analyze the shape of the Hanle curve as a function of dark time. Measurement results were converted into spin polarization kinetics for several values of applied magnetic field strength (as in Fig. 4), and the resulting curves were fitted by (10) and (12). The curves in Fig. 6 are examples of such fits. The fitting parameters were used to evaluate the initial longitudinal and transverse nuclear fields, as well as the corresponding decay times. The decay time of the longitudinal component $B^0_{\mathrm{DNP}\parallel}$ calculated by using the data for $B = 2$ mT was found to be $\tau \approx 5.5$ ms, which is close to the corresponding rise time reported above.

However, the decay time of the transverse component $B^0_{\mathrm{DNP}\perp}$ of nuclear polarization differs significantly from its rise time. Moreover, its time variation in an applied magnetic field exhibits an opposite trend: whereas the rise time increases with field strength (Fig. 5b), the decay time rapidly decreases (Fig. 7b). Accordingly, these times are approximately equal in strong magnetic fields but differ by a factor of several tens at $B = 20$ mT.

Remarkably, despite the difference in behavior between decay times, both the limit magnitudes of the DNP components and their variation with magnetic field in experiments on nuclear polarization decay are in good agreement with those determined by measuring nuclear polarization buildup (cf. Figs. 5a and 7a). The initial magnitude $B^0_{\mathrm{DNP}\parallel}$ of the longitudinal component is approximately 30 mT, which is not too different from the limit magnitude of this component obtained in experiments on polarization buildup. A similar agreement is observed for the transverse component of nuclear polarization and the nuclear spin fluctuation field, as is clearly seen by comparing Figs. 5a and 7a. As in experiments on polarization rise, the initial magnitude $B^0_{\mathrm{DNP}\perp}$ of transverse polarization increases with applied magnetic field, whereas the nuclear spin fluctuation field B_f is almost independent of applied field. A slight difference between nuclear field magnitudes measured in experiments on polarization buildup and decay should rather be attributed to a minor difference in optical excitation intensity between experiments of these two types.

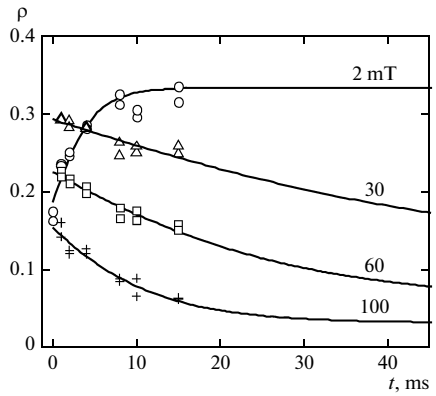

Fig. 6. Kinetics of degree of polarization at several magnetic field strengths (indicated at each curve), obtained by analyzing measurement results for various dark times. Symbols represent experimental data; solid curves are approximations by functions (10) and (12).

5. DISCUSSION

Our analysis shows that the longitudinal and transverse components of nuclear polarization in the quantum dots under study exhibit widely different dynamical patterns. The behavior of longitudinal polarization is relatively simple. After the start of optical pumping, this component increases with a characteristic time of approximately 6 ms to a limit magnitude corresponding to an effective nuclear field of 30 to 40 mT. After the end of pumping, the longitudinal component decays over a similar time scale.

The behavior of the component of dynamic nuclear polarization perpendicular to the applied magnetic field is much more complicated. Observations that

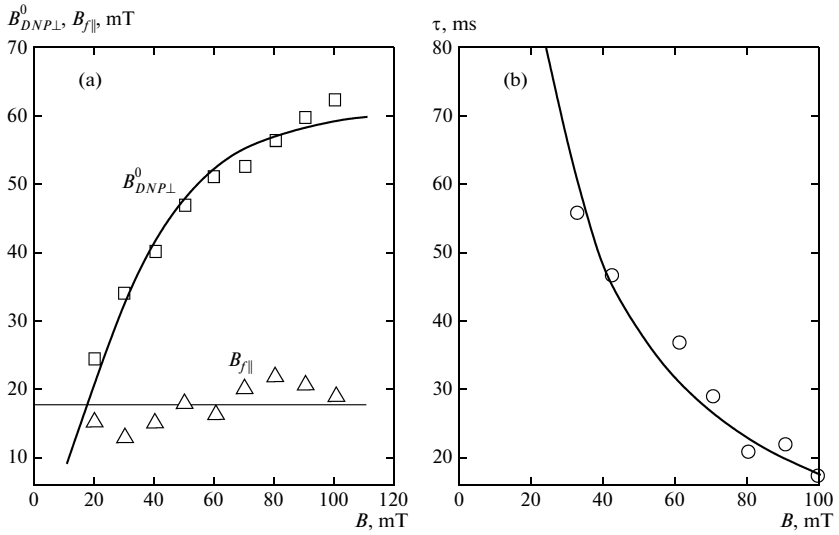

Fig. 7. (a) Field dependence of the initial magnitude $B_{\mathrm{DNP}\perp}$ of the transverse nuclear field and the nuclear spin fluctuation field B_f, obtained by analyzing kinetics of spin polarization after the end of pumping (see Fig. 3). (b) Field dependence of the $B_{\mathrm{DNP}\perp}$ decay time. The solid curves are drawn for clarity.

defy any straightforward explanation include difference between the buildup and decay times, their opposite variation with applied magnetic field, and increase in magnitude of this component with applied field strength.

In our view, these differences are mainly due to the fact that the dominant contributions to the buildup of longitudinal and transverse polarization components come from states with different spin projections on the viewing direction. Current models of nuclear polarization buildup are generally based on the classical model of angular momentum precession in isotropic space. The condition of spatial isotropy is violated in the quantum dots examined in this study because nuclei are affected by the field gradient due to the strain resulting from a mismatch between the lattice constants of the quantum dots and barrier layers. The principal axis of the field gradient is the structure growth axis, parallel to the viewing direction. The field gradient splits nuclear spin states into Kramers doublets $|\pm 1/2\rangle$, $|\pm 3/2\rangle$, etc. in indium, gallium, and arsenic nuclei, which have nonzero quadrupole moments. In an applied magnetic field, the Zeeman splitting in the doublets strongly depends on the relative orientation of gradient axis and magnetic field vector. This dependence can be described phenomenologically by introducing an anisotropic g-factor [19].

The anisotropy associated with the doublets $|\pm 1/2\rangle$ is relatively weak: the difference between the g-factor components parallel and perpendicular to the gradient axis is not greater than a factor of 2 [16, 20]. Dynamics of these states should not be too different from the nuclear spin dynamics invoked to explain the W profile of the Hanle curve [9]. In the present study, one is naturally led to hypothesize that orientation of these particular states is responsible for the buildup of the component of nuclear polarization parallel to the applied field manifesting itself by the development of a W profile. This hypothesis is consistent with the relatively simple dynamical pattern of the longitudinal component of nuclear polarization observed in our experiments.

The g-factor anisotropy associated with the states $|\pm 3/2\rangle$, $|\pm 5/2\rangle$, ..., that are split off from $|\pm 1/2\rangle$ by quadrupole interaction is much stronger, as demonstrated in relatively weak magnetic fields. In a magnetic field parallel to the gradient axis, the splitting of these states linearly increases with field strength and the corresponding g-factor is similar to that in the absence of gradient. In a perpendicular magnetic field, the splitting is a highly nonlinear function of the field, and the g-factor (i.e., the splitting of these states) almost vanishes in fields on the order of a few milliteslas [16, 20]. In terms of the classical model, this means almost no precession of angular momenta associated with these states in a field of this kind. Suppression of precession impedes nuclear spin relaxation, which is generally attributed to local magnetic field

effects (e.g., see [21]). In effect, the transverse component of polarization of the nuclear states split off by quadrupole interactions can be stabilized to some degree in weak magnetic fields [11, 12]. A superlinear increase in splitting of these states with field strength enhances the probability of spin relaxation. The ensuing higher relaxation rate may be responsible for the shorter $B_{\mathrm{DNP}\perp}$ decay times observed with increasing magnetic field strength in our experiments (see Fig. 7b).

Note the following counterintuitive observation: the time of nuclear polarization buildup after the start of pumping increases with applied field rather than decreasing (see Fig. 5b). To explain this behavior, we have to postulate that optical pumping gives rise to an additional process of $B_{\mathrm{DNP}\perp}$ relaxation, whose rate in weak magnetic fields is several times higher than in darkness. The contribution of this process decreases with increasing magnetic field strength, and the buildup and decay times of $B_{\mathrm{DNP}\perp}$ become almost equal in fields on the order of 100 mT. Furthermore, suppression of an additional relaxation process in strong magnetic fields explains the increase in limit magnitude $B^0_{\mathrm{DNP}\perp}$ with increasing field strength (see Fig. 5a).

The nature of the additional relaxation process is currently unclear. It is likely due to interaction between nuclei and photoexcited carriers. This hypothesis is in good agreement with data reported in [5], where the presence of an electron in a quantum dot was shown to increase the rate of nuclear spin relaxation by more than two orders of magnitude.

This hypothesis is also corroborated by the results of our preliminary studies demonstrating that the relaxation time of nuclear spins in quantum dots increases by about two orders of magnitude after the sample has been annealed at a higher temperature of 980°C. Annealing increases the size of quantum dots, reducing the electron density around each nucleus.

6. CONCLUSIONS

We performed an experimental study of time-dependent circular polarization of luminescence from quantum dots as a function of magnetic field perpendicular to the optical axis (time-resolved measurements of the Hanle effect). Experimental data were analyzed by using an original approach to separate treatment of the longitudinal and transverse components of nuclear polarization in quantum dots characterized by strong quadrupole splitting of nuclear spin states. The phenomenological model proposed here takes into account the contribution of nuclear spin fluctuations, which were ignored in previous analyses of experimental data on the Hanle effect. The model is validated both by our finding that nuclear spin fluctuation field is independent of applied field and by good quantitative agreement with results of other studies [6, 18]. Using this model to analyze experimental results, we obtained detailed information about the rise and decay times of each component of nuclear polarization in quantum dots in a transverse magnetic field. The rise and decay times of the component parallel to the applied field were found to be almost equal (approximately 5 ms). However, the dynamics of the transverse component is much more complicated: the corresponding rise and decay times differ widely and have opposite dependence on magnetic field strength. Furthermore, the magnitude of the transverse component created by continuous-wave pumping significantly increases with applied field strength. We attribute this unexpected behavior of nuclear polarization to nuclear spin relaxation via interaction with photoexcited carriers.

ACKNOWLEDGMENTS

This work was supported by the Government of the Russian Federation, grant no. 11.G34.31.0067; the Russian Foundation for Basic Research, project no. 09-02-00482-a; Ministry of Education and Science of the Russian Federation, state contract no. 02.740.11.0244; and Deutsche Forschungsgemeinschaft Foundation.

REFERENCES

1. C. Jeffries, *Dynamic Nuclear Orientation* (Interscience, New York, 1963; Mir, Moscow, 1965).
2. *Optical Orientation*, Ed. by F. Meier and B. P. Zakharchenya (North-Holland, Amsterdam, 1984; Nauka, Leningrad, 1989).
3. V. K. Kalevich, K. V. Kavokin, and I. A. Merkulov, in *Spin Physics in Semiconductors*, Ed. by M. I. Dyakonov (Springer, Berlin, 2008), Chap. 11, p. 309.
4. V. K. Kalevich, V. D. Kul'kov, and V. G. Fleisher, JETP Lett. **35** (1), 20 (1982).
5. P. Maletinsky, A. Badolato, and A. Imamoglu, Phys. Rev. Lett. **99**, 056804 (2007).
6. R. V. Cherbunin, S. Yu. Verbin, T. Auer, D. R. Yakovlev, D. Reuter, A. D. Wieck, I. Ya. Gerlovin, I. V. Ignatiev, D. V. Vishnevsky, and M. Bayer, Phys. Rev. B: Condens. Matter **80**, 035326 (2009).
7. A. I. Tartakovskii, T. Wright, A. Russell, V. I. Fal'ko, A. B. Van'kov, J. Skiba-Szymanska, I. Drouzas, R. S. Kolodka, M. S. Skolnick, P. W. Fry, A. Tahraoui, H.-Y. Liu, and M. Hopkinson, Phys. Rev. Lett. **98**, 026806 (2007).
8. T. Belhadj, T. Kuroda, C.-M. Simon, T. Amand, T. Mano, K. Sakoda, N. Koguchi, X. Marie, and B. Urbaszek, Phys. Rev. B: Condens. Matter **78**, 205325 (2008).
9. D. Paget, G. Lampel, B. Sapoval, and V. I. Safarov, Phys. Rev. B: Solid State **15**, 5780 (1977).
10. O. Krebs, P. Maletinsky, T. Amand, B. Urbaszek, A. Lemaïtre, P. Voisin, X. Marie, and A. Imamoglu, Phys. Rev. Lett. **104**, 056603 (2010).

11. R. V. Cherbunin, S. Yu. Verbin, K. Flisinski, I. Ya. Gerlovin, I. V. Ignatiev, D. V. Vishnevsky, D. Reuter, A. D. Wieck, D. R. Yakovlev, and M. Bayer, J. Phys.: Conf. Ser. **245**, 012055 (2010).

12. R. I. Dzhioev and V. L. Korenev, Phys. Rev. Lett. **99**, 037401 (2007).

13. S. Cortez, O. Krebs, S. Laurent, M. Senes, X. Marie, P. Voisin, R. Ferreira, G. Bastard, J.-M. Gërard, and T. Amand, Phys. Rev. Lett. **89**, 207401 (2002).

14. A. Shabaev, E. A. Stina, A. S. Bracker, D. Gammon, A. L. Efros, V. L. Korenev, and I. Merkulov, Phys. Rev. B: Condens. Matter **79**, 035322 (2009).

15. I. V. Ignatiev, S. Yu. Verbin, I. Ya. Gerlovin, R. V. Cherbunin, and Y. Masumoto, Opt. Spectrosc. **106** (3), 375 (2009).

16. A. Abragam, *Principles of Nuclear Magnetism* (Oxford University Press, Oxford, 1961; Inostrannaya Literatura, Moscow, 1965).

17. I. A. Merkulov, Al. L. Efros, and M. Rosen, Phys. Rev. B: Condens. Matter **65**, 205309 (2002).

18. M. Yu. Petrov, G. G. Kozlov, I. V. Ignatiev, R. V. Cherbunin, D. R. Yakovlev, and M. Bayer, Phys. Rev. B: Condens. Matter **80**, 125318 (2009).

19. E. S. Artemova and I. A. Merkulov, Sov. Phys. Solid State **27** (4), 694 (1985).

20. K. Flisinski, I. Ya. Gerlovin, I. V. Ignatiev, M. Yu. Petrov, S. Yu. Verbin, D. R. Yakovlev, and M. Bayer, J. Phys.: Conf. Ser. **245**, 012056 (2010).

21. M. I. D'yakonov and V. I. Perel', Sov. Phys. JETP **41** (4), 759 (1975).

Translated by A. Betev

PIII

HANLE EFFECT IN (IN,GA)AS QUANTUM DOTS: ROLE OF NUCLEAR SPIN FLUCTUATIONS

M. S. Kuznetsova, K. Flisinski, I. Ya. Gerlovin, I. V. Ignatiev, K. V. Kavokin, S. Yu. Verbin, D. Reuter, A. D. Wieck, D. Yakovlev, and M. Bayer

Published in: *Physical Review B — Condensed Matter and Materials Physics*, 2013, 87, 235320

Hanle effect in (In,Ga)As quantum dots: Role of nuclear spin fluctuations

M. S. Kuznetsova,[1] K. Flisinski,[2] I. Ya. Gerlovin,[1] I. V. Ignatiev,[1] K. V. Kavokin,[1,3] S. Yu. Verbin,[1] D. R. Yakovlev,[2,3] D. Reuter,[4] A. D. Wieck,[4] and M. Bayer[2]

[1]*Spin Optics Laboratory, St. Petersburg State University, 198504 St. Petersburg, Russia*
[2]*Experimentelle Physik 2, Technische Universität Dortmund, D-44221 Dortmund, Germany*
[3]*A. F. Ioffe Physical-Technical Institute, Russian Academy of Sciences, 194021 St. Petersburg, Russia*
[4]*Angewandte Festkörperphysik, Ruhr-Universität Bochum, D-44780 Bochum, Germany*

(Received 28 March 2013; revised manuscript received 27 May 2013; published 27 June 2013)

The role of nuclear spin fluctuations in the dynamic polarization of nuclear spins by electrons is investigated in (In,Ga)As/GaAs quantum dots. The photoluminescence polarization under circularly polarized optical pumping in transverse magnetic fields (Hanle effect) is studied. A weak additional magnetic field parallel to the optical axis is used to control the efficiency of nuclear spin cooling and the sign of nuclear spin temperature. The shape of the Hanle curve is drastically modified when changing this control field, as observed earlier in bulk semiconductors and quantum wells. However, the standard nuclear spin cooling theory, operating with the mean nuclear magnetic field (Overhauser field), fails to describe the experimental Hanle curves in a certain range of control fields. This controversy is resolved by taking into account the nuclear spin fluctuations owed to the finite number of nuclei in the quantum dot. We propose a model considering cooling of the nuclear spin system by electron spins experiencing fast vector precession in the random Overhauser fields of nuclear spin fluctuations. The model allows us to accurately describe the measured Hanle curves and to evaluate the parameters of the electron-nuclear spin system of the studied quantum dots.

DOI: 10.1103/PhysRevB.87.235320 PACS number(s): 78.67.Hc, 78.47.jd, 76.70.Hb, 73.21.La

I. INTRODUCTION

The hyperfine interaction of electron spins with the spins of lattice nuclei is able to create a considerable dynamic nuclear polarization (DNP) in semiconductors under optical pumping by circularly polarized light.[1] In this process, the angular momentum received by the electron from a photon is transferred to the nuclear spin system. In turn, the magnetic moment of polarized nuclei affects the electron spin as an effective magnetic field (Overhauser field), giving rise to splitting of electron spin states. Under conditions of strong optical pumping the splitting can reach tens of micro-eV so that the nuclear polarization becomes detectable via spectral shift by high-resolution optical spectroscopy.[2–5]

An alternative approach to detection of nuclear polarization, which does not require high spectral resolution, is to measure the electron polarization created by optical pumping in an external magnetic field. As the nonequilibrium electron spin polarization is in many cases magnetic field dependent, the Overhauser field can be detected using its effect on the mean electron spin, for example, by observing the associated changes in the circular polarization of photoluminescence (PL).[1] In a magnetic field parallel to the optical axis (longitudinal magnetic field), the nuclear polarization created by the pumping may influence the PL polarization by suppressing electron spin relaxation.[1,5–7] For optical pumping in a magnetic field perpendicular to the optical axis, the electron spin polarization is usually destroyed with increasing magnetic field (Hanle effect). In this case the Overhauser field modifies the width and shape of the dependence of the circular polarization of the PL on the magnetic field (Hanle curve), which can become nonmonotonous, and even hysteresis.[1,5,8–15]

The Hanle effect in the presence of nuclear spin polarization in bulk semiconductors and quantum wells has been theoretically treated in the model of mean Overhauser field, which has provided good qualitative and quantitative agreement with experimental data. The validity of the mean-field approach in these systems is justified by the fact that the correlation time τ_c of the electron spin at the position of a certain nucleus is much shorter than the electron spin lifetime T_s. Indeed, electrons localized at shallow impurity centers or structural imperfections rapidly lose their spin polarization to other localized or itinerant electrons via exchange scattering;[16,17] as this process is spin conserving, the mean polarization of the entire electron ensemble lives over a much longer time scale determined by spin-orbit or hyperfine interactions. As a result, the fluctuations of the Overhauser field B_N are effectively averaged out and give rise only to the electron spin relaxation, which is in this case exponential, with the decrement $\tau_s^{-1} = \gamma_e^2(\langle B_N^2\rangle - \langle B_N\rangle^2)\tau_c$, where γ_e is the electron gyromagnetic ratio.[1] This approach, called approximation of short correlation time,[8] often fails in quantum dots (QDs), where electron states are strongly localized and effectively isolated from all the other electrons. In this case, the electron spin is exposed to a virtually static nuclear spin fluctuation (NSF)[18–22] during its entire lifetime (note that the correlation time of nuclear spins, which is of the order of their transverse relaxation time $T_2 \approx 10^{-4}$s, is orders of magnitude longer than typical electron spin lifetimes). The Larmor precession of the electron spin in the fluctuating nuclear field was predicted to result in a specific nonexponential pattern of electron spin decay,[19] which was subsequently experimentally observed.[23] The influence of NSF on the evolution of the regular Overhauser field and, eventually, on the Hanle effect under dynamic polarization of nuclear spins has so far not been studied experimentally.

In this paper, we report on detailed measurements of the Hanle effect in (In,Ga)As/GaAs QDs in the weak-field range (0–20 mT field strength), where the effect of the NSF is expected to be the strongest. We have measured a set of

Hanle curves under optical excitation of moderate intensity and at different strengths of an additional magnetic field applied along the optical axis (longitudinal magnetic field). The experimental Hanle curves are compared with the results of calculations using two models, one including NSF and the other one taking into account only mean Overhauser fields. In both theories, the mean Overhauser field has been calculated within the spin temperature approach.[1] Our analysis shows that the mean-field model fails to describe the features of the Hanle curve around zero transversal field, where the so-called W structure appears in a certain range of longitudinal fields B_z. The model including NSF, on the other hand, yields good fits of the experimental data, with a reasonable choice of parameters, for all experimental conditions except for the exact compensation of the Knight field with B_z. In the latter case, nuclear quadrupole effects due to strain in the QDs probably play the dominant role.

II. EXPERIMENTAL DETAILS

A heterostructure containing 20 layers of self-assembled (In,Ga)As/GaAs QDs separated by Si-δ-doped GaAs barriers was studied. The heterostructure was annealed at temperature $T_A = 980$ °C, which resulted in the considerable decrease of mechanical stress in the QDs and in enlarging the localization volume for resident electrons due to interdiffusion of Ga and In atoms.

The sample was immersed in liquid helium at a temperature $T = 1.8$ K in a cryostat with a superconducting magnet. Magnetic fields up to 100 mT were applied perpendicular to the optical axis (Voigt geometry) along to the [110] crystallographic direction of the sample. To create an additional magnetic field, perpendicular to the main magnetic field and parallel to the optical axis, a pair of small Helmholtz coils was installed outside the cryostat.

The PL of the sample is excited by circularly polarized light from a continuous-wave Ti:sapphire laser, with the photon energy tuned to the optical transitions in the wetting layer of the sample. The degree of circular polarization of the PL is detected by a standard method using a photoelastic modulator and an analyzer (a Glan-Thompson prism). The modulator creates a time-dependent phase difference, $\Delta\varphi = (\pi/4)\sin(2\pi f t)$, between the linear components of the PL, thus converting each of the circular components (σ^+ and σ^-) into linear ones (x and y) at frequency $f = 50$ kHz. The analyzer selects one of the linear components, which was dispersed with a 0.5-m monochromator and detected by an avalanche photodiode. The signal from the photodiode was accumulated for each circular component separately in a two-channel photon-counting system. The PL polarization was recorded at the wavelength corresponding to the maximum of the PL band of the sample. Typical polarization-resolved PL spectra for the sample under study are shown in Fig. 1(a). A detailed description of these spectra can be found in Refs. 12 and 24.

The degree of PL polarization of the QDs is negative; i.e., the PL is predominately σ^- polarized for σ^+-polarized excitation. The mechanism of negative circular polarization (NCP) has been extensively discussed in Refs. 25–27, where it was shown that the presence of NCP is the result of optical

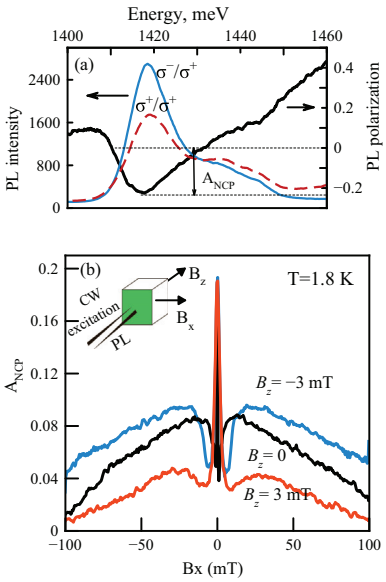

FIG. 1. (Color online) (a) The spectra of circularly cross-polarized (solid blue line) and copolarized (dashed red line) PL relative to polarization of excitation and the PL polarization degree for (In,Ga)As/GaAs QDs (black curve). (b) Overall shape of Hanle curves measured at different longitudinal magnetic fields B_z indicated at each curve. The inset shows the configuration of the experiment.

orientation of the resident electrons provided by ionization of donors outside the QDs (the doping level of our structure corresponds to one resident electron per QD on average). The amplitude of NCP is proportional to the projection of electron spin onto the optical axis z, averaged over the QD ensemble,[13]

$$A_{\mathrm{NCP}} \sim 2\,\langle S_z \rangle\,. \tag{1}$$

The amplitude of the central peak increases with rising excitation power at relatively low excitation levels. A further rise of the power results in saturation of the peak amplitude, which indicates a high level of electron spin polarization. The pump powers used in our experiments were sufficient to totally polarize the electron spin.

In this paper we use the absolute value of NCP as a measure of the electron spin orientation. We studied the dependence of PL polarization on magnetic field applied perpendicular to the optical axis. The central part of the Hanle curve, where the W-like structure is observed, was studied most carefully to understand the role of the Knight field in the optical orientation of nuclear spins. In particular, modifications of the W structure under application of small magnetic fields parallel to the optical axis were studied.

III. EXPERIMENTAL RESULTS

The general form of Hanle curves measured in the absence of longitudinal magnetic fields B_z as well as in the presence

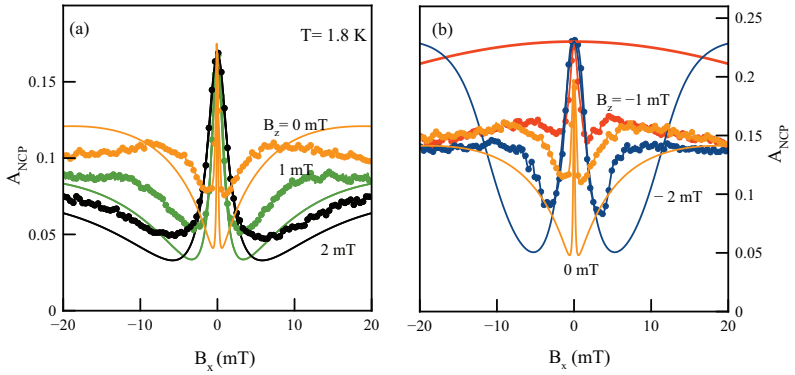

FIG. 2. (Color online) Comparison of Hanle curves calculated in the framework of the standard cooling model (solid lines) with the experimental data (points) for (a) positive and (b) negative longitudinal external fields B_z. Values of B_z are given for each curve.

of small B_z are shown in Fig. 1(b). Each curve shows the pronounced W structure consisting of the narrow central peak and two maxima positioned symmetrically relative to the peak. Application of B_z considerably affected the shape of the Hanle curve.

Namely, the central-peak width increases with B_z irrespective of its sign. At the same time, the width of the Hanle curve significantly drops when B_z is changed from -3 to $+3$ mT. This difference in behavior of the Hanle curve and its central peak is an indication that they are controlled by different components of the hyperfine interaction. According to Ref. 1, the width of the central peak and the shape of the W structure are determined by the dynamic nuclear polarization, creating an effective field parallel to the external magnetic field. The large width of the Hanle curve is due to partial stabilization of the electron spin orientation along the optical axis by the longitudinal component of the effective nuclear field of quadrupole-split nuclear spin states.[28,29] The analysis of this effect and the variation of the Hanle curve width with B_z requires a separate study; we consider hereafter only the behavior of the central part of the Hanle curve.

The effect of longitudinal magnetic fields, ranging from -20 to $+20$ mT, on the Hanle curve is shown in Fig. 2. The experiment shows that application of a positive B_z is accompanied by a monotonous increase of the width of the central peak and of the dips near the peak. The depth of the dips remains almost unchanged. At negative B_z, the behavior of the dips is not monotonous. The change of B_z from 0 to -1 mT results in almost total disappearance of the dips without noticeable change of their width. A further increase of the B_z value to -2 mT leads to the increase of both depth and width of the dips.

IV. ANALYSIS

A. Standard model for nuclear spin cooling

The electron spin orientation maintained by optical excitation is the source of a continuous flux of angular momentum into the nuclear spin system. The nuclear spin-cooling model[1,8,9,30] is based on the fact that nuclear spin orientation along the magnetic field changes the Zeeman energy of nuclear spins. As distinct from the nonequilibrium angular momentum, which decays on the time scale of hundreds of microseconds because of nuclear dipole-dipole interaction, the energy of the nuclear spin system conserves during the spin-lattice relaxation time, which is orders of magnitude longer. Because of strongly disparate time scales of spin-spin and spin-lattice relaxation, the nuclear spin system comes to a quasiequilibrium state described by an effective temperature.[31]

Lowering the spin temperature corresponds to a considerable magnetization along the magnetic field or opposite to it (depending on the sign of the spin temperature), which gives rise to the Overhauser field acting on the electron spin. The Overhauser field is parallel or antiparallel to the nuclear spin, depending on the sign of the electron g factor. In particular, it is antiparallel for the negative sign of g_e,[1] as in our case. The effective magnetic field, to which nuclei are subjected in our experiment, is the sum of the external magnetic field and of the Knight field created by spin-polarized electrons. Thus the dynamics of electron spin is determined by the joint action of the external and nuclear fields, while the dynamics of the nuclear polarization depends, in turn, on the electron spin through the Knight field. It is essential that the efficiency of nuclear spin cooling is proportional to the scalar product of the electron spin times the total field acting on the nuclei. When the external magnetic field is strictly perpendicular to the optical axis, the nuclear spin cooling occurs only due to the Knight field.

The above consideration allows one to derive a system of coupled equations for the electron spin and the effective field of nuclear polarization acting on the electron. According to Ref. 1, the system can be represented in the form

$$\mathbf{S} - \mathbf{S}_0 = \left(\mathbf{B}_{\rm tot}^{(e)} \cdot \mathbf{S}\right)/B_{1/2}, \tag{2}$$

$$\mathbf{B}_N = \mathbf{B}_{\rm tot}^{(N)} \beta b_N \frac{(I+1)\mu}{3} = \mathbf{B}_{\rm tot}^{(N)} \frac{b_N \left(\mathbf{B}_{\rm tot}^{(N)} \cdot \mathbf{S}_\parallel\right)}{\left(B_{\rm tot}^{(N)}\right)^2 + \xi B_L^2} \frac{4I(I+1)}{3}, \tag{2'}$$

where $\mathbf{B}_{\rm tot}^{(e)} = \mathbf{B} + \mathbf{B}_N$ is the sum of external and nuclear fields acting on the electron spin, $B_{1/2} = \pi/(\mu_B g_e T_e)$ is the half width of the Hanle curve in the absence of nuclear field (g_e, μ_B, and T_e are the electron g factor, the Bohr magneton, and the electron spin lifetime, respectively), $\mathbf{B}_{\rm tot}^{(N)} = \mathbf{B} + \mathbf{B}_e$ is the sum of the external magnetic field and of the Knight field acting on the nuclear spin from the electron, β is the reciprocal temperature of the nuclear spin system, and parameter b_N is the effective field of totally polarized nuclei affecting the electron spin. The magnitude of b_N is determined by the properties of the particular electron-nuclear spin system and should not depend on external conditions. The term ξB_L^2 describes the interaction between nuclear spins causing the relaxation of nuclear polarization, where B_L is the local field, which the nuclear spin "feels" from its neighbors.

Solution of these equations yields a cubic equation for the average projection of electron spin onto the direction of observation. This equation for the case when magnetic field B_x is perpendicular to the optical axis is given in Ref. 1. Simple generalization of the equation is possible for the case when an additional magnetic field B_z directed along the optical axis is present:

$$S_z\left(1+\frac{K^2}{B_{1/2}^2}B_x^2\right) - S_0\left(1+\frac{K^2}{B_{1/2}^2}B_z^2\right) = 0, \qquad (2'')$$

where

$$K = 1 + \frac{S_0 B_z + b_e S_0 S_z}{B_x^2 + 2b_e S_0 B_z + b_e^2 S_0 S_z + \xi B_L^2}.$$

In the above equations S_0 is the initial electron spin orientation created by excitation, and S_z is the z projection of the electron spin averaged over time.

To model the experimentally measured Hanle curve, we have numerically solved Eq. (2′) and obtained S_z as a function of the transverse magnetic field B_x for different values of the longitudinal magnetic field B_z in the range from -3 to $+3$ mT. The following values of the other parameters were used in the calculations: $S_0 = 1/2$, $B_{1/2} = 60$ mT, $B_L = 0.3$ mT, and $b_e = 2.0$ mT. Most of them approximately correspond to our experimental conditions and the properties of the sample studied. The exception is the value of $B_{1/2}$ extracted from the experimentally measured width of the Hanle curve. It corresponds to the electron spin life time T_e, of the order of 10^{-10} s, which is several orders of magnitude smaller than the real value in the structures of this type (see, for example, Ref. 32).

Examples of the calculated dependences are shown in Fig. 2. They indeed demonstrate behaviors similar to the measured Hanle curves. This is in particular true for positive B_z [see Fig. 2(a)], which, for the helicity of excitation used in our experiments, is codirected to the Knight field. The analysis shows that the effective nuclear field in this case is codirected to the external magnetic field and thus "amplifies" it. This amplification results in a gradual decrease of spin polarization and, correspondingly, of PL polarization beyond the central peak with rising B_z, as seen both from the calculations and from the measured curves.

When B_z is negative, the effective field is antiparallel to the Knight field, $B_e = S_0 b_e$. If $B_z = -B_e$, the compensation of the longitudinal component of total field occurs. According to Refs. 1 and 9, nuclear spin cooling is not possible in this case. This should result in the disappearance of the W structure, as it is indeed seen in Fig. 2(b) for the Hanle curve calculated for $B_z = -1$ mT. At more negative B_z, the W structure appears again, but the additional maxima run away from the central peak with increasing $|B_z|$, maintaining the same amplitude as the central peak. This behavior of the calculated Hanle curves is explained by the fact that in this case the nuclear field is directed against the total effective magnetic field affecting the nuclei. The x component of the nuclear field B_{Nx} is compensated by the transverse magnetic field B_x at some magnitude of B_x, giving rise to the additional maxima. The efficiency of the nuclear-spin pumping increases with the increase of $|B_z|$. As a result, B_{Nx} increases, and the positions of the compensation points where $B_{Nx} + B_x = 0$ are shifted to larger $|B_x|$.

These numerical results, however, are in strong contradiction to our experimental observations; see Fig. 2(b). The central peak of the measured Hanle curves is higher than the other parts of the Hanle curve at any negative B_z. We want to stress that the disagreement between the theory and the experiment cannot be eliminated for any set of values of the adjustable parameters. Therefore this contradiction is of principal importance and indicates that the model of mean nuclear field ignores some mechanism causing depolarization of the electron spin at nonzero transverse magnetic field, including points where it is totally compensated by the nuclear field. The discrepancy is evident also from the unrealistically large value of $B_{1/2}$ needed to fit, at least partly, the experimental Hanle curves within the mean-field model.

B. Effect of nuclear spin fluctuations

To extend the standard cooling model in order to account for the effects of NSF, we suppose that the effective nuclear field consists of a regular component, $\mathbf{B}_N$, created by the nuclear polarization, and a fluctuating component, $\mathbf{B}_f$, appearing due to the random orientation of the limited number of nuclear spins interacting with the electron spin.[18] The estimates given in Refs. 10 and 33 for similar QDs show that the average magnitude of the fluctuating nuclear field is of the order of tens of milliteslas. The frequency of electron spin precession about the field is orders of magnitude larger than the rate of relaxation of the electron spin T_e. Therefore the width of the Hanle curve is determined by the fluctuating nuclear field rather than by electron spin relaxation. This allowed us to fit the experimental curves without using nonrealistic values of T_e as was done in the previous paragraph. Due to fast precession only the projection of electron spin onto the field is conserved. The magnitude and the direction of the fluctuating field are randomly distributed in the QD ensemble. In the absence of other fields, such as the external magnetic field and the field of nuclear polarization, the depolarization of the electron spin by the fluctuating field reduces the observable z component of spin polarization to $1/3$ of its initial value.[19,33]

An effective optical pumping can create a dynamic nuclear polarization, whose magnitude can considerably exceed the nuclear spin fluctuations. If the transverse magnetic field is zero, the effective field of nuclear polarization is directed along the optical axis and is able to suppress the effect of

NSF. This results in the increased amplitude of the central peak of the Hanle curve. Experiments show[13,34] that the PL polarization at zero transverse magnetic field can reach 50% or even more. When $B_x \neq 0$, the nuclear polarization deviates from the optical axis, and its z component decreases, so that the NSF can reduce the electron spin polarization. In particular, the electron spin polarization at the point of mutual compensation of the external field and the field of nuclear polarization is smaller than the polarization at zero B_x. This qualitative consideration explains the small amplitudes of the additional maxima of the Hanle curves, which cannot be explained by the mean-field model.

In order to include NSF in the theory, we use the fact that the buildup time of the nuclear polarization is much longer than the correlation time of the nuclear spin fluctuation ($\approx T_2$), which is, in turn, orders of magnitude longer than the electron spin lifetime. For this reason, the nuclear spin temperature can be calculated using the value of the electron mean spin averaged over possible realizations of the NSF, while each NSF realization can be considered "frozen" (i.e., the evolution of nuclear spin during the electron spin lifetime can be neglected).[19] The dependence of the average electron spin polarization on the transverse external magnetic field within this approximation is a bell-like curve, which can be well fitted by a Lorentzian:

$$\rho(B_x) \approx \frac{\langle B_{fz}^2 \rangle}{B^2 + \langle B_f^2 \rangle}. \tag{3}$$

Here $\langle B_f^2 \rangle = \langle B_{fx}^2 \rangle + \langle B_{fy}^2 \rangle + \langle B_{fz}^2 \rangle$, where $\langle B_{f\alpha}^2 \rangle$ is the squared α component ($\alpha = x,y,z$) of the NSF averaged over the QD ensemble. Equation (3) has a simple geometrical interpretation. In each QD with realization of a particular fluctuating field $\mathbf{B}_f$, only the projection of the electron spin onto the total field, $\mathbf{B}_{\rm tot}^{(e)} = \mathbf{B}_x + \mathbf{B}_f$, survives: $S_\parallel = S_0 \cos\varphi$, where φ is the angle between the vector $\mathbf{B}_{\rm tot}^{(e)}$ and the z direction. The experimentally observable quantity $\rho(B_x)$ is proportional to the z projection of the electron spin, $S_z = S_\parallel \cos\varphi = S_0 \cos^2\varphi$, where $S_0 = 1/2$. It is obvious that in such conditions $\cos^2\varphi = B_{fz}^2/(B_{\rm tot}^{(e)})^2$. Averaging over the QD ensemble gives rise to Eq. (3) if we neglect the correlations of the quantities in the numerator and the denominator of this equation.

Some generalization of Eq. (3) is required to describe electron spin polarization under our experimental conditions. We need to take into account the regular nuclear field $\mathbf{B}_N$ with nonzero components B_{Nx} and B_{Nz} created by the dynamic polarization of nuclei. Similar to the standard mean-field model, we assume for simplicity that the electron density is homogeneously distributed over the nuclei (the so-called box model approximation),[35] which allows us to neglect the spatial variation of the Knight field. Also, since we consider weak magnetic fields, we describe all the nuclear species with a single spin temperature.[1] Since the effective field of nuclear polarization has a certain direction (in contrast to the NSF field) its components are either added to or subtracted from the respective components of the external magnetic field, depending on the experimental conditions. In addition, in our experiments, the external magnetic field has not only the transverse component but also some longitudinal one. For this case we can write down the following expressions for the z and x components of the averaged electron spin $S_\parallel$:

$$S_z = S_0 \frac{(B_z + B_{Nz})^2 + \langle B_{fz}^2 \rangle}{(B_x + B_{Nx})^2 + (B_z + B_{Nz})^2 + \langle B_f^2 \rangle}, \tag{4}$$

$$S_x = S_0 \frac{(B_z + B_{Nz})(B_x + B_{Nx})}{(B_x + B_{Nx})^2 + (B_z + B_{Nz})^2 + \langle B_f^2 \rangle}. \tag{4'}$$

Here we assume that the regular nuclear field $\mathbf{B}_N$ is directed along the total effective field $\mathbf{B}_{\rm tot}^{(N)}$ acting on the nuclei, which consists of the external magnetic field $\mathbf{B}_x + \mathbf{B}_z$ and the Knight field $\mathbf{B}_e = b_e \mathbf{S}_\parallel$, created by hyperfine interaction with the electron spin. As done in the previous paragraph, the nuclear field $\mathbf{B}_N$ is determined by Eq. (2′).

The above equation allows one to obtain the following expressions for the x and z components of the nuclear field:

$$B_{Nx} = (B_x + b_e S_x) \times \frac{b_N \left(B_z S_z + B_x S_x + b_e S_x^2 + b_e S_z^2\right)}{(B_x + b_e S_x)^2 + (B_z + b_e S_z)^2 + \xi B_L^2} \frac{4(I+1)}{3}, \tag{5}$$

$$B_{Nz} = (B_z + b_e S_z) \times \frac{b_N \left(B_z S_z + B_x S_x + b_e S_x^2 + b_e S_z^2\right)}{(B_x + b_e S_x)^2 + (B_z + b_e S_z)^2 + \xi B_L^2} \frac{4(I+1)}{3}. \tag{5'}$$

The coefficient b_e is given, in principle, by[1] $b_e = -(16\pi/3)\mu_B \zeta^2$, where μ_B is the Bohr magneton and ζ is the electron density on a nuclear site. The negative sign means that the direction of the Knight field is *opposite* to that of the electron spin. Because the electron density is dependent on the QD size, which can sufficiently vary from dot to dot, the value of ζ is unknown *a priori*.

Equations (4), (4′), (5), and (5′) contain the Cartesian components of the electron spin and of the dynamic nuclear polarization as unknown quantities. We found them by numerical solution of these equations for transverse magnetic fields in the range from -20 to $+20$ mT and for the several values of the longitudinal magnetic field used in experiment.

In the calculations, the coefficient b_e has been chosen such that the Knight field compensates the z component of the magnetic field at the point where the dips near the central peak of the Hanle curve disappear (see Fig. 3). The quantities b_N, B_{fz}, and ξB_L^2 were considered fitting parameters and varied to get the best correspondence with the experimentally obtained Hanle curves. To compare the calculated results with experimental data we multiplied the calculated values of S_z by a factor α, which takes into account the reduced magnitude of PL polarization. This reduction is presumably due to the fact that some QDs are charge neutral and their PL is nonpolarized. $\alpha = 0.2 \pm 0.02$ for curves measured at negative B_z and 0.16 ± 0.01 for positive values of B_z. The latter curves were measured at a slightly lower power of excitation. The possible reason for the pump-power dependence of α is the creation of photoinduced electrons, which slightly change the fraction of charged QDs.

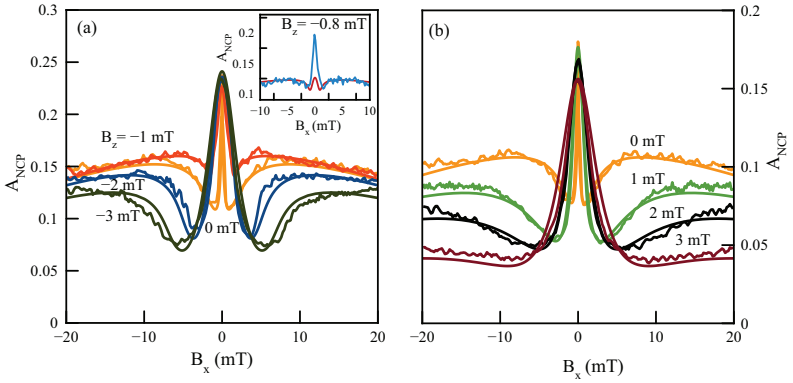

FIG. 3. (Color online) Experimentally measured Hanle curves (noisy lines) and results of calculations taking into account the NSF (smooth solid lines) for (a) negative and (b) positive longitudinal external fields B_z. Values of B_z are given near each curve. The inset shows the central parts of experimental and calculated Hanle curves in the case of mutual compensation of B_z and B_e. The fitting parameters are $b_N = 400$ mT, $\sqrt{\langle B_f^2 \rangle} = 25$ mT, $b_e = 2$ mT.

We should note that Eqs. (4), (4′), (5), and (5′) are interconnected cubic equations. Their solution is unstable in the most general case, complicating the determination of fitting parameters. To simplify the calculations, we performed them in two steps. In the first one, we excluded the x component of electron spin from the equations because it weakly affects the nuclear polarization. In addition, we neglected the small difference in orientation of effective fields $\mathbf{B}_{\rm tot}^{(e)}$ and $\mathbf{B}_{\rm tot}^{(N)}$ and also introduced a fitting parameter:

$$b'_N = \frac{b_N \left(B_{\rm tot}^{(N)}\right)^2}{\left(B_{\rm tot}^{(N)}\right)^2 + \xi B_L^2}, \tag{6}$$

which characterizes the real nuclear field acting on the electron spin. This reduces the system of equations to one equation of fifth order for S_z:

$$\rho = \frac{S_z}{S_0} = \frac{2B_{ez}}{b_e} = \frac{\left[B_z B_x^2 + (B_z - S_0 b'_N)(B_{ez} + B_z)^2\right]^2 + \langle B_{fz}^2 \rangle \left[B_x^2 + (B_{ez} + B_z)^2\right]}{B_x^2 \left[B_x^2 + (B_{ez} + B_z)^2 - S_0 b'_N (B_{ez} + B_z)\right]^2 + \left[B_z B_x^2 + (B_z - S_0 b'_N)(B_{ez} + B_z)^2\right]^2 + \langle B_f^2 \rangle \left[B_x^2 + (B_{ez} + B_z)^2\right]}. \tag{7}$$

We solved Eq. (7) numerically, which allowed us to determine the range of possible values for quantities b_N and B_{fz}. In the second step, we solved the whole system of Eqs. (4), (4′), (5), and (5′) and used their real roots for modeling the Hanle curves, slightly varying the fitting parameters determined in the first step. We find that the best coincidence with the experimental data is achieved with virtually the same values of b_N and B_{fz} as in the first step of the fitting.

Examples of the calculated Hanle curves are shown in Fig. 3. As seen there, reasonable agreement between calculated and measured curves is observed for positive as well as for negative B_z. Some deviations from the experiment occur for magnetic fields B_z in the range from -0.5 to -1 mT, where the theoretically calculated amplitude of the central peak is considerably smaller than the one observed experimentally (see inset in Fig. 3). The strong decrease of the peak amplitude obtained in the calculations is due to the depolarization of the electron spin by the nuclear spin fluctuations, when the longitudinal component of total field disappears and the nuclear field does not build up. Experiments also show a decrease of the central peak of about 20%, which is, however, significantly smaller than the one predicted theoretically. A possible reason for this discrepancy between the theory and the experiment could be related to the spread of Knight fields in the QD ensemble, which is ignored in the theory. Another possible reason is the polarization of quadrupole-split nuclear spin states, which can stabilize the electron spin polarization.[28] Further study is needed to clarify this problem.

The results of the calculations allow us to conclude that the effect of nuclear spin fluctuations is indeed important for the QDs under study. The good agreement between theory and experiment for the whole range of B_z (with the only exception mentioned above) allows us to consider in more detail the physical meaning of the parameters obtained

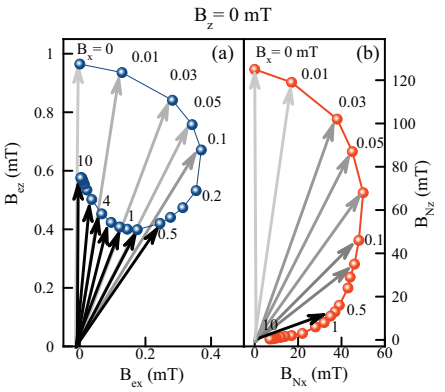

FIG. 4. (Color online) Evolution (a) of Knight field B_e and (b) of nuclear field B_N at $B_z = 0$ under changing external magnetic field B_x. Values of B_x (in mT) are given for some curves (points at the trajectories). The step between points is not constant. Arrows show respective $\mathbf{B}_e$ and $\mathbf{B}_N$ vectors.

from the fitting and their dependence on the longitudinal magnetic field.

We find that the NSF amplitude $\sqrt{\langle B_f^2 \rangle}$ can be chosen close to 25 mT for all the Hanle curves measured at various longitudinal magnetic fields. This value is somewhat larger than the one obtained in another experiment with similar QDs.[13] A possible reason for this overestimation of the NSF amplitude is the increase of the wings of the Hanle curves due to polarization of quadrupole–split nuclear spin states, which becomes noticeable at magnetic fields $|B_x| \sim 20$ mT and larger.[24] By adding this polarization phenomenologically into the model, we were able to reduce the calculated NSF amplitude. We ignore here the quadrupole effects to avoid a complication of the analysis.

We have also verified the validity of the assumption of an isotropic distribution of NSF by replacing $\langle B_{fz}^2 \rangle \to \beta \langle B_{fz}^2 \rangle$ in the numerator of Eq. (7) and optimizing the factor β. The optimal value of β was found to be in the range from 1.2 to 1.4. We suppose that some asymmetry of the distribution of nuclear spin fluctuations can also be due to the quadrupole stabilization of nuclear spins along the growth axis.

The good overall correspondence of the simulated and measured Hanle curves confirms the validity of the model developed. In the framework of this model, we can get a clear idea about the vector representation of the time-averaged electron spin and nuclear polarization in the system under study. Figure 4 schematically shows the evolution of the respective vectors under variation of the transverse magnetic field B_x and for zero longitudinal field. For uniformity, the electron spin and the nuclear polarization are presented as effective fields, B_e and B_N, respectively. The diagrams are shown only for positive values of B_x. For negative B_x, the x components of vectors B_e and B_N are negative so that the diagrams are symmetrical relative to the vertical axes.

The nuclear field at zero B_x is controlled only by the Knight field, which is directed along the z axis. When a small transverse magnetic field, $B_x \ll B_e$, is applied, the nuclear field deviates from the z axis, so that its x component becomes orders of magnitude larger than the magnetic field B_x. For example, $B_{Nx} \approx 50$ mT at $B_x = 0.1$ mT; see Fig. 4(b). This is a clear illustration of the "amplification" of the external magnetic field by the nuclear field.[1] The electron spin polarization follows the nuclear field, which becomes quickly tilted with magnetic field and depolarizes the electron spin. This behavior of the electron spin explains the small width of the central peak of the Hanle curve. For a further increase of the magnetic field, the magnitude of the nuclear field rapidly drops so that $|\mathbf{B}_N| \leqslant |\mathbf{B}_x|$ at $B_x \geqslant 10$ mT.

Application of a longitudinal magnetic field with a magnitude larger than that of the Knight field significantly changes the behavior of the electron and nuclear polarizations, as demonstrated in Fig. 5 for $|B_z| = 2$ mT. An increase of the transverse magnetic field B_x is accompanied by inclination and reduction of the Knight field; however, the reduction is not as fast as at $B_z = 0$. The direction of the Knight field inclination depends on the sign of the longitudinal magnetic field; see Figs. 5(a) and 5(b). The nuclear field $\mathbf{B}_N$ is directed along the z axis at zero transverse magnetic field and has the maximal value $B_N = b_N S_0 = 200$ mT at positive B_z when the Knight

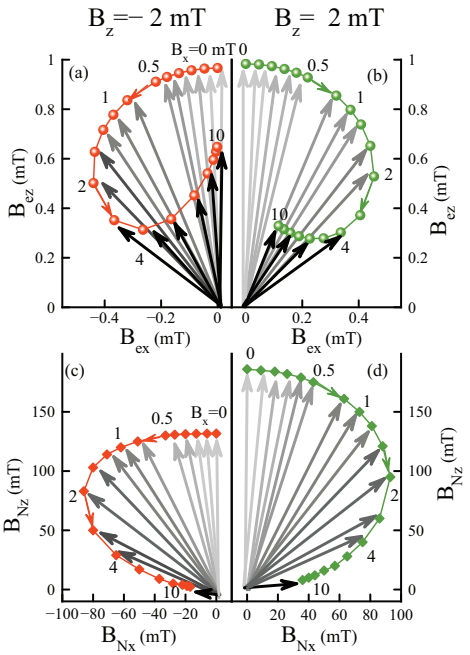

FIG. 5. (Color online) Evolution of (a) and (b) the electron and (c) and (d) nuclear fields for application of negative [(a) and (c)] and positive [(b) and (d)] longitudinal magnetic fields with relatively large magnitudes. Similar to Fig. 4 the diagrams are shown only for positive B_x.

field and the longitudinal magnetic field add up [Fig. 5(d)]. At opposite (negative) sign of B_z when the fields are subtracted from each other, the total effective field acting on the nuclei is smaller, which results in some reduction of the nuclear polarization [Fig. 5(c)]. The direction of inclination of the nuclear field is also dependent on the sign of B_z. In particular, the x component of the nuclear field is negative at negative B_z, so that compensation of the transverse magnetic field occurs at $B_x \approx 10$ mT. This compensation results in partial restoration of the electron spin polarization and its reorientation again along the z axis; see Fig. 5(a). The decrease of the magnitude of the Knight field relative of its initial value at $B_x = 0$ mT is the effect of the nuclear spin fluctuations, as discussed above.

V. CONCLUSION

The experimental study of electron spin polarization in singly charged (In,Ga)As/GaAs QDs as a function of an applied transverse magnetic field for simultaneously applied small longitudinal magnetic field highlights a number of specific features of the hyperfine interaction in these systems. The analysis of experimental data has confirmed the prediction of Ref. 19 about the significant influence of nuclear spin fluctuations on the electron spin orientation due to strong localization of the electron in QDs. The observed behavior is considerably different from that in extended semiconductor alloys studied in many works,[1] in which the electron density is spread out over a huge number of nuclei and the effect of the NSF, as a rule, is negligibly small. The analysis allows us to evaluate the maximal value of the effective field of nuclear polarization created in studied quantum dots by optical pumping to be about 200 mT. We have also found that the effective field acting on the nuclei from the electron spin (Knight field) in the sample under study is near 1 mT when the electron spin is almost fully oriented.

We have restricted our analysis to the range of transverse magnetic fields $|B_x| < 20$ mT (see Figs. 2) for two reasons: (i) the effect of the NSF is most prominent in this range, and (ii) the effect of the quadrupole splitting of the nuclear spin states is small. However, the results of our calculations show that the quadrupole effect cannot be totally ignored. In particular, it may be responsible for an anisotropy of the nuclear spin fluctuations and a rise of the wings of the Hanle curve. Another possible manifestation of the quadrupole effect is the relatively large amplitude of the central peak for mutual compensation of the Knight field and the z component of the external magnetic field.

The consideration of the NSF field has allowed us to quantitatively describe the Hanle curves in the range of relatively small external field and to evaluate random and regular nuclear fields acting on the electron. We have also found that the magnitude of the nuclear polarization obtained from the simplified analysis based on neglecting the transverse component of the Knight field gives rise to almost the same result as the exact calculation. Therefore the simplified model can be useful for an express analysis of the experimentally measured Hanle curves.

ACKNOWLEDGMENTS

This work was supported by the Deutsche Forschungsgemeinschaft, the Russian Foundation for Basic Research, and EU FET SPANGL4Q. The financial support from the Russian Ministry of Education and Science (Contract No. 11.G34.31.0067 with SPbSU and leading scientist A. V. Kavokin) is acknowledged.

[1] *Optical Orientation*, edited by B. P. Zakharchenya and F. Meier (North-Holland, Amsterdam, 1984).
[2] S. W. Brown, T. A. Kennedy, D. Gammon, and E. S. Snow, Phys. Rev. B **54**, R17339 (1996).
[3] D. Gammon, Al. L. Efros, T. A. Kennedy, M. Rosen, D. S. Katzer, D. Park, S. W. Brown, V. L. Korenev, and I. A. Merkulov, Phys. Rev. Lett. **86**, 5176 (2001).
[4] O. Krebs, P. Maletinsky, T. Amand, B. Urbaszek, A. Lemaître, P. Voisin, X. Marie, and A. Imamoglu, Phys. Rev. Lett. **104**, 056603 (2010).
[5] R. V. Cherbunin, S. Yu. Verbin, T. Auer, D. R. Yakovlev, D. Reuter, A. D. Wieck, I. Ya. Gerlovin, I. V. Ignatiev, D. V. Vishnevsky, and M. Bayer, Phys. Rev. B **80**, 035326 (2009).
[6] P. Maletinsky, A. Badolato, and A. Imamoglu, Phys. Rev. Lett. **99**, 056804 (2007).
[7] P. Maletinsky, C. W. Lai, A. Badolato, and A. Imamoglu, Phys. Rev. B **75**, 035409 (2007).
[8] V. K. Kalevich, K. V. Kavokin, and I. A. Merkulov, in *Spin Physics in Semiconductors*, edited by M. I. Dyakonov, Springer Series in Solid-State Sciences, Vol. 157 (Springer, Berlin, 2008), Chap. 11, p. 309.
[9] D. Paget, G. Lampel, B. Sapoval, and V. I. Safarov, Phys. Rev. B **15**, 5780 (1977).
[10] B. Pal and Y. Masumoto, Phys. Rev. B **80**, 125334 (2009).
[11] T. Auer, R. Oulton, A. Bauschulte, D. R. Yakovlev, M. Bayer, S. Yu. Verbin, R. V. Cherbunin, D. Reuter, and A. D. Wieck, Phys. Rev. B **80**, 205303 (2009).
[12] K. Flisinski, I. Ya. Gerlovin, I. V. Ignatiev, M. Yu. Petrov, S. Yu. Verbin, D. R. Yakovlev, D. Reuter, A. D. Wieck, and M. Bayer, Phys. Rev. B **82**, 081308(R) (2010).
[13] R. V. Cherbunin, K. Flisinski, I. Ya. Gerlovin, I. V. Ignatiev, M. S. Kuznetsova, M. Yu. Petrov, D. R. Yakovlev, D. Reuter, A. D. Wieck, and M. Bayer, Phys. Rev. B **84**, 041304 (2011).
[14] Y. Masumoto, K. Toshiyuki, Ts. Suzuki, and M. Ikezawa, Phys. Rev. B **77**, 115331 (2008).
[15] B. Urbaszek, X. Marie, T. Amand, O. Krebs, P. Voisin, P. Malentinsky, A. Högele, and A. Imamoglu, Rev. Mod. Phys. **85**, 79 (2013).
[16] K. V. Kavokin, Semicond. Sci. Technol. **23**, 114009 (2008).
[17] D. Paget, Phys. Rev. B **24**, 3776 (1981).
[18] I. A. Merkulov, G. Alvarez, D. R. Yakovlev, and T. C. Schulthess, Phys. Rev. B **81**, 115107 (2010).

[19]I. A. Merkulov, Al. L. Efros, and M. Rosen, Phys. Rev. B **65**, 205309 (2002).
[20]A. V. Khaetskii, D. Loss, and L. Glazman, Phys. Rev. Lett. **88**, 186802 (2002).
[21]M. S. Rudner and L. S. Levitov, Phys. Rev. Lett. **99**, 036602 (2007).
[22]M. S. Rudner, F. H. L. Koppens, J. A. Folk, L. M. K. Vandersypen, and L. S. Levitov, Phys. Rev. B **84**, 075339 (2011).
[23]P. F. Braun, X. Marie, L. Lombez, B. Urbaszek, T. Amand, P. Renucci, V. K. Kalevich, K. V. Kavokin, O. Krebs, P. Voisin, and Y. Masumoto, Phys. Rev. Lett. **94**, 116601 (2005).
[24]S. Yu. Verbin, I. Ya. Gerlovin, I. V. Ignatiev, M. S. Kuznetsova, R. V. Cherbunin, K. Flisinski, D. R. Yakovlev, and M. Bayer, Zh. Eksp. Teor. Fiz. **141**, 778 (2012) [Sov. Phys. JETP **114**, 681 (2012)].
[25]S. Cortez, O. Krebs, S. Laurent, M. Senes, X. Marie, P. Voisin, R. Ferreira, G. Bastard, J.-M. Gérard, and T. Amand, Phys. Rev. Lett. **89**, 207401 (2002).
[26]A. Shabaev, E. A. Stinaff, A. S. Bracker, D. Gammon, A. L. Efros, V. L. Korenev, and I. Merkulov, Phys. Rev. B **79**, 035322 (2009).
[27]I. V. Ignatiev, S. Yu. Verbin, I. Ya. Gerlovin, R. V. Cherbunin, and Y. Masumoto, Opt. Spektrosk. **106**, 427 (2009) [Opt. Spektrosc. **106**, 375 (2009)].
[28]R. I. Dzhioev and V. L. Korenev, Phys. Rev. Lett. **99**, 037401 (2007).
[29]P. Maletinsky, M. Kroner, and A. Imamoglu, Nat. Phys. **5**, 407 (2009).
[30]M. I. Dyakonov and V. I. Perel, Zh. Eksp. Teor. Fiz. **68**, 1514 (1975) [Sov. Phys JETP **41**, 759 (1975)].
[31]A. Abragam, *Principles of Nuclear Magnetism* (Clarendon, Oxford, 1962).
[32]R. Oulton, A. Greilich, S. Yu. Verbin, R. V. Cherbunin, T. Auer, D. R. Yakovlev, M. Bayer, I. A. Merkulov, V. Stavarache, D. Reuter, and A. D. Wieck, Phys. Rev. Lett. **98**, 107401 (2007).
[33]M. Yu. Petrov, I. V. Ignatiev, S. V. Poltavtsev, A. Greilich, A. Bauschulte, D. R. Yakovlev, and M. Bayer, Phys. Rev. B **78**, 045315 (2008).
[34]M. Ikezawa, B. Pal, Y. Masumoto, I. V. Ignatiev, S. Yu. Verbin, and I. Ya. Gerlovin, Phys. Rev. B **72**, 153302 (2005).
[35]G. G. Kozlov, Zh. Eksp. Teor. Fiz. **132**, 918 (2007) [Sov. Phys. JETP **105**, 803 (2007)].

PIV

RESONANT NUCLEAR SPIN PUMPING IN (IN,GA)AS QUANTUM DOTS

R. V. Cherbunin, K. Flisinski, I. Ya. Gerlovin, I. V. Ignatiev, M. S. Kuznetsova, M. Yu. Petrov, D. R. Yakovlev, D. Reuter, A. D. Wieck, and M. Bayer

Published in: *Physical Review B — Condensed Matter and Materials Physics*, 2011, 84 (4), 041304(R)

PHYSICAL REVIEW B **84**, 041304(R) (2011)

Resonant nuclear spin pumping in (In,Ga)As quantum dots

R. V. Cherbunin,[1,2] K. Flisinski,[1] I. Ya. Gerlovin,[2] I. V. Ignatiev,[2] M. S. Kuznetsova,[2] M. Yu. Petrov,[2] D. R. Yakovlev,[1,3] D. Reuter,[4] A. D. Wieck,[4] and M. Bayer[1]

[1]*Experimentelle Physik 2, Technische Universität Dortmund, D-44221 Dortmund, Germany*

[2]*Physics Department, St. Petersburg State University, 198504 St. Petersburg, Russia*

[3]*A. F. Ioffe Physical-Technical Institute, Russian Academy of Sciences, 194021 St. Petersburg, Russia*

[4]*Angewandte Festkörperphysik, Ruhr-Universität Bochum, D-44780 Bochum, Germany*

(Received 27 May 2011; published 19 July 2011)

We report on the observation of resonant optical pumping of nuclear spin polarization in an ensemble of singly charged (In,Ga)As/GaAs quantum dots subject to a transverse magnetic field. Electron spin orientation by circularly polarized light with the polarization modulated at the nuclear spin transition frequency is found to create a significant nuclear spin polarization, precessing about the magnetic field. Synchronous rf field application along the optical excitation axis considerably enhances the effect. Nuclear spin resonances for all isotopes in the quantum dots are found in that way. In particular, transitions between states split off from the $|\pm 1/2\rangle$ doublets by the nuclear quadrupole interaction are identified.

DOI: 10.1103/PhysRevB.84.041304 PACS number(s): 78.67.Hc, 78.47.jd, 76.70.Hb, 73.21.La

The spin dynamics in semiconductor quantum dots (QDs) has been an object of intense theoretical and experimental research during the past decade.[1–6] In a QD the spin of a confined electron is strongly coupled to the spins of the lattice nuclei. The coupling strength is given by the contact hyperfine interaction, which is enhanced due to strong localization of the electron in the QD.[2,3] Hyperfine coupling destroys electron spin polarization via interaction with random fluctuations of the effective nuclear magnetic field.[2] A way to overcome this is by creating a strong polarization of the nuclear spins.[3]

An efficient technique to reach significant nuclear spin polarization (NSP) is optical pumping.[7] A relatively strong nuclear polarization (tens of percent) can be created by optical pumping of QDs in a magnetic field parallel to the optical axis (longitudinal field).[4–6] Optical pumping can create dynamic nuclear polarization also in a transverse magnetic field.[7–9] It is commonly accepted[1,7] that the NSP components orthogonal to the magnetic field rapidly relax due to a dipole-dipole interaction between the nuclear spins so that only the longitudinal component is conserved and may be accumulated. The appearance of this longitudinal component corresponds to a difference in population of nuclear Zeeman sublevels and, therefore, is usually treated in terms of "nuclear spin cooling."[1,7]

In this Rapid Communication we experimentally demonstrate that not only longitudinal but also transverse NSP components of remarkable magnitude can be created in QDs. We find that polarization-modulated optical excitation of singly charged (In,Ga)As/GaAs QDs results in a strong change of the dependence of photoluminescence (PL) polarization on a transverse magnetic field (Hanle curve). Evaluation of the characteristic times of nuclear spin dynamics allows us to conclude that the polarization is due to resonant pumping of the nuclear spin system. We identify resonances related to spin transitions of the gallium, indium, and arsenic nuclei which are influenced by magnetic field and quadrupole interaction. We suggest that the observed effect is a clear indication of a phasing of the nuclear spin states that corresponds to the creation of transverse NSP components precessing about the magnetic field.

The heterostructure under study contains 20 layers of (In,Ga)As QDs sandwiched between GaAs barriers with *n*-type modulation doping. Donor ionization supplies every dot with, on average, a single resident electron. The original structure grown by molecular-beam epitaxy on a (100) GaAs substrate was thermally annealed at a temperature of 980 °C, resulting in a reduction of the In content in the QDs due to interdiffusion of In and Ga and a high-energy shift of the lowest QD optical transition to ∼1.42 eV. Further optical properties of the sample can be found in Ref. 10. The sample is placed in a cryostat with a superconducting magnet for moderate magnetic fields with strengths up to fraction of a tesla perpendicular to the structure growth axis (Voigt geometry), either along the [110] or the [010] crystallographic axes. The experiments are done at a sample temperature $T = 1.6$ K.

The PL is excited by a continuous-wave Ti:sapphire laser tuned to a photon energy of 1.481 eV, corresponding to the wetting layer optical transition. An electro-optical modulator followed by a quarter-wave plate is used to modulate the polarization helicity of optical excitation. The PL is dispersed by a 0.5-m spectrometer and detected with a silicon avalanche photodiode. The degree of circular polarization of the PL, $\rho = (I^{++} - I^{+-})/(I^{++} + I^{+-})$, is determined from the PL signals detected for a fixed helicity but different helicities of excitation. Here I^{++} (I^{+-}) is the PL intensity for copolarization (cross polarization) of excitation and detection. An acousto-optical modulator is used for amplitude modulation of excitation.

The spin polarization of the resident electrons is monitored through the negative circular polarization (NCP), $\rho < 0$, of the PL from singly charged QDs.[11,12] The NCP measured at the PL maximum of the QD ensemble is proportional to the mean electron spin polarization along the optical axis (z axis).[12] Because the resident electrons are interacting with the QD nuclei, the presence of NSP influences the NCP. Therefore, NCP variation can be used to monitor the nuclear spin state.

Figure 1 shows the magnetic field dependence of the NCP amplitude measured for different excitation protocols. All curves show a decrease of NCP (the Hanle effect) with increasing magnetic field. For continuous-wave excitation with fixed polarization helicity (cw) the Hanle curve consists of a

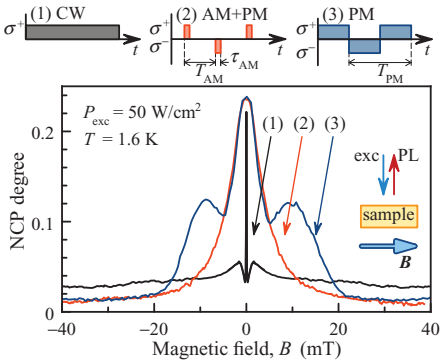

FIG. 1. (Color online) Hanle curves measured for cw optical excitation [curve (1)], for modulated polarization of the excitation [$T_{PM} = 40$ μs, curve (3)], and for polarization and amplitude modulation of the excitation [$T_{AM} = 20$ μs, $\tau_{AM} = 5$ μs, curve (2)]. The top panels sketch these different timing protocols.

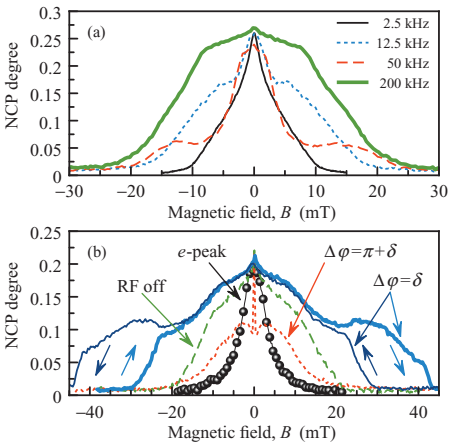

FIG. 2. (Color online) (a) Hanle curves measured for excitation polarization modulated at different frequencies. (b) Effect of rf field on the Hanle curve measured at $f_{PM} = 250$ kHz. The solid curves are measured applying a cophased rf field ($\delta = 20^\circ$) with amplitude $B_{RF} = 0.5$ mT when the magnetic field is scanned in straight (thick line) and reverse (thin line) directions. The dotted curve is measured applying an antiphased rf field. The dashed curve is measured with no rf field. The circled curve is measured in the absence of nuclear polarization. $P_{exc} = 25$ W/cm^2.

narrow central peak and broad shoulders, together forming the so-called W structure.[8] The W structure clearly indicates NSP that has built up for these excitation conditions. When amplitude modulation (AM) with a low on-off time ratio is used, the Hanle curve has a Lorentzian shape. Switching on polarization modulation (PM) in addition to the amplitude modulation ("AM + PM" protocol in the inset of Fig. 1) does not change notably the Hanle curves, meaning that nuclear polarization does not develop under such excitation conditions and the Hanle curve is determined solely by electron spin dynamics. Therefore we call the curve measured in that way the electronic peak ("e peak").

The Hanle curve measured for polarization modulation only [curve (3) in Fig. 1] shows two additional maxima at approximately $B = \pm 10$ mT. The appearance of such additional maxima is the main topic of this Rapid Communication. Hanle curves for various modulation frequencies f_{PM} are given in Fig. 2(a). At small f_{PM}, the Hanle curve consists of a central peak and hardly visible sidebands. The sidebands become more pronounced for higher frequencies, but their amplitude drops so that they disappear at $f_{PM} > 100$ kHz. Simultaneously the central peak becomes wider and additional shoulders appear on it. The frequency shift of the shoulders indicates their resonant character.

An even stronger modification of the Hanle curve is observed when a rf field that is synchronous with the modulation of polarization, as shown in Fig. 2(b), is applied to the sample. We use a sinusoidal rf field, $U_{rf} = U_0 \sin(\omega_{PM} t + \Delta\varphi)$, generated by Helmholtz coils in the sample vicinity (see details in Ref. 13). The coils generate a rf field with a magnetic component directed along the optical axis, having an amplitude B_{rf}^0 of fractions of millitesla. The phase of the rf field $\Delta\varphi$ is chosen either nearly the same as that of polarization modulation or opposite to it. As seen in Fig. 2(b), cophase rf excitation considerably broadens the Hanle curve, giving rise to additional resonances and a hysteresislike behavior. The resonances appear far beyond the electronic Hanle curve. Antiphase rf, on the contrary, considerably suppresses the NCP except at $B = 0$. A phase-dependent effect of joint optical polarization modulation and rf-field application was earlier reported for bulk (Al,Ga)As.[14]

To identify the resonances which contribute to the Hanle curves, we analyze the nuclear spin splitting in a transverse magnetic field. The calculations are made taking into account the quadrupole splitting of nuclear spin states caused by the strain-induced gradient of the crystal field as well as the statistical population of crystal sites by Ga and In atoms. The QDs under study contain several types of nuclei (including isotopes): ^{69}Ga, ^{71}Ga, ^{75}As, ^{113}In, and ^{115}In. The principle axis of the strain-induced gradient is directed along the growth axis (z axis), and determines the quadrupole splitting in the Ga and In as well as As nuclei on symmetric lattice sites (with neighbors of one type). Calculations show[13] that the strain gives rise to a splitting of the nuclear states into doublets $|\pm 1/2\rangle$, $|\pm 3/2\rangle$, etc., which is comparable to or larger than the Zeeman splitting of the doublets in the appled magnetic field range. Further, the Zeeman splitting of the states $|\pm 1/2\rangle$ is increased by factor of $\sim$2 in weak magnetic fields, and the Zeeman splitting of the states $|\pm 3/2\rangle$ is strongly nonlinear [see Fig. 3(a)]. The transitions $|+1/2\rangle \leftrightarrow |-1/2\rangle$ should give rise to resonances, whose magnetic-field-dependent energies can be calculated according to $\hbar\omega_{PM} = 2\gamma_N B$, where γ_N is the nuclear gyromagnetic ratio. The transitions $|+n/2\rangle \leftrightarrow |-n/2\rangle$ with $n = 3,5,\ldots$ lead to additional resonances due to the

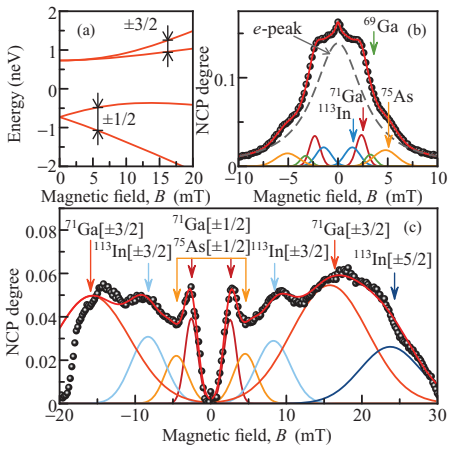

FIG. 3. (Color online) (a) Zeeman splitting of the quadrupole interaction-influenced nuclear spin states of ^{71}Ga. (b) and (c) Hanle curves (circled lines) measured at $f_{PM} = 67$ kHz in the absence (b) and in the presence (c) of rf field and their Gaussian decomposition (solid lines). The peak positions of Gaussians are chosen in accordance with the spin splitting of respective nuclear species. The dashed curve in (b) is the *e* peak.

mixing of the $|\pm(n-1)/2\rangle$ states with the $|\pm n/2\rangle$ states in a magnetic field, having resonance energies depending strongly on the quadrupole splitting. These resonances are responsible for the wide parts of the Hanle curve because larger magnetic fields are required to split the states $|\pm n/2\rangle$ with $n \geqslant 3$. The As nuclei with one or two In atoms in their surroundings are strongly influenced by the electric field gradient from their neighbors, and can give separate resonances with, however, a small amplitude because of the small In concentration in the QDs under study, which does not allow us to identify them.

We calculate the splittings of nuclear spin states by the magnetic field and the quadrupole interaction assuming a strain magnitude $\varepsilon_{zz} = 0.01$ as estimated in Ref. 13. Each resonance at a calculated energy is modeled by a Gaussian with amplitude and width as fit parameters. Our analysis shows that the Hanle curves measured at different modulation frequencies can be described well using the calculated resonance energies. An example for such an analysis is given in Figs. 3(b) and 3(c).

The Hanle curve measured for 67-kHz frequency of excitation-polarization modulation without rf-field application is shown in Fig. 3(b). The curve can be fitted using $|+1/2\rangle \leftrightarrow |-1/2\rangle$ transition resonances only. Although the resonance amplitudes cannot be uniquely determined, the fitting clearly shows that the ^{71}Ga and ^{75}As resonances are most intense. This conclusion is in agreement with the observations made using another technique.[13] Similar results are obtained for other frequencies of polarization modulation.

The analysis of a Hanle curve measured with rf-field application is shown in Fig. 3(c). To work out the resonances more clearly, we subtracted the *e* peak from the experimentally measured Hanle curves. The central part of the curve is given by the resonances $|+1/2\rangle \leftrightarrow |-1/2\rangle$, as discussed above. The wide part of the Hanle curve can be well described by the resonances $|+3/2\rangle \leftrightarrow |-3/2\rangle$ for the In and Ga nuclei, as well by the resonances $|+5/2\rangle \leftrightarrow |-5/2\rangle$ for the In nuclei.

We want to note here that the explanation of the Hanle curve peculiarities by peaks centered at certain resonance fields is not generally accepted, but rather the object of discussion. In Ref. 15, a peculiarity similar to the ones observed here was considered as a peak. Further, the authors of Refs. 7, 16, and 17 observed experimentally dispersionlike peculiarities superimposed on a smooth Hanle curve. These peculiarities were treated as manifestations of optically induced nuclear magnetic resonance (NMR). This conclusion was supported by a theoretical analysis in Ref. 18 for relatively weak resonant optical pumping. The theory of NMR (Ref. 19) also predicts a dispersionlike contour for a classical NMR signal. The dynamics of the electron-nuclear spin system subject to strong optical pumping with modulated polarization should behave more complexly, however. To the best of our knowledge, there are no theoretical models so far which can quantitatively describe the nuclear spin dynamics in this case. A qualitative analysis in the frame of the nuclear spin cooling model predicts a bistability of the electron-nuclear spin system for resonant pumping conditions.[7,20] Such bistability was indeed observed in an (Al,Ga)As epitaxial layer, but the behavior of electron spin polarization was strongly different from the one theoretically predicted.[20]

We assume that the key point for understanding the origin of the resonances observed in our work is the appearance of a significant component of nuclear polarization in the plane perpendicular to the external magnetic field (transverse component). This component, created by optical pumping with resonantly modulated polarization precesses in the (yz) plane about the magnetic field, and can be conserved if the pumping is faster than the transverse relaxation destroying this component. The relaxation is mainly caused by the dipole-dipole interaction between the nuclear spins with a spin flip rate in the order of 10^4 Hz.[7] At the same time, $\sim 10^8$ events of electron polarization per second occur in each QD at the intensity of optical excitation used in our experiments. This excitation rate is by orders of magnitude larger than the dipole-dipole relaxation rate. In addition, the precession frequency of the transverse component is also considerably larger than 10^4 Hz. Under these conditions, the transverse component of the nuclear polarization is not totally destroyed and can support the polarization of the electron spin. The role of this component has not been discussed so far. We want to emphasize that the appearance of such a component cannot be related to a redistribution of populations among Zeeman sublevels and, therefore, cannot be treated in the frame of the nuclear spin cooling theory, which assumes that the transverse relaxation of the nuclear spins rapidly destroys this component.

The creation of a transverse component is a resonant process, as our experiments show. For excitation with constant polarization of light, polarized nuclear spins are created with arbitrary phases so that a transverse component is not created. Only resonant modulation of the optical polarization results in cophase pumping of a large number of nuclear spins, giving rise to resonant amplification of the transverse component of nuclear polarization.

A longitudinal component of nuclear polarization should not appear at strictly resonant pumping, as predicted by the theory of NMR.[19] (In,Ga)As QDs contain, however, several types of nuclei with different resonance frequencies for a given magnetic field so that the majority of nuclei is out of resonance. For these nuclei a longitudinal component may appear. Its direction depends on the signs of the electron g factor and of the mismatch of frequencies $\Delta\omega$ of the nuclear spin precession and the polarization modulation.[7] The electron g factor is negative for (In,Ga)As QDs, so that the longitudinal component is directed against the external magnetic field if $\Delta\omega > 0$, that is, when the resonance frequency of the nuclei is larger than that of polarization modulation. The effective nuclear field created by this component partially compensates the external magnetic field, favoring a further increase of electron spin polarization. The effect should be largest for the resonances observed at the highest magnetic field for a given frequency of polarization modulation because $\Delta\omega > 0$ for the other nuclear spin resonances.

The increase of electron spin polarization corresponds to an increase of the Knight field acting on the nuclei through the polarized electron and promotes accumulation of a longitudinal component of nuclear polarization. The effective nuclear field created by this component partially compensates the external field and favors a further increase of the electron polarization. This positive feedback causes a bistability in the electron-nuclear spin system.[7,9,20] We believe it is this process that is responsible for the hysteresis observed in our case [see Fig. 2(b)]. A quantitative analysis of this process requires, however, a more sophisticated theory.

The proposed model can explain also the modification of the resonance effects when applying a synchronous rf field. This field adds to the Knight field for cophase modulation, thus amplifying the observed effects. On the contrary, an antiphase rf field suppresses the Knight field, thereby eliminating all resonance effects.

In conclusion, we have observed a significant nuclear polarization in the plane perpendicular to the external magnetic field in semiconductor QDs. The polarization is created by circularly polarized optical pumping modulated at a frequency that is resonant to one of the nuclear spin transitions. The effect, which may be termed resonant optical pumping of nuclear spin polarization, is evidenced by several intense peaks in the Hanle curve. The number of peaks increases for joint action of polarization modulation of optical excitation and synchronous rf-field application. In particular, the rf field enhances resonances related to transitions between $|\pm 3/2\rangle$ nuclear states split off from the $|\pm 1/2\rangle$ states by a quadrupole interaction. The magnetic fields at which the peaks occur coincide with those calculated theoretically, assuming a quadrupole splitting of nuclear states induced by a strain field of magnitude $\varepsilon_{zz} = 0.01$. Quantitative modeling of the observed effect is a challenging theoretical problem for further studies. Resonant optical pumping also enhances significantly the sensitivity of NMR signal detection due to the creation of a high nonequilibrium nuclear magnetization. We believe that further improvement of this technique may be a promising way toward nano-NMR.

The authors thank K. V. Kavokin and I. A. Merkulov for fruitful discussions. This work was supported by the Deutsche Forschungsgemeinschaft, the EU Seventh Framework Programme (Grant No. 237252, Spin-optronics), the Russian Foundation for Basic Research, and the Russian Ministry of Science and Education. M.Y.P. thanks the "Dynasty" Foundation.

[1] *Spin Physics in Semiconductors*, edited by by M. I. Dyakonov (Springer, Berlin, 2008).
[2] I. A. Merkulov, Al. L. Efros, and M. Rosen, Phys. Rev. B **65**, 205309 (2002).
[3] A. V. Khaetskii, D. Loss, and L. Glazman, Phys. Rev. Lett. **88**, 186802 (2002).
[4] D. Gammon *et al.*, Phys. Rev. Lett. **86**, 5176 (2001).
[5] P.-F. Braun *et al.*, Phys. Rev. B **74**, 245306 (2006).
[6] A. I. Tartakovskii *et al.*, Phys. Rev. Lett. **98**, 026806 (2007).
[7] *Optical Orientation*, edited by by B. P. Zakharchenya and F. Meier (North-Holland, Amsterdam, 1984).
[8] D. Paget, G. Lampel, B. Sapoval, and V. I. Safarov, Phys. Rev. B **15**, 5780 (1977).
[9] O. Krebs *et al.*, Phys. Rev. Lett. **104**, 056603 (2010).
[10] R. V. Cherbunin *et al.*, Phys. Rev. B **80**, 035326 (2009).
[11] S. Cortez, O. Krebs, S. Laurent, M. Senes, X. Marie, P. Voisin, R. Ferreira, G. Bastard, J.-M. Gérard, and T. Amand, Phys. Rev. Lett. **89**, 207401 (2002).
[12] I. V. Ignatiev, S. Yu. Verbin, I. Ya. Gerlovin, R. V. Cherbunin, and Y. Masumoto, Opt. Spektrosk. **106**, 427 (2009) [Opt. Spectrosc. **106**, 375 (2009)].
[13] K. Flisinski *et al.*, Phys. Rev. B **82**, 081308(R) (2010).
[14] V. G. Fleisher, R. I. Dzhioev, and B. P. Zakharchenya, Pis'ma Zh. Eksp. Teor. Fiz. **23**, 22 (1976) [Sov. Phys. JETP Lett. **23**, 18 (1976)].
[15] Yu. G. Kusraev, E. S. Artemova, R. I. Dzhioev, B. P. Zakharchenya, I. A. Merkulov, and V. G. Fleisher, Fiz. Tverd. Tela (Leningrad) **24**, 2705 (1982) [Sov. Phys. Solid State **24**, 2705 (1982)].
[16] V. K. Kalevich, V. D. Kulkov, and V. G. Fleisher, Fiz. Tverd. Tela (Leningrad) **22**, 1208 (1980) [Sov. Phys. Solid State **22**, 1208 (1980)].
[17] M. Eickhoff, B. Lenzman, G. Flinn, and D. Suter, Phys. Rev. B **65**, 125301 (2002).
[18] I. A. Merkulov and M. N. Tkachuk, Zh. Eksp. Teor. Fiz. **83**, 620 (1982) [Sov. Phys. JETP **56**, 342 (1982)].
[19] A. Abragam, *Principles of Nuclear Magnetism* (Oxford University Press, Oxford, UK, 1962).
[20] R. I. Dzhioev, I. A. Merkulov, M. N. Tkachuk, and V. G. Fleisher, Zh. Eksp. Teor. Fiz. **83**, 2252 (1982) [Sov. Phys. JETP **56**, 1304 (1982)].